Power Loss and Voltage Profile Mitigation Using Distribution Generation (DG) and DSTATCOM: (Case Study of Awash Melkasa Distribution Feeder).

Tewachew Alem Kassie

A thesis submitted to the Department of Power and Control Engineering

School of Electrical Engineering and Computing

Presented in Partial Fulfillment of the Requirements for the Degree of Master's in Electrical Power and Control Engineering

(Power System Engineering)

Office of Graduate Studies

Adama Science and Technology University

June, 2024

Adama, Ethiopia

Power Loss and Voltage Profile Mitigation Using Distribution Generation (DG) and DSTATCOM (Case Study Awash Melkasa Distribution Feeder).

Tewachew Alem Kassie

Advisor: Dr. Tefera Terefe Y.

A thesis submitted to the Department of Power and Control Engineering

School of Electrical Engineering and Computing

Presented in Partial Fulfillment of the Requirements for the Degree of Master's in Electrical Power and Control Engineering

(Power System Engineering)

Office of Graduate Studies

Adama Science and Technology University

June, 2024

Adama, Ethiopia

DECLARATION

I hereby declare that this Master Thesis having **"Power Loss and Voltage Profile Mitigation Using Distribution Generation (DG) and D-STATCOM (Case Study Awash Melkasa Distribution Feeder)."** is my own work and has not been submitted for the award of any academic degree, diploma or certificate in any other university. All sources of materials that u sed for this thesis have been duly acknowledged through citation.

Tewachew Alem Kassie	_____________	____________
Name of Student	Signature	Date

RECOMMENDATION

I, the advisor of this thesis, hereby certify that I have read the revised version of the thesis entitled **“Power Loss and Voltage Profile Mitigation Using Distribution Generation (DG) and DSTATCOM :(Case Study Awash Melkasa Distribution Feeder).”** Prepared under my guidance by Tewachew Alem submitted in partial fulfillment of the requirements for degr ee of Master’s of Science in Electrical Power and Control Engineering (Power System Engine ering). Therefore, I recommend the submission of revised version of the thesis to the departm ent following the applicable procedures.

Dr. Tefera Terefe Y.

__________________________	___________________	___________________
Advisor	Signature	Date

APPROVAL PAGE OF MSc. THESIS

I, the advisor of the thesis entitled "**Power Loss and Voltage Profile Mitigation Using Distr ibution Generation (DG) and DSTATCOM (Case Study Awash Melkasa Distribution Fe eder)**" and developed by Tewachew Alem Kassie, hereby certify that the recommendation and suggestions made by the board of examiners are appropriately incorporated into the final version of the thesis.

Dr. Tefera Terefe.Y

Advisor	Signature	Date

We, the undersigned, members of the Board of Examiners of the thesis by Tewachew Alem Kassie have read and evaluated the thesis proposal entitled **"Power Loss and Voltage Profile Mitigation Using DG and DSTATCOM (Case Study on Awash Melkasa Distribution Fe eder)"** and examined the candidate during open defense. This is, therefore, to certify that the thesis is accepted for partial fulfillment of the requirement of the degree of Master of Science in Electrical Power and Control Engineering (Power System Engineering).

Chairperson	Signature	Date
Internal Examiner	Signature	Date
External Examiner	Signature	Date

Final approval and acceptance of the thesis is contingent upon submission of its final copy to the Office of Postgraduate Studies (OPGS) through the Department Graduate Council (DGC) and School Graduate Committee (SGC).

Department Head	Signature	Date
School Dean	Signature	Date
Office of Postgraduate Studies, Dean	Signature	Date

ACKNOWLEDGEMENTS

First and foremost, I would like to take this opportunity to give glory to Medhanialem and to Kidanemihiret, with whom the completion of this work would have been impossible. I express my gratitude to Dr. Tefera Terefe Ayalew, my thesis advisor. Throughout my research and writing process, Dr. Tefera Terefe's office was always accessible whenever I encountered difficulties or had inquiries. His valuable input and insightful discussions covered a wide range of topics, and he consistently encouraged me to take ownership of this paper. Additionally, he provided guidance whenever he felt it was necessary, steering me in the right direction.

Lastly, I would like to sincerely acknowledge and appreciate my family as well as my friends (Woinshet Lera, Misgana Tulu, Birhan Mamo, and Abnet Eshetu) for their unwavering support and constant encouragement during my academic journey and the entire process of researching and writing this thesis. Their presence and assistance have been instrumental in the realization of this achievement, and I am truly grateful for their contributions.

TABLE OF CONTENTS

Table of contents Page numbers

DECLARATION i

RECOMMENDATION ii

APPROVAL PAGE OF MSc. THESIS iii

ACKNOWLEDGEMENTS iv

TABLE OF CONTENTS v

LIST OF TABLES ix

LIST OF FIGURES xi

ACRONYMS xiii

ABSTRACT xvi

CHAPTER ONE 1

1. Background of the study 1

1.1. Statement of problem 3

1.2. Objectives 4

1.2.1 General objective: 4

1.2.2 Specific objectives: 4

1.3. Scope and Limitation of the study 4

1.4. Significant of the study 4

1.5. Organizations of the Thesis 5

CHAPTER TWO 6

2. Theoretical Background and Literature Review 6
2.1. Introduction 6
2.2. Electric power distribution system 6
2.3. Power Loss and Voltage Drop in Radial Distribution Network 7
2.4. Power Loss and Voltage Profile Mitigation Methods 10
2.5. Distribution Static Synchronous Compensator (D-STATCOM) 14
2.6. Solar Based Distribution Generation 18
2.7. Mathematical Modeling of DG and D-STATCOM 19
2.7.1. Mathematical Modeling of Solar-DG or PVDG system 19
2.7.2. Mathematical Modeling of DSTATCOM 19
2.8. Literature Review 23
CHAPTER THREE 27
3. Material and Methods 27
3.1. Introduction 27
3.2. Materials 27
3.3. Methods 27
3.4. Data Collection 29
3.5. Overhead Distribution Line Impedance Calculation 31
3.6. Modeling of Awash Melkasa Radial Distribution Network 39
3.6.1 Single Line Diagram of Distribution Network 39

3.6.2. Per-Unit Value of Distribution Network 41

3.6.3 Description of Proposed Distribution Feeder 42

3.7. Resource Feasibility Study of Distribution Generation 43

3.7.1. Solar Energy Resource Assessment 43

3.7.2. Wind Resource Assessment 43

3.7.3. Resource Assessment of DSTATCOM 46

3.8. Power Flow Analysis of Radial Distribution System 47

3.8.1 Backward-Forward Sweep Load Flow Analysis of Radial Distribution System.... 47

3.8.2 Integration PQ Model of DG and of Static Model of DSTATCOM in BFS Load Flow Algorithm 52

3.9. Optimal Placement and Sizing of DG and DSTATCOM 53

3.10. Whale Optimization Algorithm 54

3.11. Problem Formulation of Multi-Objective function 57

3.12. Implementation of the WOA Algorithm to Identify the Optimal Size and Placement of DSTATCOM and DG 63

CHAPTER FOUR 67

4.SIMULATION RESULT ANALYSIS AND DISCUSSION 67

4.1 Scenario I: Base case or current system 67

4.2 Scenario II: DG Integration Only 69

4.3 Scenario III: Only D-STATCOM Integration 71

4.4 Scenario IV: Simultaneous DG and DSTATCOM Integration 73

4.5 General Discussion of the Results 75

4.6. Cost Analysis and payback period 77

5.CONCLUSIONS AND RECOMMENDATIONS 82

5.1. Conclusions 82

5.2 Recommendations 83

5.3. Suggestions for Further Work 83

REFERENCE 84

APPENDIXES i

Appendixes-A: Annually Interruption Data for Awash Melkasa substation outgoing Feeders.. i

Appendix- B: Standard conductor type and impedance per km viii

Appendix -C: Sample MATLAB code for This Thesis xii

Appendix-C1: Subprogram for the formation of BIBC Matrix xii

Appendix-C2: Base case Backward-forward Sweep load flow xiv

LIST OF TABLES

Table 3.1: Feeder name, bus bar voltage, and length of Awash Melkasa substation feeders (Appendix-A1) 31
Table 3.2: Overhead conductor parameters used in the feeder (Appendix-B) 33
Table 3.1: GMR Factor (k) and Strand Relationship for AAC conductor 33
Table 3.3: Overhead conductors positive sequence impedance 33
Table 3.3 Awash Melkasa substation 15kv feeder line data and bus data of Dera feeder (F-5) (Appendix-A2) 34
Table 3.4: proposed distribution feeder description 42
Table 3.4: monthly average data of the solar irradiance (kWh/$m2$/day) 43
Table 3.5: Monthly average wind speed (m/s) at ten-meter height 45
Table 3.6: Monthly average wind speed (m/s) at fifty-meter height 45
Table 3.7: Comparison of STATCOM and DSTATCOM (Tejas, Bhavesh , & Naimish, 2020) 46
Table 3.8: Parameters of WOA algorithm and boundary of decision variables of the objective function 64
Table 4.1: Result summary of Scenario-II 70
Table 4.2: Result summary of Scenario-III 72
Table 4.3: Results Summary of Scenario-IV 74
Table 4.4: Result Summary of all Scenarios 76
Table 4.5: Ethiopia Electricity Prices 78
Table 4.6: Result summary of cost analysis 81
Table Appendix-A1: Three-year (2013,2014 and 2015E.C) interruption i
Table Appendix-A2:2013 E.C interruption data of Awash Melkasa substation outgoing feeder ii
Table Appendix-A3:2015 E.C interruption data of Awash Melkasa substation outgoing feeder iii
Table Appendix-A4: feeder of Awash Melkasa distribution substation with their network types iv
Table Appendix-A5 distribution transformer capacity and voltage level of F-5 feeder vi

Table Appendix-B: All Aluminum Conductor (AAC) ix
Table Appedix-B1: Conductor type of F-5 feeder with length and impedance x

LIST OF FIGURES

Figure 1.1: Location of the site (Awash Melkasa, Ethiopia) Ethiopia) (www.Maps.com, 2023) ...3
Figure 2.1: Electric power distribution system (Singh, 2018) ...7
Figure 2.2: Losses in distribution network (Singh, 2018)...9
Figure 2.3: Schematic diagram of D-STATCOM...15
Figure 2.4: Operation principle of D_STATCOM (Mohammed, Ahmet, & Yeliz, 2015)...17
Figure 2.5: Two bus radial distribution system...20
Figure 2.6: Phasor diagram of voltage and current of two- buses radial distribution system (Bikash, Aashish, Jalpa H., & Mohan, 2022) ...20
Figure 2.7: Single Line diagram of two-bus radial distribution system with DSTATCOM...21
Figure 2.8: Voltage & Current Phasor diagram representation of D-STATCOM integration..21
Figure 3.1: Block diagram of the thesis methodology ...28
Figure 3.2: Single line diagram of Awash Melkasa substation...30
Figure 3.3: the coverage area of F-5 feeder ...30
Figure 3.4: overhead distribution line of distribution system (Abayneh, 2022) ...32
Figure 3.6: typical wind turbine power output versus wind speed (Sachidonondo & Moneesh, 2023) ...44
Figure 3.7: Sample radial distribution system...49
Figure 3.8: Bubble net search shrinking encircling mechanism (P.Dinakara, V.C. Veera, & T.Gowri, 2019)...56
Figure 3.9: Bubble net search spiral updating position mechanism (P.Dinakara, V.C. Veera, & T.Gowri, 2019)...57
Figure 3.10: Schematic diagram of an RDS including PV &DSTATCOM ...58
Figure 3.11: Sample radial distribution system and voltage phasor diagram ...60
Figure 3.12: Flowchart proposed whale optimization algorithm ...66
Figure 4.1: Base case voltage profile of Awash Melkasa F-5 feeder...68
Figure 4.2: Base case active and reactive power loss of feeder F-five ...68
Figure 4.3: Voltage profile improvement using integration of DG...69
Figure 4.4: Total active and reactive power loss before and after DG installation...70

Figure 4.5: Voltage profile improvement using D-STATCOM..71
Figure 4.6: Total active and reactive power loss before and after DSTATCOM installation...72
Figure 4.7: Voltage profile improvement using integration DG and D-STATCOM................73
Figure 4.8: Power Loss after Simultaneously DG and D-STATCOM 75
Figure 4.9: Voltage profile enhancement comparisons for all scenarios 76
Figure 4.10: Total Power Loss Mitigation of all Scenarios 77

ACRONYMS

Abbreviations	Description
AAC	All Aluminum Conductor
AVB	Automatic Voltage Booster
BCBV	Branch Current to Bus Voltage
BFS	Backward/Forward Sweep
BIBC	Bus Injection to Branch Current
DC	Direct Current
DG	Distribution Generation
DLF	Distribution Load Flow
D_STATCOM	Distribution Static Var Compensator
DT	Distribution Transformer
EEP	Ethiopia Electric Power
EEU	Ethiopia Electric Utility
F-5	Feeder-Five
FACT	Flexible AC Transmission
GMR	Geometric Mean Ratio
HT	High Tension
IA-GA	Immune Algorithm-Genetic Algorithm
IEEE	Institute of Electrical and Electronics Engineering
KCL	Kirchhoff Current Law
KV	Kilo Volte

KVL	Kirchhoff Voltage Law
KW	Kilo Watt
KWH	Kilo Watt hour
KVAR	Kilo-VAR
LT	Low Tension
LV	Low Voltage
MFA	Moth Flame Algorithm
MFO	Moth Flame Optimization
MOF	Multi-Objective Function
MV	Medium Voltage
MVA	Mega-Volt Ampere
MVAR	Mega-VAR
NB	Number of Bus
NOC	Nominal Operation Cell
NTL	Non-Technical Loss
P	Power
PDS	Power Distribution System
PF	Power Factor
PL	Peak Load
PSO	Particle Swarm Optimization
PV	Photovoltaic
PV-DG	Photovoltaic- Distributed Generation
Q	Reactive Power
R/X	Resistance/Reactance
RDN	Radial Distribution Network
RDS	Radial Distribution System

SCRC	Series Capacitor Reactor Compensator
SSSC	Static Synchronous Series Compensator
STATCOM	Static Synchronous compensator
STC	Standard Test Condition
SVC	Static Var Compensator
TNDI	Total Number Duration Interruption
TNFI	Total Number Frequency Interruption
TPL	Total Active Power Load
TQL	Total Reactive Power
TSSC	Thyristor-Switched Series Capacitor
TSSR	Thyristor-Switched Series Reactor
UPFC	Unified Power Flow Compensator

ABSTRACT

Distribution networks face several problems such as power loss, low voltage profiles, frequent and prolonged power interruptions at customer sites, and lowest level of voltage at system nodes. Awash Melkasa Distribution Feeder similarly faces this kind of problems. Major issues of the feeder are high frequency of interruptions, power losses, and voltage drops. In order to mitigate power loss and voltage deviation, the optimal sizing and placement of distribution static compensators (D-STATCOM) and solar-based distributed generation (DG) in the Awash Melkasa distribution system, Dera (F-5) distribution feeder, were used in this thesis. Dera (F-5) distribution feeder on Awash Melkasa distribution system has 117 branches and 118 buses. The load flow analysis of the distribution feeder has been simulated in MATLAB using the backward/forward sweep algorithm to determine power loss and voltage deviation. The existing system real and reactive power losses are 1298.84 KW and 987.991KVAr respectively and forty-five and 12/100 (45.12%) buses have below standard voltage levels. An optimization problem has been formulated as multi-objective functions comprising total real power loss, total reactive power loss, and voltage deviation for optimal siting and sizing of DG and D-STATCOM using Whale optimization algorithm. The simulation results were tested by considering base case (scenario -I), Only DG integration (scenario -II), only D- STATCOM integration (scenario-III), and simultaneously DG and D-STATCOM integration (scenario-IV) scenarios. The simulation result indicates that active power loss reduction percentages were 44.5578%, 26.456%, and 79.117% for scenario-II, scenario-III, and scenario-IV best-case, respectively. Similarly, reactive power loss reduction percentages were 44.6838%, 26.497%, and 79.218% for the same scenarios. Additionally, the minimum voltage level in the base case improved from 0.8689 p.u. to 0.95 p.u., 0.955204 p.u., and 0.972127 p.u. Therefore, based on the results, scenario IV is the preferred option for reducing power loss and enhancing voltage profile. The optimal simultaneous placement and sizing of DG and DSTATCOM were determined to be at buses 55 and 105 of the F-five feeder, with the DG rated at 1,049 MW and the DSTATCOM rated at 1,214 MVAr, respectively. Furthermore, the payback period of the proposed solution indicates four year and three months.

Keyword: *Backward/Forward Sweep Algorithm, DG, D-STATCOM, Power Loss, Voltage profile, and Whale Optimization Algorithm.*

CHAPTER ONE

1. Background of the study

A power system is a complex interconnection of various electricity-carrying utility systems. The distribution system, transmission system, and generating system are the three subsystems which make together the electric utility system. Lower voltage and more concentrated power distribution to customers occur at the substation level. The number of transmission lines in distribution system larger than the transmission system. The majority of customers are only involved in one of the distribution system's three phases. As a result, each line has a separate power flow, and the system is usually unbalanced. Lateral distributors and primary or main feeders are used in distribution circuits. The main feeder travels across the main load centers after leaving the substation. The individual load is connected to the lateral distributors. The distribution transformers at the ends of the lateral distributors are used to link each individual load point to the main feeder. A single circuit main feeder with a wide range of resistance and reactance values is seen in many practical distribution systems. A radial distribution network, thus, consists of a primary feeder and several laterals that branch out of its nodes (Talukdar, 2019).

The distribution system's main problems are power outages, low voltage profiles, frequent and long-lasting interruptions, distorted voltage and current at the customer's end, and unstable voltage at the system node. Each of the mentioned problems has a unique source; for instance, there can be technical and non-technical causes of power loss. The feeder's length and loading state are the causes. One unwanted phenomenon that happened in the power system was loss in the distribution and transmission systems. Ethiopia now has an overall power loss of 18.66% (Alyu, 2022).

Distributed Generations position in distribution systems to decrease phase unbalancing and power loss and mitigate the profile of voltage. A decreasing the power losses and mitigation of voltage profile at common point of coupling in a real distribution system. Placement of DG did not outcome the requirement of reactive power for the network, ensuing in under voltage at various buses. This under voltage issue was resolved through the optimal position of DSTATCOM (Muquthiar, Gadana, & Visali, 2022).

The study area of this thesis is located in the Central Oromia Region of Ethiopia. Awash Melkasa located in the East Shewa Zone southeast of the capital, Addis Ababa and 9.29mi from Adama. Awash Melkasa substation has 132 kV incoming feeder from Awash hydropower generation II.

There are two transformers a capacity of 25MVA and 31MVA which steps down the incoming voltage to 15kVand 33kV respectively. Two transformers operate independently to the feeders. Distribution feeder voltage s' further steps dawn by distribution transformer to supply the customer loads. Awash melkasa substation has eight outgoing feeders to deliver electrical energy to industry load, commercial load and domestic loads (Report, 2013-2015).

Demographics

Zone: East Shewa

Region: Oromia

Location: 08°24′0″N 39°19′59″E

Lat/long (dec): 8.4,39,33333

Site selection

Specific site location is an important factor for the selection of power loss and voltage drop problem mitigation of Awash Melkassa distribution feeder. A good location can increase both the economy of Ethiopia Electric Utility and customer. Crucial points that need to be considered for reduce power loss and mitigate the voltage profile to improve power quality of this site. Site selection for power loss and voltage profile problems in a distribution system involves identifying the locations where these issues are occurring (Report, 2013-2015).

The most problems in this site are:

- Power loss
- Voltage drops
- High power interruption rate

Figure 1.1: Location of the site (Awash Melkasa, Ethiopia) Ethiopia) *(www.Maps.com, 2023)*

1.1. Statement of problem

The electrical energy demand of the Awash Melkasa distribution system has been rapidly growing due to the expansion of industries and the high growth rate of commercial and residential load and also, consumers at the end of the Feeder have been experiencing low voltage levels due to extended line. As a result, the distribution feeders which transfer power from substation to the customers have poor power quality.

Distribution feeders that travel long distance have high resistance to reluctance ratio (R/X) which is causes high power losses and voltage deviation. The coverage area of Dera (F-5) distribution feeder from the Awash Melkasa distribution system spans 163.95 km. This feeder supplies power to several small towns, including Koshim, Sire Megbiya water pump, and Sire Golo water pump, which operate at voltage levels of 3x289V, 3x340V, and 3x337V, respectively. This indicates that the feeder faces significant challenges, including a high frequency of interruptions, power losses, and voltage drop.

These issues result in economic losses for utilities and customers. This regard, finding loss reduction and voltage profile enhancement mechanisms for the distribution networks is a critical issue. Integration of D-STATCOM and solar-based distributed generation (DG) in Awash Melkasa distribution substation, Dera (F-5) distribution feeder is proposed to solve the problem. The significance of this thesis lies in enhancing the utility's economic efficiency, improving customer satisfaction, and increasing power quality and sustainability.

1.2. Objectives

1.2.1 General objective:

To enhance the efficiency and reliability of Awash Melkasa Distribution Feeder by mitigating power loss and voltage profile through the optimal integration of Distribution Generation (DG) and Distribution Static Compensator (DSTATCOM).

1.2.2 Specific objectives:

The specific objectives of this thesis are:

- ✓ Analyzing and modeling of distribution feeder to determine power loss and voltage deviation using backward/forward sweep algorithm.
- ✓ Formulate a multi-objective function for optimal placement and sizing of DG and D-STATCOM using whale optimization algorithm.
- ✓ Improve voltage profile of Awash Melkasa distribution feeder (F-5).
- ✓ Reduce power loss of Awash Melkasa distribution feeder.
- ✓ Increase economy of utility and customer.

1.3. Scope and Limitation of the study

The scope of the thesis covers, studying distribution network voltage profile mitigation and power loss reduction for the Awash Melkasa distribution feeders. The study focused on reducing power loss, and improving voltage profile for distribution systems by optimal DG and D-STATCOM placement and sizing using whale optimization algorithm.

The scope of the thesis is to analyze, modeling, simulate and evaluate the performance of the distribution network with or without DG and D-STATCOM in order to minimize the power losses and mitigate bus voltage profile of the selected case study using MATLAB software.

The thesis is limited to investigating only the impact on power losses and voltage profile mitigation using software tools. This study does not include the investigation of the impacts of harmonics and protection levels on the distribution network.

1.4. Significant of the study

This thesis work has several significant aspects, including:

- ➢ Reduction of power loss in the distribution network

- Maintaining the voltage profile within a standard voltage range
- Motivating consumers and utilities to use renewable energy resources
- Reducing environmental pollution and minimizing the cost of transmission

Additionally, this work has made a substantial contribution to the application of whale optimization algorithm in power system applications.

1.5. Organizations of the Thesis

The organization of the thesis has been made in such a way that the reader finds an introduction, literature review of different methods for mitigating voltage deviation and power loss reduction, results of the simulations, conclusion and future work. The layout of the thesis is as follows:

Chapter one gives an introduction background, statement of the problem, objectives of the study, scope, methodology followed in the thesis work and finally it provides the thesis outline.

Chapter two gives the detail of theoretical background and review of different literatures related to voltage profile and power loss mitigation in the distribution network and optimization techniques used to solve voltage drop and power loss reduction in the distribution network.

Chapter three describes modeling and analysis of Awash Melkasa distribution feeder. Data collection process, the type of data collected for Dera (F-5) distribution feeder and modeling of the distribution network.

Chapter four presents simulation studies using MATLAB software and analysis of the results.

Chapter five includes the conclusions, recommendations and suggestions for future work to further investigate the research work carried out in this thesis with the whale optimization algorithm to find the best location and the size of DG and D-STATCOM. Finally, the base case is compared with that the compensated system and economic analysis has performed for the selected mechanism.

CHAPTER TWO

2. Theoretical Background and Literature Review

2.1. Introduction

This chapter examines the study's literature reviews and relevant theoretical basis. The electric power distribution system is dealt with in Section 2.2, and the voltage drop and power loss in the radial distribution network are addressed in Section 2.3. Methods for reducing power loss and improving voltage profile are covered in section 2.4. The distribution of static synchronous compensators is reviewed in Section 2.5. The solar-based distribution generation is presented in Section 2.6. DG and D-STATCOM modeling is discussed in Section 2.7. In section 2.8, the literature review is discussed.

2.2. Electric power distribution system

Power distribution systems comprise essential electrical components and infrastructure that facilitate the delivery of electrical energy from a power transmission system to end users. Typically, the topology of distribution systems is radial, so that power goes from substations to end users through main lines or feeders (Pareja, Lezama, & Carmona, 2023).

A distribution system originates at a distribution substation and includes the line, poles, transformers and other equipment needed to deliver electric power to the customer at the required voltage level. Transport energy from the transmission system to end user customer, industry, transport center and power-dependent infrastructure (Daware, 2018).

Ethiopia electric power system voltage level at primary transmission system is 400kv, 230kv, and 132kv.Sub-transmission systems voltage is 66kv and 45kv and 33kv and 15kv as distribution system voltage. Distribution substation is used to step down the voltage to 33kv and 15kv and distribute with outgoing feeders connected in a radial structure (Alyu, 2022).

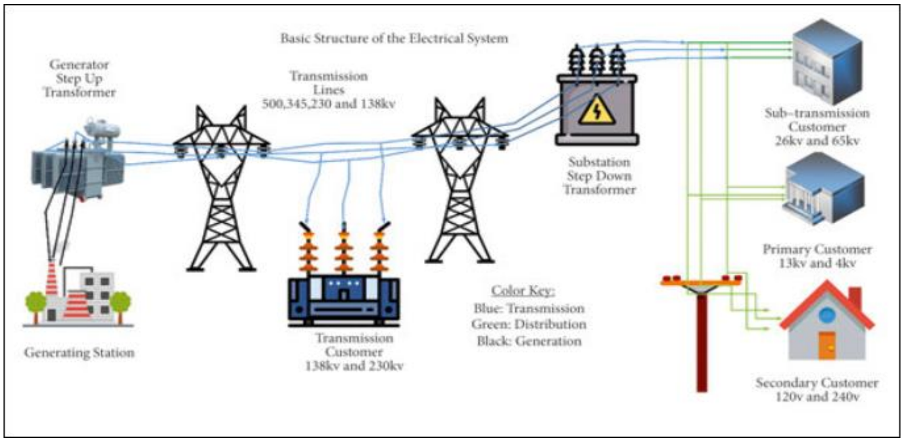

Figure 2.1: Electric power distribution system *(Singh, 2018)*

2.3. Power Loss and Voltage Drop in Radial Distribution Network

Power losses and voltage drops are the most prevalent issues in the Awash Melkasa radial distribution network. In the network, a high R/X ratio results in massive voltage drop and power loss. At the low voltage side with the load, especially Awash Melkasa(F-5) feeder's voltage drop is 290V at the Koshim site. In this thesis, primarily investigate voltage drop and loss of power mitigation for the F-5 distribution feeder.

Electric power loss is described as voltage drop and power loss. Electrical power losses in distribution networks are impacted by losses through transformers, insulators, and distribution lines. The two types of power loss are true power loss and reactive power loss. Line resistance produces true power loss, while reactive elements induce reactive power loss (Abayneh, 2022).

Distribution networks are an important part of a power supply system since the supply of electricity to consumers is ensured by an efficient distribution system. In general, the radial distribution network has a low X/R ration, which leads to more power losses and voltage drop. A large amount of total power losses in the power grid occurs in the distribution network accounting for about 13% of the total network generation (Benalia, Madji, & Benaissa, 2020). The increment of reactive power demand in distribution system creates manifold challenges especially in loss profile management due to most of the loads consist of reactive loads. This significantly increases the current flow in transmission and distribution system which also increase the $I^2 * R$ and $I^2 * R$ losses in the lines. In distribution 70% of total power losses in power system occur while the rest of 30% occurs at transmission and sub-transmission system (Bazilah, et al., 2020).

Power loss created in the distribution networks is divided into two main parts, 60% of which is wasted in the lines and 40% in the transformer (Alireza, Yiming, Negar, & Mohammad, 2021). Power losses can be divided into two categories that are technical and non-technical.

Technical losses may occur due to natural events, design malfunction, overloading and the types of material being used in the system, whereas power losses of non-technical nature involve measurement monitoring issues and power theft (Khan, et al., 2022).

The losses to be in the power distribution network can be classified as:

- Technical losses
- Non-Technical losses

Technical losses: The distribution network experiences technical losses as a result of current flowing through conductors and magnetic losses in transformers, which generate heat within the network. This covers primary and secondary network resistive losses. The losses in KWh meters, resistive losses in the services drops, and resistive losses in the winding and core of the distribution transformer. Technical losses often depending on the features and configuration of the network. Primary and secondary distribution lines in the power network experience the majority of losses (Singh, 2018).

Non-Technical Losses (NTL): Non-technical losses are losses that are dependent on human activity. The unlawful attempt to reduce or completely avoid paying a utility bill for the use of electric energy is known as energy theft. NTL can be caused by a variety of factors, including misread meters, underperforming or non-performing meters, tampering with the meter to provide false readings that are then used to create incorrect consumption statistics in billing, creating unauthorized connections, and direct tapping. This causes customers refuse to pay for the power that uses (Singh, 2018).

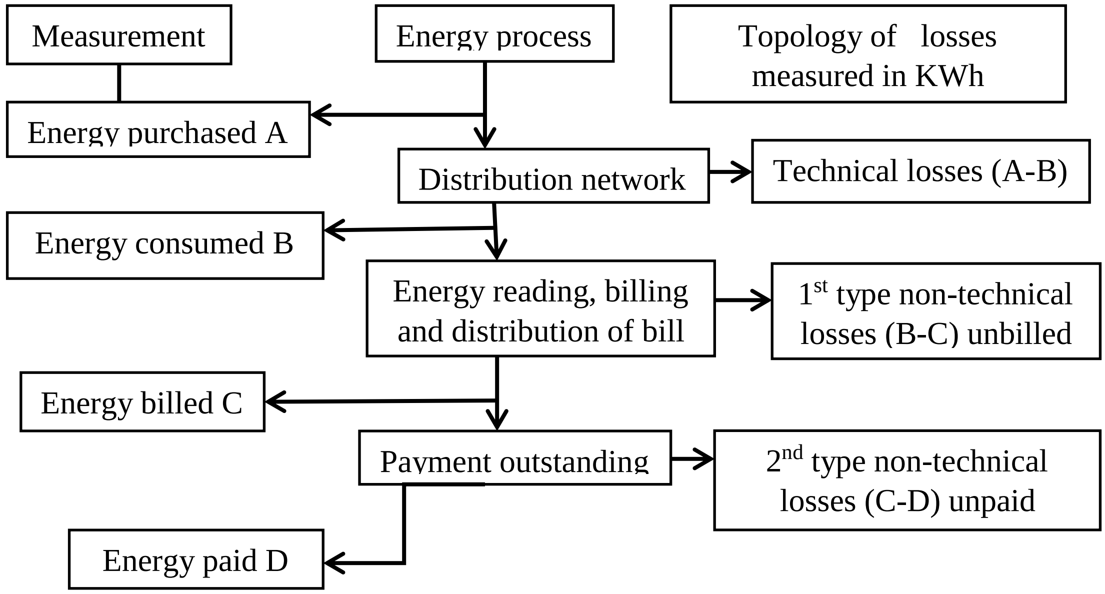

Figure 2.2: Losses in distribution network *(Singh, 2018)*

Reasons for high distribution losses (Singh, 2018)

Long distribution lines: Losses occur in the network when distribution is extended without testing. 15 kV and 400/380-volt lines are hastily extended, usually in rural locations where loads are dispersed across a wide area. High line losses and a high R/X ratio is the outcomes.

Insufficient conductor size: Insufficient conductor size causes feeder overloading and additional losses. The KVA x KM method should be used to determine the conductor size. Since radial feeders typically feed the loads, extending the feeder resulted in higher current losses.

Distribution transformer-related losses: The key component of the distribution system is the distribution transformer. Various kinds of losses are contingent upon it. Transformer with higher and lower ratings.

Low voltage level: Most of the domestic and commercial loads are inductive so small variation in voltage effect the performance of equipment and increase losses in system. Low voltage level at consumer end effect the life of electric goods also

Distribution transformer Location: When a distribution transformer (DT) is positioned incorrectly, energy is lost in the system. For example, customers who are farthest away from the DTs receive much lower voltages than customers who are closer to the DTs.

Poor quality of equipment: High losses are a result of poor-quality equipment since it does not meet electrical standards and draws a lot of current. Heat and I^2R losses were induced by high current.

Low power factor: It has been noted that in most of LT distribution circuits, the power factor ranges from 0.65 to 0.75. Since the majority of domestic, commercial and industry loads are inductive and require high current at any given load, there will be higher losses corresponding to I^2R losses.

Poor high-to-low tension ratio: A 1:1 HT/LT ratio is ideal. However, the ratio is currently 1:6.25 as a result of the LT lines' further extension in the State's extensive electrification of the domestic sector.

Unbalanced phase: The load cannot be distributed equally among all the phases due to the random distribution of the load locations. Power losses occur due to the current flowing in the neutral during this unbalanced phase.

Transformer Losses: The resistive losses in the windings and the iron losses in the core are examples of distribution transformer losses. Nowadays, ordinary silicon steel makes up the majority of a transformer's core. This causes an increase in copper and iron losses within the transformer.

Direct tapping by non-customers: Direct tapping of power by non-customers is common in several places, mainly in the domestic and agricultural sectors. The stolen energy cannot be measured and, thus, is not identifiable to any one party because it is frequently impossible to identify the offender. Thus, stolen energy is regarded as part of line losses.

Current customers are pilfering: The main reason why the electrical utilities lose money is because of current customers' pilfering or theft. The most common methods are to directly bypass the meter and to tamper with it. Physical jerks, the placement of powerful magnets, or the insertion of foreign objects into the disc rotation can all be methods of tampering.

2.4. Power Loss and Voltage Profile Mitigation Methods

There are various methods for mitigating the voltage profile and power loss, which raises the power quality of the distribution system of the outgoing feeders from the Awash Melkasa substation. Network reconfiguring, updating the conductors, compensating for reactive power, installing an automatic voltage booster, locating and sizing distribution transformers, Flexible AC Transmission System Device, Distributed Flexible AC Transmission System, and distributed generation are some of these techniques. Suggestion for enhancement of Awash Melkasa distribution feeder by DG and D-STATCOM to mitigation power loss and voltage profile. An analysis was conducted on the D-STATCOM and DG penetration allocation to save investment costs and improve system performance overall in terms of real power loss reduction and voltage profile improvement.

Power loss reduction and voltage profile improvement are important challenges for the power network. Various methods are implemented for reducing the power loss as well as improving the voltage profile in the network. One of the conventional methods is the use of a reactive power compensation source. The main advantages of this method are improving voltage, reducing power losses, and increasing the capacity of the feeder. Injecting reactive current into the distribution network increases the power loss and voltage deviations. Distribution network reactive compensation is necessary, and installing a reactive compensator in an optimal location with optimal size will reduce the cost of losses and improve the voltage profile. (Alireza, Yiming, Negar, & Mohammad, 2021).

Distribution systems are usually designed to propagate power in a radial distribution network, hence posing challenges for the integration of renewable distributed generation resources. Distributed generation units in the system improves the voltage profile and reduce the overall power loss (Khan, et al., 2022).

Network reconfiguration: Modifying the distribution network to change the network topology is known as network reconfiguration. The percentage of power loss tends to decrease as power flow increases. To enhance network reliability, a smoother demand pattern, and an improved voltage profile network reconfiguration offers major benefits (S.Balakumar, Akililu, Samuel, & K.Bamash, 2021).

The separation of current feeders to create parallel power flow routes and the creation of a new tree structure by opening and closing system switches (Singh, 2018).

Feeder reconfiguration allows loads to be transferred from severely loaded feeders to lighter-laden feeders, and from higher- resistance routs to lower-resistance routs to achieve the lowest loss, where the resistance route is the entire resistance from the source to the load point. Such transfers are successful not only in terms of changing the amount of loads on the switched feeder and lowering losses, but also in terms of improving the voltage profile on the feeders and lowering total system power losses. Feeder reconfiguration, on the other hand, is successful if the distribution feeders are automated and not too far apart. For un-automated and fare apart feeders, feeder reconfiguration may not be cost effective (Abayneh, 2022).

Conductor updating: To reduce the active power losses, replace the existing conductor with one of the optimal conductor sizes. The load growth is rapid. The conductor sizes are chosen for a minimized initial capital investment. This plan is very effective in reducing losses and enhancing the voltage profile (Singh, 2018).

Reactive power compensating: The benefits of reactive power compensation in the distribution system include voltage profile variation, higher power flow capacity, mitigated system capacity, and reduced power losses. In general, if the size and position are optimized, reactive power compensation is an efficient way to improve the voltage profile and loss of a distribution network. This can be performed by putting in various reactive compensating devices (Alyu, 2022).

The load on the distribution system is mostly inductive and requires large reactive power. Shunt capacitor provide reactive power compensation at its location, independent of the load (Singh, 2018).

Distribution Transformers Locating and Sizing: The location and size of distribution transformers (DTs) should be determined with the load. This will help to minimize technical loss in the secondary distribution system (Singh, 2018).

The secondary of the transformer is maintained at a tolerable voltage level. Distribution transformers should be positioned as close to the load center as feasible. In addition, large transformers must be changed out with transformers with limited ratings that service a small number of customers (Alyu, 2022).

Automatic voltage booster: In distribution systems, autotransformers known as Automatic Voltage Booster (AVB) are installed to solve the issue of voltage deviation. They maintain the electrical distribution network's voltages within a predetermined range. The optimal operation of electrical devices is guaranteed by voltage regulation. Usually, electrical equipment is designed to operate within a specific voltage range. Device performance is usually insufficient and unsatisfactory as a result of poor regulation of voltage (Asmaa, Abdullah, & Heba, 2022).

Distributed generation: DG can be classified into four major types based on their terminal characteristics in terms of active and reactive power-delivering capability as follows (Tesfay, 2018):

1. Type 1: DG is limited to injecting P.
2. Type 2: DG is limited to injecting Q.
3. Type 3: A DG with the ability to inject both P and Q.
4. Type 4: A DG that can inject P but consume Q.

Micro turbines, fuel cells, and photovoltaic systems are excellent examples of Type 1 energy sources that can be integrated into the grid with the use of converters and inverters. Capacitors and reactive power compensators could be Type 2. DG units classified as Type 3 are synchronous machines, such as gas turbines and cogeneration. Type 4 is mainly induction generators that are used in wind farms.

Advantages of DGs in Power Systems Applications (Alyu, 2022):

DG units have various advantages in power system applications which are the main reason behind its widespread acceptance. Some main technical and economic benefits are:

- Reducing losses in the power system
- Improvement of the voltage profile
- Increasing energy efficiency
- Improving reliability and regional consequences of system failure
- Improving power quality and security
- Lower operating cost because of peak shaving
- Enhanced productivity
- Deferred investment for upgrade facilities

Flexible AC Transmission System Device: FACTS devices are frequently used to improve power quality and stability. FACTS devices come in different types, each having unique characteristics, benefits, and drawbacks. FACTS devices enable control over transmission system parameters of interest, which are essential to the grid's smooth operation. They can be employed alone or in combination with other types of FACTS devices (Adetokun & Muriithi, 2021).

FACTS devices are (Abayneh, 2022):

- Shunt connected controllers such as Static Synchronous Compensator (STATCOM) and Static VAR Compensator (SVC).
- Series connected controllers such as static synchronous series compensator (SSSC), series capacitive reactance compensator (SCRC), Thyristor-switched series capacitor (TCSC), and Thyristor-controlled series reactor (TCSR).

- A combination of shunt and series connected controllers such as unified power flow controller (UPFC), and Thyristor-controlled phase shifting transformer (TCPST).
- Those FACTS devices are used to improve grid voltage stability and power quality.
- The basic applications of FACTS devices are (Alyu, 2022):
- Power flow control, reactive power compensation, and increase of transmission capability.
- Power quality improvement, Power conditioning, Voltage control, and Stability improvement.

Distributed Flexible AC Transmission System:

D-FACTS devices connect in series, shunt and series-shunt to distribution feeder lines. D-FACTS devices are smaller and less expensive than traditional FACTS devices which may make them better candidates for wide scale deployment for distribution power system. From a power systems perspective, D-FACTS devices have many potential benefits (Ganguly, Manna, Mondal, & Roy, 2020).

Recently Distributed Flexible AC transmission system (D-FACTs) has been introduced to overcome most of the problem posed by FACTs devices (Bhavna , 2023).

- D-FACTs devices are power modular,
- Small in size and light in weight.
- Less expensive
- better candidates for wide scale deployment
- Generally, modules are rated about 10 KVA to 15KVA

D-FACTs devices are DSSC, DSTATCOM and DPFC which used to improve power network handling capacity, voltage regulation, system stability and harmonic reduction (Bhavna , 2023).

- DSSC is used to alter line impedance to control the power dynamically.
- DSTATCOM used to mitigate the voltage profile of the line acting as current source.
- DPFC has the capability of simultaneously adjusting all the parameters of power system: line impedance, bus voltage magnitude and power angle (Bhavna , 2023).

2.5. Distribution Static Synchronous Compensator (D-STATCOM)

The D-STATCOM is a three-phase shunt connected Voltage Source Converter (VSC) designed for use in the distribution network to compensate for the bus voltage to provide better performance of distribution power system. At the point of common coupling, the device can inject or absorb both active and reactive current (PCC). D- STATCOM's to inject active power over a lengthy period is essentially impossible due to the energy storage restriction. D-STATCOM cannot inject active power over a lengthy period due to the energy storage restriction. The operation is mostly in a steady state with reactive power being the power exchange between D-STATCOM and the distribution network system (Abayneh, 2022).

Distribution static compensator constructed from combination of DC source, a combined transformer, and combined VSC, thus connected in shunt to change control unit and current system. A DC capacitor, inverter modules, an AC filter, a transformer to match the inverter output to the line voltage, and a PWM control are the essential parts of D-STATCOM. A voltage source in the D-STATCOM installation transforms a three-phase AC-DC voltage before connecting it to the AC line through the reactor and capacitor connections. This configuration helps in maintaining the appropriate voltage levels and reactive power compensation (Zaenab, Riskiani, Idar, & Agus, 2022).

The three main components of D-STATCOM (Zaenab, Riskiani, Idar, & Agus, 2022).

1). IGBT or GTO-based DC to AC inverter: this inverter is used to create a leading or lagging active current in the voltage output to control magnitude and phase based on required compensation.

2).LC filter: The LC filter is used to reduce harmonics and match the inverter output impedance. The LC filter was chosen because of its compatibility with the type of distribution network and the harmonic that occur in the converter output.

3). Control block: The controller used when pure-wave D-STATCOM module switches are required.

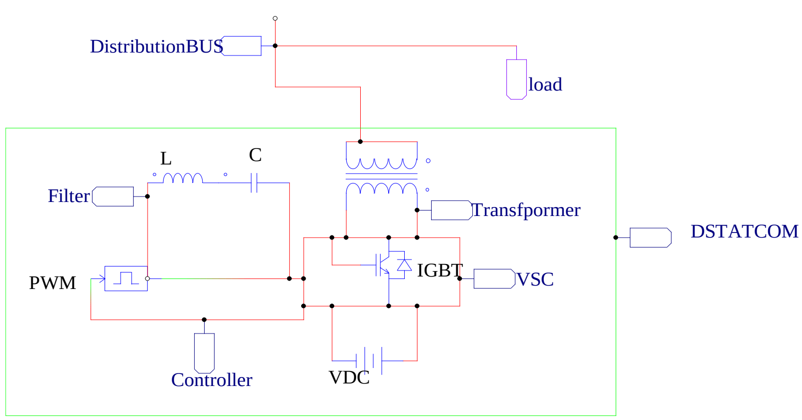

Figure 2.3: Schematic diagram of D-STATCOM

Operation Principle of DSTATCOM

The basic principle of DSATATCOM is the same as the synchronous machine. The synchronous machine provides a leading current when over-excitation and a lagging current when under-excitation. D-STATCOM can absorb and generate similarly reactive power as a synchronous machine and can swap real power if provided with an external DC source (Zaenab, Riskiani, Idar, & Agus, 2022).

The DC-link energy storage device, an output filter, a coupling transformer, and an inverter compose DSTATCOM blow the figure. The three-phase AC output voltages are generated from the DC voltage across the storage device using VSI. Through a coupling transformer, the generated voltages are connected to the distribution network in phase.

The effective control of active and reactive power flow between the DSTATCOM and the distribution system is properly adjusting the phase and magnitude of the DSTATCOM output voltages. The inverter output voltage (V_S), the voltage drops due to coupling impedance, and the voltage at the point of common coupling (PCC). Thus, are V_S, $V_{L,}$ V_C Coupling, V_{PCC}, and, respectively (Mohammed, Ahmet, & Yeliz, 2015).

Operation conditions of DSTATCOM (Mohammed, Ahmet, & Yeliz, 2015)

1) **If V_L equal to V_{PCC}**, the reactive power exchange between the distribution line and DSTATCOM is zero, and then DSTATCOM does not generate or absorb reactive power.
2) **When V_L greater than V_{PCC}**, DSTATCOM performs an inductive reactance connected at its terminal. The current flows through transformer reactance from DSTATCOM to the distribution line, and the device produces capacitive reactive power.
3) **If V_{PCC} greater than V_L**, DSTATCOM performs a capacitive reactance connected at its terminal, Then the current flows from the distribution line to DSTATCOM, and resulting in the device absorbing inductive reactive power.
4) If the switch devices do not lose less real power than the DC capacitor required for switching, the DSTATCOM switches real power (Zaenab, Riskiani, Idar, & Agus, 2022).

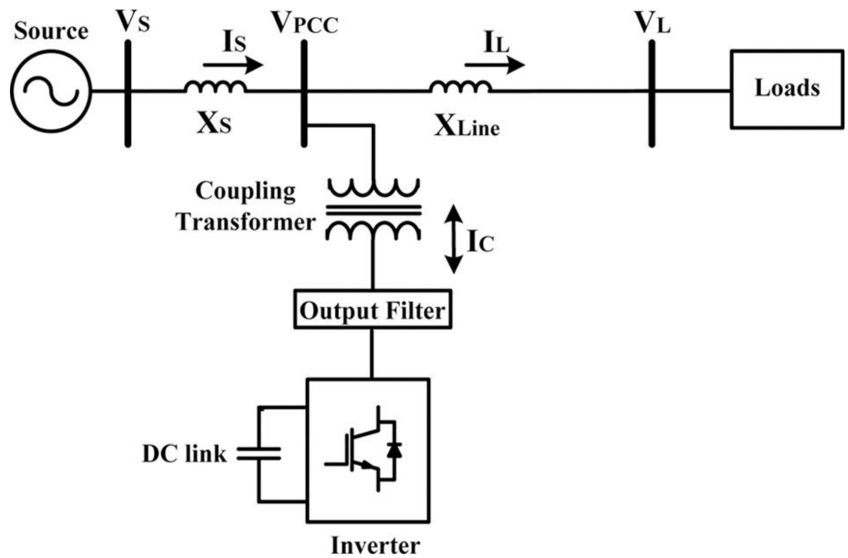

Figure 2.4: Operation principle of D_STATCOM *(Mohammed, Ahmet, & Yeliz, 2015)*

Advantages of DSTATCOM rather than FACTs device are (Bhavna , 2023)

- Distributed nature
- Small in size and Weight
- Less expensive
- Multirole in the circuit
- Augmentation with DG
- Power module device
- Has fast response<10ms

The main problems that face in Awash Melkasa distribution feeder are voltage drop and power loss. Based on this problem select DSTATCOM from above D-FACTs device to reduce power loss and mitigate voltage profile of Awash Melkasa distribution feeder.

The important point use DSTATCOM for mitigation voltage profile in distribution feeder of Awash Melkasa. Based on the above advantages, select D-STATCOM for voltage profile mitigation of the Awash Melkasa distribution feeder.

Distribute nature, augmentation with DG, module device, and small size and weight of DSTATC OM best chose in distribution power network to installation. As a result of the economic aspect, DSTATCOM is less expensive than the FACT devices. DSTATCOM regulates voltage, which has a very fast response of less than 10 ms compared to FACTS devices. DSTATCOM is more flexible for radial distribution power systems because of the value of reactive power that is absorbed or generated according to requirements.

2.6. Solar Based Distribution Generation

Implementing photovoltaic system distribution generation (PVDG) has several advantages, including improving power loss, and system stability, mitigating the voltage profile, and reducing distribution stress. However, realizing benefits necessitates optimal placement and sizing of PVDG. This study proposes a multi-objective artificial immune algorithm to determine the optimal location and size.

Distribution generation (DG) is electrical power generation system design at the customer load site. They have ability to reduce technical loss, improve voltage profile and power quality of distribution network (Dikio & Ezenwa, 2018).

Distribution generation integration into medium voltage distribution feeder. Photovoltaic-based distribution generation is connected to the distribution feeder through an inverter, which can control active and reactive power in the distribution network. Adding PVDG into a conventional single power source distribution network will result in bidirectional power flow during normal and fault conditions (Hermanus, Ramesh, & Raj, 2020).

Improper placement of PVDG in the distribution network can result in issues such as increased power loss, voltage rise problems, and reduced power quality in the system. These losses in the distribution network directly influence the operation cost of the distribution network and poor voltage profile, especially in high loads.

The distribution networks directly affect the operational cost of the system and can also lead to a poor voltage profile, especially in the condition of high load. Thus, problems solved through optimal placement and sizing of PVDG at carefully identified buses can effectively minimize the problem (Ayooluwa, et al., 2022). Hence, in order to avoid reverse power flow, which can be harmful to the operation of power systems, especially at the distribution network, energy storage facilities can be included

The advantages of PVDG integration in distribution network (Ayooluwa, et al., 2022).

- Reduce distribution cost
- Reduce power loss in distribution network
- Improve voltage profile
- Avoid pollution and clean environment

- Provision backup power advent the power outage from distribution system
- Abundantly available energy from sun
- Cheapest energy source compares to other
- Easy installation and setup
- Sufficient technology for deployment for both domestic and industrial purpose
- Minimum maintenance cost

2.7. Mathematical Modeling of DG and D-STATCOM

2.7.1. Mathematical Modeling of Solar-DG or PVDG system

Solar energy is freely accessible renewable energy and totally liberated from pollution. the output of solar PV depends on its geographical atmosphere. Its application for power production as renewable energy source overcomes society's dependence on fossil fuels and wood charcoal. The output power PV and its efficiency can be calculated as shown below in equation 2.1 and 2.2, 2.3 and 2.4 (Bikash, Aashish, Jalpa H., & Mohan, 2022).

$$\begin{cases} p^{pv} = aG\eta^{pv} \\ \eta^{pv} = \eta^{STC}[1+\alpha(T^{cell}-25)] \end{cases} \tag{2.1}$$

Where,

P^{PV} is the power output of PV; "a" is the panel area in meters squared (m^2) and "G" is incident solar radiation (W/m2). η^{PV} and η^{STC} represent the efficiency in the determined operating condition and under Standard Test Conditions (STC).

Cell temperature in ^0C is T^{cell}, and in percentage per ^0C temperature, and the co-efficient "α" is represented. After equation (2.1) merging a new equation (2.2) is formulated. These developed equations will give the output power under STC.

$$\begin{cases} p^{pv} = p^{STC}\{\frac{G}{100}[1+\alpha(T^{cell}-T^{0})] \\ T^{cell} = T^{am} + (\frac{T^{NOC}-20}{800})G \end{cases} \tag{2.2}$$

Where, T^{NOC} = Nominal operating cell temperature in ^0C, T^{am} = ambient temperatures in ^0C, and T^0 = 25 ^0C.

2.7.2. Mathematical Modeling of DSTATCOM

DSTATCOM is shunt-connected to medium voltage distribution power network. It performs two operations, namely, supplying and absorbing the reactive power in the network. When the system is voltage drop and power loss, the compensating current is injected at the DSTATCOM-allocated bus to control the system voltage. Single diagram two-bus radial distribution system and two-bus radial distribution system with DSTATCOM are presented in Figures 2.5 and 2.6, respectively. Here, considering a balanced distribution power network. The (R_L+jX_L) is the impedance of the line between m and n buses. Voltage and current phasor representation of the two-bus radial distribution system and with DSTATCOM is shown in Figure 2.7 and 2.8 respectively. The loads connected at the buses are expressed by (P_i+jQ_i) and (P_j+jQ_j), where the voltages are V_i and V_j (Bikash, Aashish, Jalpa H., & Mohan, 2022).

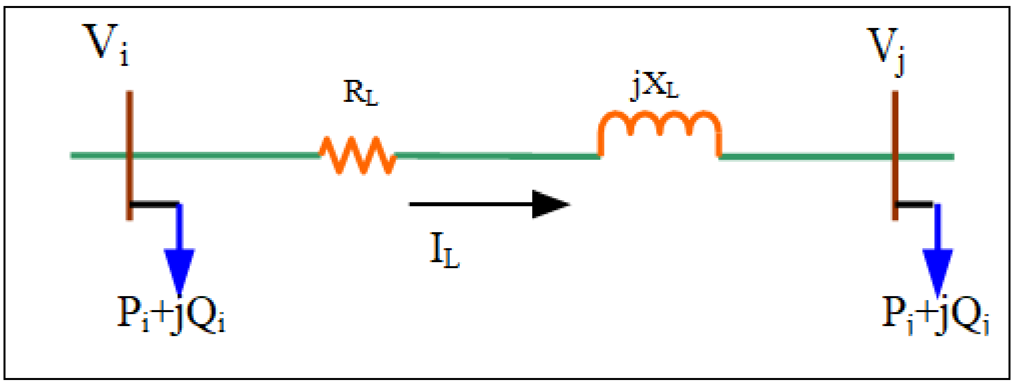

Figure 2.5: Two bus radial distribution system

The voltage equation is as follows, from the two-bus radial distribution system.

$$V_{i+1} = V_i\angle\theta_i - (R_i - jX_i)I_i\angle\delta \tag{2.3}$$

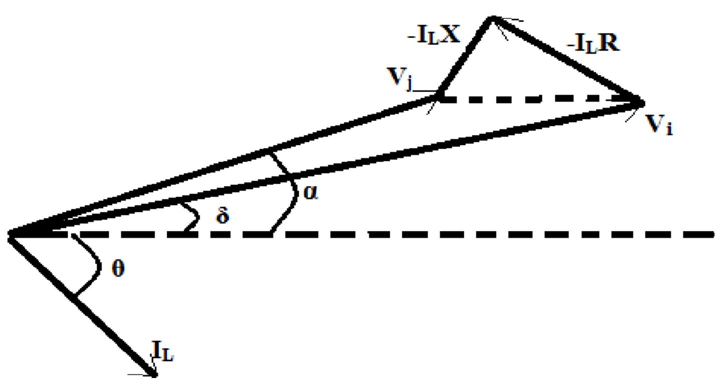

Figure 2.6: Phasor diagram of voltage and current of two- buses radial distribution system *(Bikash, Aashish, Jalpa H., & Mohan, 2022)*

The voltage and current relation from the phasor diagram are expressed in equation (2.4).

$$V_j\angle\alpha = V_i\angle - \delta(R_L + jX_L)I_L\angle\theta \tag{2.4}$$

The backward/forward sweep algorithm is used for Load flow analysis to calculate the voltage and current. The voltages of buses in the radial distribution system are usually less than one per unit so the bus voltages are compensated to the desired value by integrating a DSTATCOM in the optimal distribution system location. For this study, D-STATCOM only injects reactive power therefore the current it injects must be in quadrature with the system's voltage.

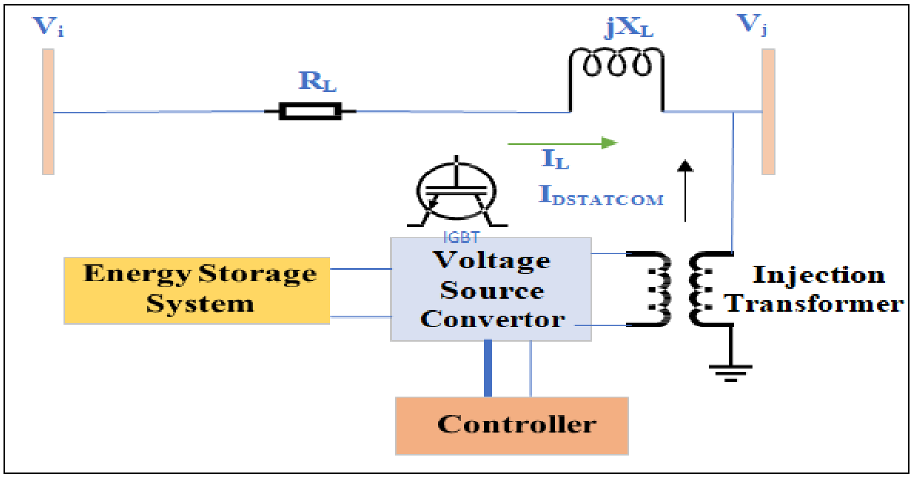

Figure 2.7: Single Line diagram of two-bus radial distribution system with DSTATCOM

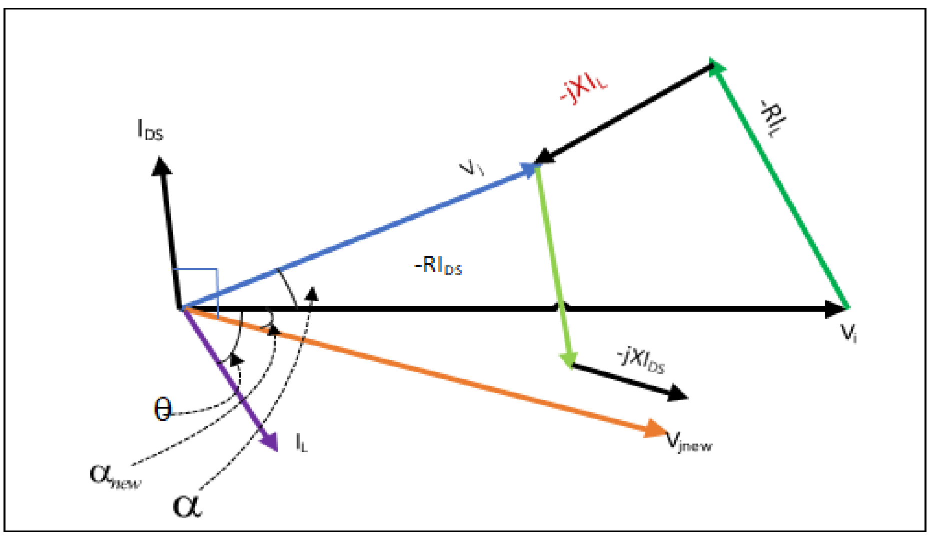

Figure 2.8: Voltage & Current Phasor diagram representation of D-STATCOM integration

The vector diagram of two buses of a distribution system after integration of D-STATCOM is shown in Figure 2.8 and the relation between voltage and current is given in equation (2.7).

$$V_{jnew}\angle\alpha_{new} = V_i\angle\delta(R_L + jX_L)\{I_L\angle\theta(R_L + jX_L) + I_{DS}\angle(\alpha_{new} + \frac{\pi}{2})\} \quad (2.5)$$

Where; V_{jnew} : voltage of J bus after integration of DSTATCOM; $V_i\angle\delta$: voltage of bus I.

$I_L\angle\theta$: Current flow in the line; $I_{DS}\angle(\alpha_{new} + \frac{\pi}{2})$: injected current by DSTATCOM.

The current I_L and I_{DST} flow simultaneously line/branch after installation of DSATCOM in the (j) bus. The reactive power injected by DSTATCOM for mitigation of the system voltage, such as the correction voltage, at bus (j) till V_{jnew} is given:

$$I_{DSTATCOM} = (V_{jnew}\angle\alpha_{new})\{I_{DSTATCOM}\angle(\frac{\pi}{2}+\alpha_{new})\} \tag{2.6}$$

The angle changes and the current injected by DSTATCOM will be zero when the voltage is equal after and before the integration of DSTATCOM, i.e., V_j=V_{jnew}. Mathematically, as boundary condition, it is represented as:

$$V_{jnew} = V_j \Rightarrow \begin{cases} I_{DSTATCOM} = 0 \\ \alpha_{new} = \alpha \end{cases} \tag{2.7}$$

Separating imaginary and real part of equation (2.5) we can get:

$$\begin{cases} V_{jnew}\cos\alpha_{new} = real(ZI_L\angle\theta) - RI_{DS}\cos(\alpha_{new}+\frac{\pi}{2}) + XI_{DS}\sin(\alpha_{new}+\frac{\pi}{2}) \\ V_{jnew}\sin\alpha_{new} = imag(ZI_L\angle\theta) - XI_{DS}\cos(\alpha_{new}+\frac{\pi}{2}) - RI_{DS}\sin(\alpha_{new}+\frac{\pi}{2}) \end{cases} \tag{2.8}$$

Let as use notation

$$T = real(V_i\angle\delta) - real(ZI_L)\ ;\ E = imag(V_i\angle\delta) - imag(ZI_L)\,;$$

$$w = -R; w_1 = -X; A = |V_{jnew}|; h = |I_{DS}|; x = \alpha_{new}$$

Substitute variables and constants in the above equations (2.8).

$$\begin{cases} A\cos x = T - wh\sin x - w_1h\cos x \\ A\sin x = E - w_1h\sin x + wh\cos x \end{cases} \tag{2.9}$$

T, E, w & w_1 are constants so calculating variables x, h, from equation (2.9). Calculate equation (2.10).

$$h = \frac{A\cos x - T}{-wh\sin x - w_1h\cos x} = \frac{A\cos x - E}{w_1h\sin x + wh\cos x} \tag{2.10}$$

Equating the above equation (2.10) and taking Y=sin(x), and rearrangement is equation (2.11).

$$[(Tw_1 - Ew)^2 + (Tw - Ew_1)^2]Y^2 + 2(Tw_1 - Ew)AwY + A^2w^2 - Tw + Ew_1 = 0 \tag{2.11}$$

Let's assume m = Tw_1-Ew and m_1 = Tw-Ew_1 so, equation (2.11) changes to

$$(m^2 + m_1^{\,2})Y^2 + 2(Amw)Y + (A^2w^2 - m_1) = 0 \tag{2.12}$$

The equation (2.16) is a quadratic equation with variable Y so the solution is given as

$$Y = 2Amw \pm \sqrt{\frac{(2Amw)^2 - 4(m^2 + m_1{}^2)(A^2w^2 - m_1{}^2)}{2(m^2 + m_1^2)}} \tag{2.13}$$

Consider the load flow result, from equation (2.13) are explain under the following boundary conditions.

If $A = V_{jnew} = V_j$ then $I_{DS} = 0$ and $\alpha_{new} = \alpha$ after testing the condition on load flow results, the correct answer selected is equation (2.17). Finally, variables are computed.

The voltage phase angle is $\alpha_{new} = x = \sin^{-1}(Y)$

The voltage, reactive power, and current injected at bus j are calculated as follows.

$$\begin{cases} V_{jnew} = |V_{jnew}| \angle \alpha_{new} \\ I_{DST} = |I_{DST}| \angle(\alpha_{new} + \frac{\pi}{2}) = h\angle(\alpha_{new} + \frac{\pi}{2}) \\ jQ_{DS} = V_{jnew} I_{DST}{}^* \end{cases} \tag{2.14}$$

The injected voltage at bus ‘j’ is given by equation (2.14), the current through DSTATCOM and reactive power injected by DSTATCOM can be found from equation (2.14) (Bikash, Aashish, Jalpa H., & Mohan, 2022).

2.8. Literature Review

(Prashant, Anwar, Sarwar, Ahmed, & Sherif, 2022) “Optimal location and sizing of distribution generator in power system network with power quality enhancement using fuzzy logic-controlled D-STATCOM”. This research presents the location and sizing selection of multiple distributed generators for boosting performance of the radial distribution system in the case of constant power and constant impedance load flow. The selection of DG and D-STATACOM location is decided in this article in terms of real power loss, accuracy, and sensitivity. The positioning and sizing of DG and D-STATCOM are analyzed with the genetic algorithm and the heuristic probability distribution method. The proposed analytical approach for the system is tested on the IEEE33 bus system. As a result, the author concluded that, the performance of the system with genetic algorithm give better solution in comparison to heuristic PDF for determining the optimal location and sizing of DG and D-STATCOM. However, the distribution network load flow analysis base system does not consider the optimal placement and sizing of DG and D-STATCOM in the IEEE33 bus for constant power and constant impedance load flow. Since load demand is fixed for all buses, selection of bus for DG and D-STATCOM placement and sizing is assessed in terms of minimum real power loss, improved accuracy and improved sensitivity factor by integration of DG and D-STATCOM.

(Khan, et al., 2022) The research used four types of DGs, such as type-1: only contribute to the real power, type-2: only compensate the reactive power, type-3: contribute both active and reactive power, and type-4: contribute active power but consume reactive power in the system were used during the whole optimization process. These algorithms were deployed to find the optimum DG values from the combination of random DG population. Honey badger algorithm (HBA) was used to size the DGs optimally in IEEE 33-bus and 69-bus power distribution test bench systems to boost the overall voltage profile and stability by minimizing the power losses in a system. The results of the simulation the power losses are reduced and voltage profile and stability improvement are observed. However, researchers are used four different types of DG to reduce the power loss, voltage profile and stability improvement. But not analyzed which combination of DG most efficient to minimize power loss and improve voltage more to test IEEE-33 and 69 bus system.

(Muhammad, Syed, & Omar, 2022)"A novel hybrid optimization-based algorithm for the single and multi-objective achievement with DG allocations in distribution networks" The research proposed distribution generation allocation problem focuses on three objectives that is reduction of real power loss, minimization of voltage deviation and maximization of voltage stability indices. Case studies of the research are simulated with IEEE 33-bus and IEEE 69-bus test system, for optimal allocation of DG units by considering different power factor. This work considered various power factors of DG which is unity PF, 0.95 PF and optimal PF for DG allocation. To examine the effect of the PF of DG on the power loss reduction, optimum DG sitting and sizing with optimal power factor are carried out utilizing the established method. However, this research did not identify the types of DG system. The payback period of the DG connection in distribution network are not analyzed.

(S.Balakumar, Akililu, Samuel, & K.Bamash, 2021) "Improvement of Voltage Profile and Loss Reduction in Distribution Network Using Moth Flame Algorithm: Wolaita Sodo, Ethiopia" The researcher can be solving the problem of voltage stability and line loss in distribution network use algorithm to determine the appropriate location and size of Static Var compensator (SVC) are Moth Flame Optimization and Particle Swarm Optimization. The objective function of the research is defined to minimize the voltage deviation and power loss. The results were checked with the aid of MATLAB software on Wolaita Sodo radial distribution network of 34 bus data. The results obtained from the test system were compared with the result of MFA and PSO. This comparison was done to know the computational time of proposed techniques. The performance of the MFA based SVC was superior in distribution system and highlighted the importance of device. As a result, MFO algorithm is used in this article to find the optimum location, size and SVC units to improve the voltage profile and minimize the power loss in Wolaita Sodo distribution of the 34-bus system. However, the research is doing not include Multiple SVC system and did not consider the dynamism of control, harmonic distortion and space requirement of SVC. The cost effectiveness of SVC integration in distribution system is not analyzed.

(Kallon, Nyakoe, & Muriithi, 2021) "Development of D-STATCOM Optimal Sizing and Location Techniques Based on IA-GA for Power Loss Reduction and Voltage Profile Enhancement in an RDN" The author considers the increasing of voltage drop and power loss in the radial distribution network. As a result, the author proposes to minimize voltage drop and power loss use D-STATCOM by IA-GA optimization. The research uses an innovative technique based on hybridized Immune and Genetic Algorithm for optimal D-STATCOM placement and sizing for three distinct load levels (light, medium, and peak loads) is proposed. Simulation and analysis of the proposed algorithm were carried out using IEEE-33 bus radial distribution network in MATLAB. The simulation results show decrease in power loss and improve voltage profile. The author compares the existing approaches with the proposed method. As a result, the proposed method produces better outcomes.

(Saad & Abdeljabbar , 2020) "An Improved Backward/Forward Sweep Power Flow Method Based on a New Network Information Organization for Radial Distribution Systems" The researchers present unlike transmission systems, the conductors used in distribution networks are characterized by high R/X ratio and a radial structure with large number of nodes, branches, and complex topology configuration. Due to this load flow analysis use Jacobian-based methods such as Newton-Raphson, Gauss-Seidel, and Fast-decoupled methods are failed with such network. Jacobian-based methods for load flow analysis were not appropriate to solve practical problem in distribution network. The author shows the prefer method for load flow analyzing in distribution system is backward/forward sweep approach. Backward/forward sweep approach is powerful computational time and convergence.

(Tanish, Srijan, & Tajender, 2022)“Load flow Analysis Using Forward and Backward Sweep, and Minimizing Power Losses Using Genetic Algorithm” The author presents a backward/forward sweep method to solve to analyses the load flow in radial system. The R/X ratios of distribution system having radial structure are high. Newton-Raphson and fast decoupled methods are failed with distribution system. The proposed method is one of the most effective methods for load-flow analysis of the radial distribution system.it is easy to implement and there is no needs of complex renumbering of branches and nodes, or any matrix calculation. This method uses only the linear equations based on Kirchhoff’s formulation and is used to determine power losses for each bus branch and voltage magnitude for each node.

The reviewed literature presents various methods for the optimal allocation and sizing of Distributed Generation (DG) and Distribution Static Compensator (D-STATCOM) to address power loss and voltage drop issues in distribution feeders. However, these research have certain limitations often employ single-objective function optimization without considering multi-objective, and the values of weighting factors for multi-objective functions were based on theoretical assumptions, rather than a systematic approach, they fail to consider both real and reactive power loss, as well as other associated constraints; in the optimization process, and there is a lack of comprehensive cost analysis after the integration of DG, D-STATCOM, SVC, and STATCOM.

This study aims to address the gaps identified in the previous works. The key contributions of this study include developing a multi-objective optimization function that considers both real and reactive power loss reduction, as well as voltage deviation; incorporating an economic impact analysis of DG and D-STATCOM integration; and addressing system constraints in the Whale Optimization Algorithm (WOA) simulation. Moreover, this research explores the integration of DG and D-STATCOM in a distribution network, with the dual objectives of power loss minimization and voltage profile improvement.

CHAPTER THREE

3. Material and Methods

3.1. Introduction

Ethiopian distribution system mostly, outgoing feeder is 15kV, and feeders are connected radially. Mostly them 15kV feeders are used to feed up to 80 distribution transformers (Abayneh, 2022). this study, a 15kV feeder feeds up to 106 distribution transformers. Awash Melkas distribution, transformers are used to step down the voltage on the feeders to a utilization voltage of 380 volts three-phase or 220 volts single-phase. The power (F-5 feeder) is delivered to the small rural towns of Dera, Etaya, Huruta, and Srie. Section 3.1 presents an introduction; Section 3.2 presents materials, section 3.3 present methodology, section 3.4 present data collection; Section 3.5 discusses modeling and analysis of the Awash Melkasa distribution system.

Load flow analysis is presented in Section 3.6; section 4.7 present resource feasibility of distribution generation; section 3.8 discusses comparison of DSTATCOM and STATCOM; section 3.9 presents power flow analysis of radial distribution system; section 3.10 presents optimal placement and sizing of DG and DSTATCOM; section 3.11 discusses whale optimization algorithm; section 3.12 presents problem formulation and multi-objective function, and proposed work implementation discussed in section 3.13.

3.2. Materials

Software used in this thesis study includes Math Type 7.8, Microsoft Office 2019, Visio 2019, and MATLAB/2021a. A computer program called MATLAB is utilized as a programming language to write algorithm code. Microsoft Office is used for editing the thesis documentation. Math Type 7.0 is used to write mathematical equations and formulas, while Visio is utilized to create the diagrammatical model of the feeder.

3.3. Methods

Different methods which used for accomplish this thesis work is showed in Figure 3.1 and general explanation in below section.

Literature Review: First, a comprehensive review of the literature on distribution systems performance enhancement was done. This review looked at several journals, books, documents, and theses.

We looked at the theoretical explanations of distribution static compensator (D-STATCOM) and distributed generation (DG). Models of these compensating devices were also investigated for possible integration into load flow analysis.

Data collection and analysis: Various input data required for the modeling of the feeder and formation of optimization problem were gathered from the Ethiopia Electric Utility (EEU), Adama district.

Modeling and Optimization Problem Formulation: The modeling of the selected feeder has been conducted based on the obtained data. Additionally, the modeling of the photovoltaic distributed generator (PV-DG) and the static model of the distribution static compensator (D-STATCOM) have also been realized.

Computer Simulation: The simulation was carried out using MATLAB/programming version 2021a. The purpose of this simulation was to determine the optimal location and size of the compensating devices, as well as to analyze the system performance before and after the integration of these devices.

Finally, a comparative analysis was performed to determine the most effective method for enhancing distribution system performance. This analysis compared three scenarios: (1) only DG integration, (2) only D-STATCOM integration, and (3) simultaneous DG and D-STATCOM integration.

Conclusion: Based on the comprehensive analysis and simulation outcomes, a conclusion was formulated. This conclusion summarizes the key findings from the comparative analysis.

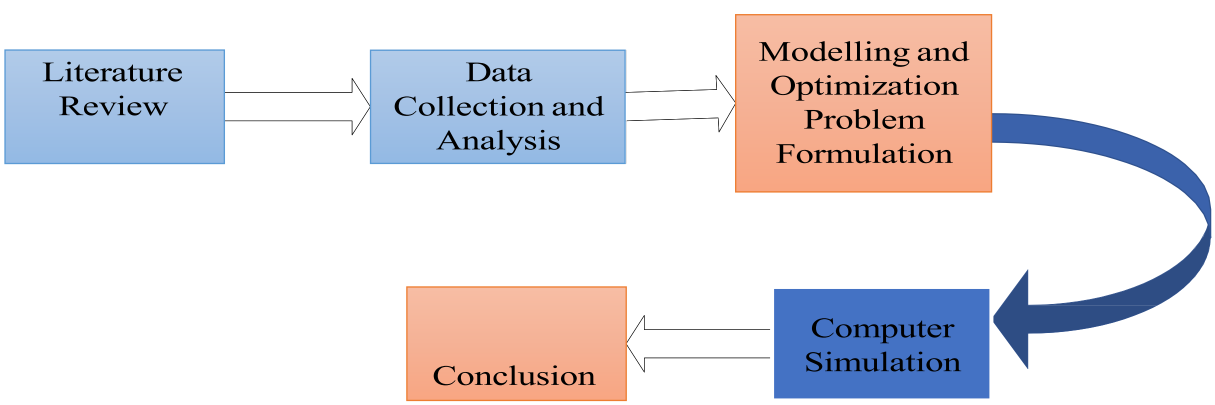

Figure 3.1: Block diagram of the thesis methodology

3.4. Data Collection

The necessary data for this thesis has been gathered from Awash Melkasa distribution substation, Dera customer service center, from Adama district Ethiopian electric utility (EEU) and Engineering office of Ethiopian electric power (EEP). The secondary data have been gathered from past recorded of feeders from both institutions.

- loading (peak load) data of the substation,
- interruption data of the feeder,
- The line data, the bus data, type conductor and size.
- Rout of the feeder and rating of distribution transformer.

Awash Melkasa substation have only one 132 kV incoming feeders, from Awash hydropower station and five 15 kV and three 33 kV outgoing feeders. There are two power transformers capacity of 31 MVA and 25 MVA, which step dawn into 33kV and 15 kV feeders respectively.

- F-01, supply 15kV to the small town near to Awash Melkasa.
- F-02, and F-03, supply 15kV to the Wenji sugarcane irrigation.
- F-04, supply 15kV to the Awash sulphate production factory
- F-05(Dera), supply 15 kV to partially (Dera city, etaya city), and totally cover (Huruta city, Seriy city and the end site Koshim city).
- Amude, supply 33kV to rural small city.
- Industry 1, supply 33kV to the SUNSHINE industry.
- Industry 2, supply 33kV to the ANTENXS industry.

Feeder 01 is distributing electric power in Awash Melkasa city while nearby areas. Industry 1, industry 2 and feeder 04 feeders are fixed line supply to industry. Thus, Feeder 02 and feeder 03 are distribute electric power to Awash sugarcane irrigation. Also, there is no sufficient data for analysis. Therefore, feeder 05 is selected for analysis and mitigation of their power loss and voltage profile. Depend on the following reason feeder five is selected for the study.

- Long distance coverage
- high-power interruption and
- High power demand

Distributed electric power for residential, commercial, and factories and also some are as which have sensitive loads that cause for distribution feeder affected by power loss and voltage drop.

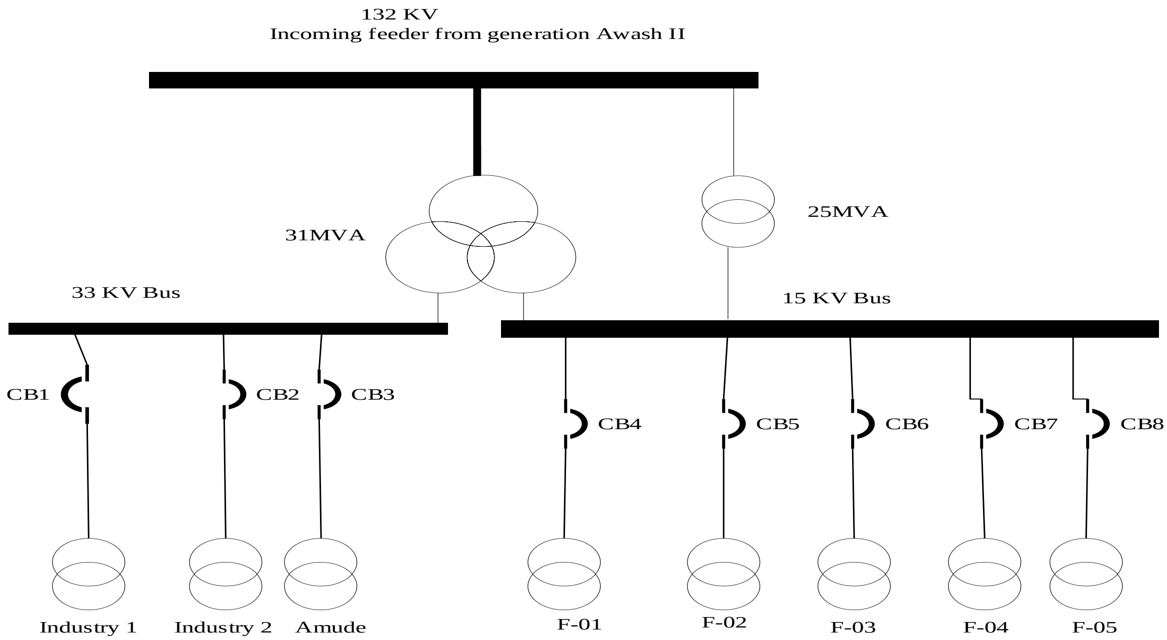

Figure 3.2: Single line diagram of Awash Melkasa substation

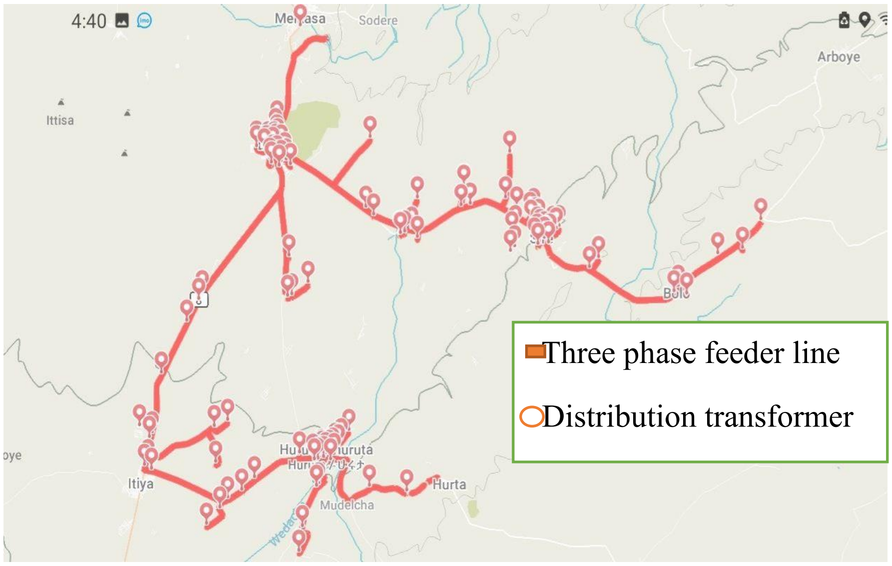

Figure 3.3: the coverage area of F-5 feeder

Table 3.1: Feeder name, bus bar voltage, and length of Awash Melkasa substation feeders (Appendix-A1)

Feeder Name	Bus bar voltage (kV)	Length (KM)	Total interruption frequency from 2013-2015 E.C	Peak load (mw) 2014E.C
F-01	15	6.836	76	1.67
F-02	15	11.568	213	0.89
F-03	15	4.886	371	1.44
F-04	15	97.637	1252	4.22
F-05	15	163.975	1892	6.32
Amude	33	91.437	970	1.46
Industry 1	33	38.645	841	5.55
Industry 2	33	38.645	326	4.37

The following facts observed during data analysis led to the selection of the F-5 feeder for this case study from the 15 kV Awash Melkasa substation power distribution feeders.

- Increased power consumption.
- Distribution lines are quite long.
- High power interruption rate.

3.5. Overhead Distribution Line Impedance Calculation

The distribution line configuration arrangement can affect the impedance of the line especially the inductance of the line. There are different configurations styles exist. But the selected distribution feeder line has a triangular configuration as shown below in figure (3.4.) Conductors are arranged at equal distance between them.in each phase flux linkage and inductance are the same. If current in the conductor are balanced, the impedance of the conductor is symmetrical.

The inductance would be different, resulting in unequal voltage drops in the three phases. As a result, voltage at end of line will be different for each step. To ensure the voltage drop is equal in all conductors, the common practice is arranging the conductor symmetrically or exchange location of conductor at regular interval.

Overhead line of F-05 distribution feeder from Awash Melkasa substation to end users. Dera F-5 distribution line use four type of all aluminum conductors (AAC) at primary distribution network. The primaries of distribution feeder conductor size are connected by $AAC_{95}mm^2$, AAC_{50} mm^2, $AAC_{35}mm^2$and AAC_{25} mm^2.

The impedance of the conductor used in the power distribution system depends upon the material, dimensions, and configuration of the wires and length with the spacing between them. The conductors that are used in Awash Melkasa distribution feeders are stranded conductors and 50 Hz frequency also applied for calculating the inductive reactance.

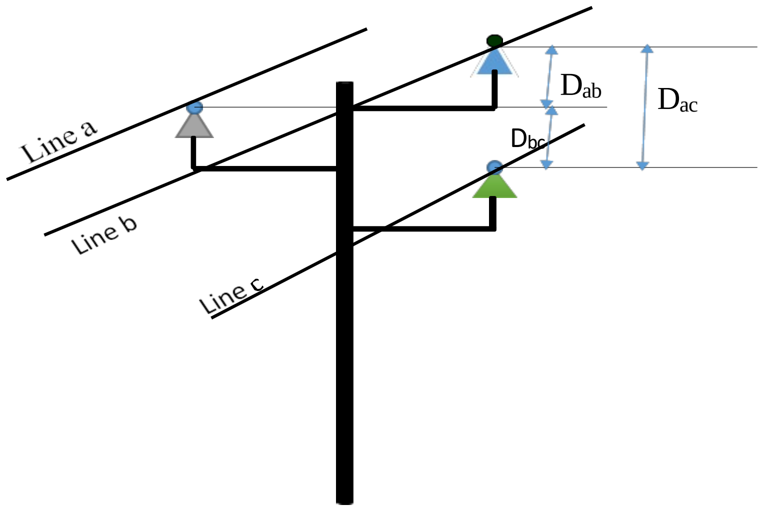

Figure 3.4: overhead distribution line of distribution system *(Abayneh, 2022)*

$$Z_a = R_a + j0.06283\ln\left(\frac{D}{GRM_a}\right)\frac{\Omega}{km} \tag{3.1}$$

$$D = \sqrt[3]{\left(D_{ab} * D_{bc} * D_{ac}\right)} \tag{3.2}$$

Since the conductors that are used in distribution feeders are stranded conductors. For stranded conductors, the GMRa is given by:

$$GMR_a = k * r \tag{3.3}$$

Where: GMR_a =Geometric mean ratio of conductor

k = the GMR factor, r = actual conductor radius

Z_a = impedance of conductor a in Ω/km, R_a = resistance of conductor i in Ω/km$D$=distance between conductors in meter, Dab=Separation distance (in meter) of conductors a and b, Dbc= Separation distance (in meter) of conductors b and c and Dac= Separation distance (in meter) of conductors a and c. Based on Table 3.1, the impedance of the conductor can be evaluated as the following: For AAC_{50}, AAC_{35}, AAC_{25} and AAC_{95} conductor type. The positive sequence impedance for AAC_{50} can be calculated using equation (3.1) as follow.

Table 3.2: Overhead conductor parameters used in the feeder (Appendix-B)

Conductor Type	Conductor size (mm^2)	Number of wires	Overall diameter of conductor (mm)	Actual diameter (mm)	Resistance (Ω/km)
AAC	25	7	6.3	5.56	1.18080
AAC	35	7	7.5	6.864	0.83320
AAC	50	7	9	7.9377	0.57860
AAC	95	19	12.5	10.897	0.30840

Table 3.1: GMR Factor (k) and Strand Relationship for AAC conductor

Standard	GMR factor, k
7	0.7256
19	0.7577
37	0.7678
61	0.7722

Using equation 3.1, Table 3.1 and table 3.2 the following results are obtained.

$$\begin{cases} Z_a = R_a + j0.062832\ln\left(\dfrac{D}{GMR_a}\right)\Omega/km \\ Z_{50} = 0.5785 + j0.062832\ln\left(\dfrac{0.72135}{0.00288}\right)\Omega/km \\ Z_{25} = 1.181 + j0.062832\ln\left(\dfrac{0.72135}{0.00202}\right)\Omega/km \\ Z_{35} = 0.9669 + j0.062832\ln\left(\dfrac{0.72135}{0.00249}\right)\Omega/km \end{cases}$$

Table 3.3: Overhead conductors positive sequence impedance

Type of Conductor	Resistor (Ω/km)	Reactance (Ω/km)	Impedance (Ω/km)
AAC_{25}	1.181	0.736	1.181 + j0.3736
AAC_{35}	0.9669	0.3561	*0.9669 + j0.3561*
AAC_{50}	0.5785	0.3470	*0.5785 + j0.3470*
AAC_{95}	0.3085	0.3244	*0.3085 + j0.3244*

The line segments total positive sequence impedances are obtained by multiplying the impedance perkilometer by its length as tabulated in Table 3.3. Since the distribution lines are relatively short, the shunt admittance of overhead lines is neglected.

Table 3.3 Awash Melkasa substation 15kv feeder line data and bus data of Dera feeder (F-5) (Appendix-B1)

Bus data						Line data	
From bus	To bus	Length (km)	Conductor type	R(Ω)	X(Ω)	Active power(mw)	Reactive power(kvar)
1	2	4.962	AAC50	2.870517	1.721814	0	0
2	3	0.55	AAC50	0.31817	0.19085	0.16	0.12
3	4	0.48	AAC50	0.27768	0.16656	0.16	0.12
4	5	0.43	AAC50	0.393355	0.155594	0.16	0.12
5	6	0.38	AAC50	0.21983	0.13186	0.04	0.03
6	7	0.17	AAC50	0.098345	0.5899	0.252	0.189
7	8	0.19	AAC50	0.109915	0.06593	0	0
8	9	0.24	AAC50	0.13884	0.08328	0	0
9	10	0.42	AAC50	0.24297	0.14574	0	0
10	11	0.044	AAC50	0.025454	0.015268	0.16	0.12
11	12	0.65	AAC50	0.376025	0.22555	0.6	0.12

12	13	0.25	AAC50	0.144625	0.08675	0.08	0.06
13	14	1.6	AAC50	0.9256	0.5552	0	0
14	15	8.8	AAC50	5.0908	3.0536	0.04	0.03
15	16	0.55	AAC50	0.318175	0.19085	0.04	0.03
16	17	1.7	AAC50	0.98345	0.5899	0.08	0.06
17	18	3.8	AAC50	2.1983	1.3186	0.02	0.015
18	19	4.1	AAC50	2.37185	1.4227	0	0
19	20	0.45	AAC50	0.260325	0.15615	0.04	0.03
20	21	1.1	AAC50	0.6363	0.3817	0.08	0.06
21	22	2.4	AAC50	1.3884	0.8328	0.16	0.12
22	23	0.39	AAC50	0.225615	0.13533	0.04	0.03
23	24	0.48	AAC50	0.27768	0.16656	0.08	0.06
24	25	0.16	AAC50	0.09256	0.05552	0.08	0.06
25	26	0.605	AAC35	0.363587	0.210254	0.02	0.015
26	27	5.4	AAC50	3.1239	1.8738	0.08	0.06
27	28	0.39	AAC50	0.225615	0.13533	0.04	0.03
28	29	1.2	AAC50	0.6942	0.4164	0.04	0.03
29	30	1.2	AAC50	0.6942	0.4164	0	0
30	31	3.8	AAC50	2.1983	1.3186	0	0
31	32	1.1	AAC50	0.6942	0.3817	0.04	0.03
32	33	0.31	AAC50	0.179335	0.10757	0.08	0.06
33	34	0.43	AAC50	0.248755	0.14921	0.04	0.03
34	35	0.28	AAC50	0.16198	0.09716	0	0
35	36	0.15	AAC50	0.86775	0.05205	0.252	0.189
36	37	0.29	AAC50	0.167765	0.10063	0.02	0.015

37	38	0.058	AAC50	0.033553	0.020126	0.252	0.189
38	39	0.27	AAC50	0.156195	0.09369	0.08	0.06
7	40	0.39	AAC50	0.225615	0.13533	0.16	0.12
40	41	0.26	AAC50	0.15041	0.09022	0.252	0.189
41	42	0.46	AAC50	0.26611	0.15962	0.04	0.03
42	43	0.81	AAC50	0.468585	0.28107	0.02	0.015
43	44	0.2	AAC50	0.1157	0.0694	0.08	0.06
44	45	0.74	AAC50	0.42809	0.25678	0.252	0.189
8	46	0.15	AAC50	0.086775	0.05205	0.04	0.03
46	47	0.3	AAC50	0.17355	0.1041	0	0
47	48	0.58	AAC50	0.33553	0.20126	0.08	0.06
48	49	0.35	AAC50	0.202475	0.12145	0.252	0.189
49	50	0.57	AAC50	0.329745	0.19779	0.252	0.189
50	51	0.11	AAC50	0.063635	0.03817	0	0
51	52	8.2	AAC50	4.7437	2.8454	0.16	0.12
52	53	2.9	AAC50	1.67765	1.0063	0.02	0.015
53	54	0.86	AAC50	0.49751	0.29842	0.252	0.189
54	55	2.3	AAC50	1.33055	0.7981	0.04	0.03
55	56	0.46	AAC50	0.26611	0.15962	0.02	0.015
56	57	1	AAC50	0.5785	0.347	0	0
57	58	3.4	AAC95	1.0489	1.10296	0.04	0.03
58	59	0.12	AAC95	0.03702	0.038928	0.08	0.06
59	60	0.69	AAC50	0.399165	0.23943	0	0
60	61	2.4	AAC50	1.3884	0.8328	0.08	0.06
61	62	1.5	AAC50	0.86775	0.05205	0.04	0.03

62	63	0.23	AAC50	0.133055	0.07981	0.08	0.06
63	64	0.83	AAC50	0.480155	0.28801	0.02	0.015
64	65	0.34	AAC50	0.19669	0.11798	0.08	0.06
65	66	0.38	AAC50	0.21983	0.13186	0.16	0.12
66	67	0.65	AAC50	0.376025	0.22555	0.04	0.03
67	68	0.31	AAC35	0.179335	0.10757	0.252	0.189
68	69	0.59	AAC50	0.341315	0.20473	0.16	0.12
69	70	0.53	AAC50	0.306605	0.18391	0.08	0.06
70	71	3.7	AAC50	2.14045	1.2839	0.04	0.03
9	72	0.16	AAC50	0.09256	0.05552	0.04	0.03
72	73	6.6	AAC50	3.8181	2.2902	0.04	0.03
73	74	0.038	AAC50	0.021983	0.013186	0.02	0.05
13	75	0.42	AAC50	0.24297	0.14574	0.16	0.12
75	76	1.2	AAC50	0.6942	0.4164	0.08	0.06
76	77	3.3	AAC50	1.90905	1.1451	0.02	0.015
77	78	2.3	AAC50	1.33055	0.7981	0.04	0.03
19	79	2.1	AAC50	1.21485	0.7287	0.04	0.03
79	80	0.28	AAC50	0.16198	0.09716	0.16	0.12
80	81	0.51	AAC25	0.295035	0.12697	0.08	0.06
30	82	0.43	AAC50	0.60231	0.190536	0.02	0.015
82	83	4.5	AAC95	1.38825	1.4598	0.04	0.03
83	84	3	AAC95	0.9255	0.9732	0.02	0.015
84	85	0.19	AAC95	0.058615	0.061636	0.04	0.03
85	86	1.4	AAC95	0.4319	0.45416	0.04	0.03
31	87	7.3	AAC50	4.22305	2.5331	0.04	0.03

87	88	0.64	AAC50	0.37024	0.22208	0.08	0.06
88	89	1.3	AAC50	0.75205	0.4511	0.08	0.06
89	90	0.66	AAC50	0.38181	0.22902	0.16	0.12
90	91	1.8	AAC50	1.0413	0.6246	0.08	0.06
35	92	0.21	AAC50	0.121485	0.07287	0.08	0.06
92	93	2.1	AAC50	1.21485	0.7287	0.08	0.06
93	94	0.24	AAC50	0.13884	0.08328	0.04	0.03
94	95	2.9	AAC50	1.67765	1.0063	0.04	0.03
95	96	2.7	AAC50	1.56195	0.9369	0.04	0.03
47	97	0.026	AAC50	0.015041	0.009022	0.16	0.12
97	98	0.18	AAC50	0.10413	0.06246	0.02	0.015
98	99	0.012	AAC50	0.006942	0.004164	0.252	0.189
99	100	0.11	AAC50	0.063635	0.03817	0.504	0.378
51	101	0.4	AAC50	0.2314	0.1388	0.252	0.189
101	102	0.4	AAC50	0.2314	0.1388	0.252	0.189
102	103	5.93	AAC50	3.430505	2.05771	0.02	0.015
103	104	2.87	AAC50	1.660295	0.99589	0.08	0.06
104	105	0.31	AAC50	0.179335	0.10757	0.252	0.189
58	106	0.45	AAC50	0.260325	0.156656	0.08	0.06
106	107	0.48	AAC50	0.27768	0.16656	0.16	0.12
107	108	0.53	AAC50	0.306605	0.18391	0.08	0.06
108	109	0.34	AAC50	0.19669	0.11798	0.16	0.12
109	110	0.06	AAC50	0.03471	0.02082	0.16	0.12
110	111	0.006	AAC50	0.003471	0.002082	0.16	0.12
111	112	4.4	AAC50	2.5454	1.5268	0.16	0.12

60	113	1.3	AAC50	0.75205	0.4511	0.04	0.03
113	114	0.01	AAC50	0.005785	0.00347	0.16	0.12
114	115	0.52	AAC50	0.30082	0.18044	0.16	0.12
115	116	3	AAC50	1.7355	1.041	0.08	0.06
116	117	1	AAC50	0.5785	0.3470	0.08	0.06
117	118	0.53	AAC50	0.306605	0.18391	0.16	0.12

3.6. Modeling of Awash Melkasa Radial Distribution Network

3.6.1 Single Line Diagram of Distribution Network

A single-line diagram is a visual representation where loads are connected to the network. Transmission (distribution) lines and machinery of an electrical system are connected using a single-line model and standard symbols (Argaw, 2021). It is helpful for operators to determine the electrical placement of various devices and components and is used for maintenance tasks and tracking the location of faults. A distribution diagram for an MV and LV system should clearly show the main, sub-main, and distribution panel boards together with a symbol-based representation of the network's loads. it shows the location and connections of the static load, circuit breaker, generator, transformer, and transmission line (Ayman, 2022).

Figure (3.5) shows the Awash Melkasa radial distribution substation feeder 5. It has 117 branches and a 118-bus system. There are 106 transformer loads and 12 common connecting nodes from 118 buses. Every bus has a unique voltage level and both active and reactive power in the feede

Figure 3.5: Sigle line diagram of Awash Melkasa (F-5) distribution feeder

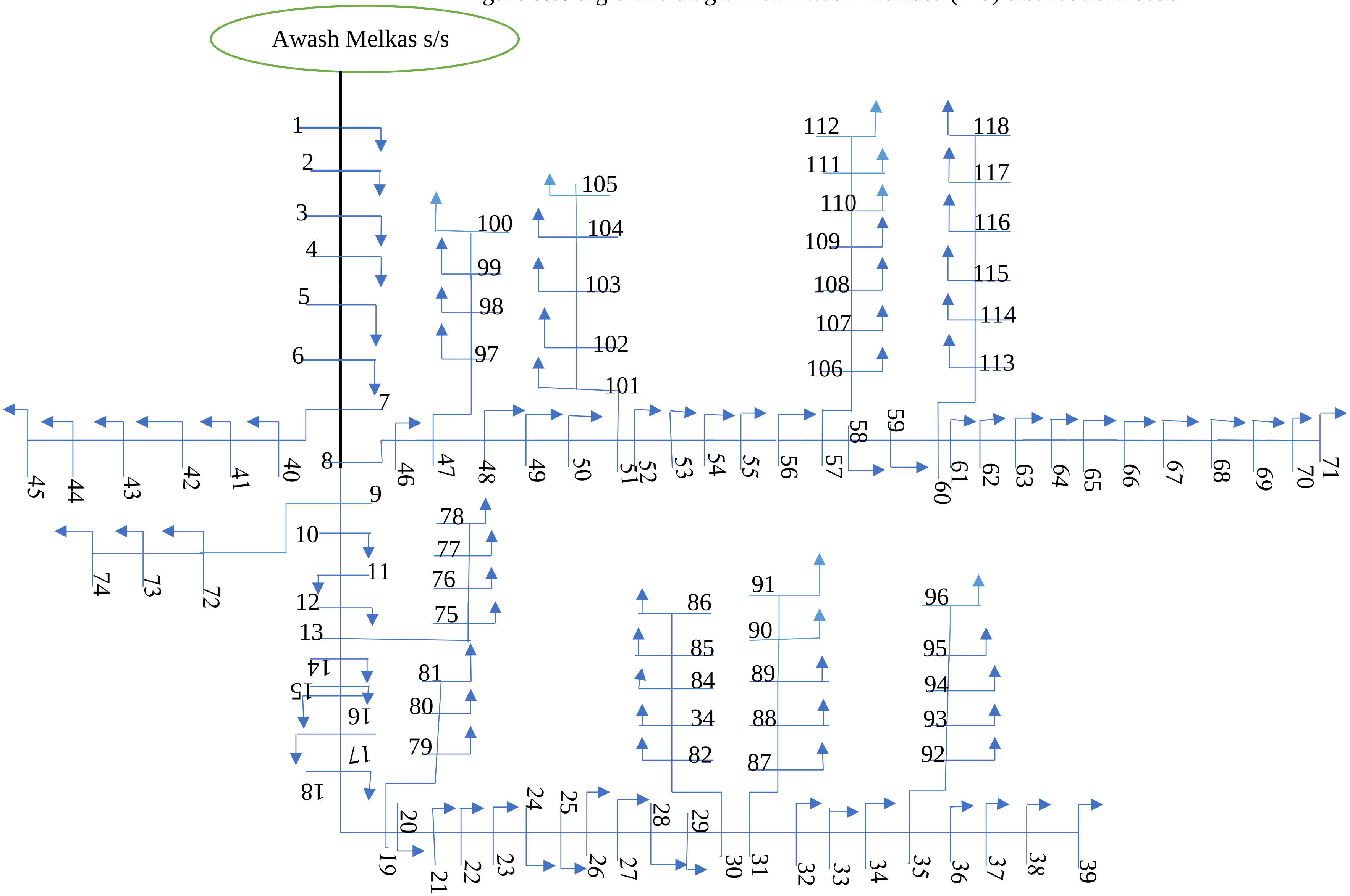

3.6.2. Per-Unit Value of Distribution Network

A per-unit system is a mathematical technique that expresses quantities about a selected base value, which is used in power engineering to normalize and simplify electrical computations. It helps ev aluate and contrast electrical systems, apparatus and component. All reactance within this particular system has the capacity to be articulated in either percentage or per unit terms. A minimum of four fundamental quantities is deemed necessary to fully characterize a per-unit framework: namely volt-amperes, voltage, current, and impedance (Asghar, 2024).

$$per-unit = \frac{actual\ quantity}{base\ value\ of\ \ quantity} \tag{3.4}$$

In order to define a per-unit system, it is crucial to determine the parameters of voltage, current, power, and impedance as follows (Asghar, 2024).

$$I_{pu} = \frac{I_{actual(Amps)}}{I_{Base}(Amps)} = \frac{I}{I_B},\ V_{pu} = \frac{V_{actual(Volts)}}{V_{Base}(Volts)} = \frac{V}{V_B}, \tag{3.5}$$

$$S_{pu} = \frac{S_{actual(VA)}}{S_{Base}(VA)} = \frac{S}{S_B},\ Z_{pu} = \frac{Z_{actual(Ohm)}}{Z_{Base}(Ohm)} = \frac{Z}{Z_B} \tag{3.6}$$

The evaluation of any two of the four specified base values, that is v_{base}, I_{base}, S_{base} and Z_{base}. The two base values can be calculated based on their fundamental circuit relationships. Based on the given base values calculated impedance and current under equation 3.7 (Asghar, 2024).

$$I_{base} = \frac{S_{base}}{V_{base}},\ Z_{base} = \frac{V_{base}^2}{S_{base}} \tag{3.7}$$

The apparent power and system voltage base values used for this thesis are appropriate parameters. V_{base}=15 a KV and S_{base}=100 an MVA. The predetermined base value of the power distribution system, calculated by equation 3.7 above, sets the base values of current and impedance.

$$I_{base} = \frac{S_{base}}{V_{base}} = \frac{100MVA}{15KV} = 6.667KA,\ Z_{base} = \frac{V^2{}_{base}}{S_{base}} = \frac{(15KV)^2}{100MVA} = 2.25\Omega$$

The base values of load power and system voltage are known in this thesis. A known quantity is applied to calculate the network's base values for current and impedance. Thus, the real and reactive load at each bus in the radial distribution network can be expressed as a per-unit value using the following formula.

$$\begin{cases} Bus\ real\ \ power = \dfrac{\mathrm{Re}\,al\ load\ value}{base\ MVA} \\ Bus\ reactive\ \ power = \dfrac{\mathrm{Re}\,active\ load\ value}{base\ MVA} \end{cases} \tag{3.8}$$

3.6.3 Description of Proposed Distribution Feeder

Data provided by Adama district design and planning office, operation office of EEU and Awash Melkasa distribution substation. Feeder-5 (the Dera feeder) is the selected feeder. Awash Melkasa substation connected to F-5 feeder, it travels 163.95 kilometers.

All of the system's buses have loads linked to them outside of the root node. Due to the non-linear loads in the residential, commercial, and industrial sectors, the voltage on this network drops below the standard level on the distribution bus system. Table 3.2 displays an overview of all the data that was gathered in the test system. The total of all the loads in the radial distribution system, including active and reactive, are as follows:

$$\begin{cases} TPL\left(KW\right) = \sum_{m}^{nb} PL\left(m\right) \\ TQL\left(KVAr\right) = \sum_{m}^{nb} \left(m\right) \end{cases} \tag{3.9}$$

Where; m=1, 2, 3………nb and nb is number of bus

Table 3.4: proposed distribution feeder description

Description	Feeder-5(Dera) RDN
Number of lateral lines	117
Number of bus	118
Network real load (MW)	6.62
Network reactive load (MVAr)	3.972
System voltage (KV)	15
Line impedance (Ω)	2.25
Power transformer	1. 132kv/33kv @31MW 2. 132kv/15kv @25 MW
Distribution transformer	15kv/0.4kv

3.7. Resource Feasibility Study of Distribution Generation

The solar and wind power plant energy outputs are strongly dependent on the sun radiation and the wind speed respectively which are stochastic in nature. Therefore, the feasibility of resources for either solar and or wind type DG installation has to be first studied before the study of their optimal size and appropriate bus location.

3.7.1. Solar Energy Resource Assessment

Feasibility of solar power-based DG installation on a given area should be studied before installing a solar panel at a given place. The sunshine hour and solar irradiance must enable to generate electricity from PV cells. The solar irradiance (kw-hr/m2/day) data of the two years taken from NASA is shown in the table 3.4.

Table 3.4: monthly average data of the solar irradiance (kWh/$\boldsymbol{m}$^2/day)

Year	Jan	Feb	Mar	Apr	May	Jun	Jul	Aug	Sep	Oct	Nov	Dec
2021	6.66	6.3	7.51	6.55	6.46	6.23	4.37	5.97	5.6	6.2	6.47	6.39
2022	6.09	6.9	7.03	6.69	6.97	5.98	4.74	5.48	5.58	5.93	6.22	6.01
Monthly average	6.38	6.6	7.27	6.62	6.72	6.11	4.56	5.73	5.59	6.07	6.35	6.2

3.7.2. Wind Resource Assessment

The consumption of energy increases from day to day and the issue of the environment is getting worse. Therefore, wind power is one of the solutions to reduce environmental stress. The availab ility of wind energy depends mainly on wind speed which is a random variable.

Wind Turbine Power Output Variation with Wind Speed

A wind energy conversion system's (WECS) power output is directly proportional to the cube of the wind speed at the wind turbine's height, as Figure (3.7) shows. Estimating wind speed accurately at a specific location is crucial to the size and energy production of wind turbines. The direction and speed of the wind continue to shift over time. One of the best ways to predict wind potential is to look at the average monthly wind speed. Furthermore, know the wind turbine's cut-in and cut-off speeds before installation.

Cut-in speed is a wind speed at which the turbine initially rotates and begins to produce power.

Cut-out speed is the highest wind speed at which there is a risk of rotor damage due to the strong forces acting on the turbine structure.

Wind speed varies depending on the area of operation and is variable. In the four cases that are discussed below, wind energy was produced (Sachidonondo & Moneesh, 2023).

Case 1: When the wind speed is below the cut-in speed, the wind turbine is not producing enough electricity at very low wind speeds. This is often between 3 and 5 m/s.

Case 2: A wind turbine produces electricity when wind speed exceeds the cut-in speed. This represents the range of wind speeds above (3-5 m/s) and below the rated speed (12-15 m/s). Wind energy generation is quite low, so to maximize power generation, maximum power tracking is required.

Case 3: The zone's wind speed (15–18 m/s) produces the most power.

Case 4: The wind turbine isn't producing electricity when the wind speed is higher than 25 m/s.

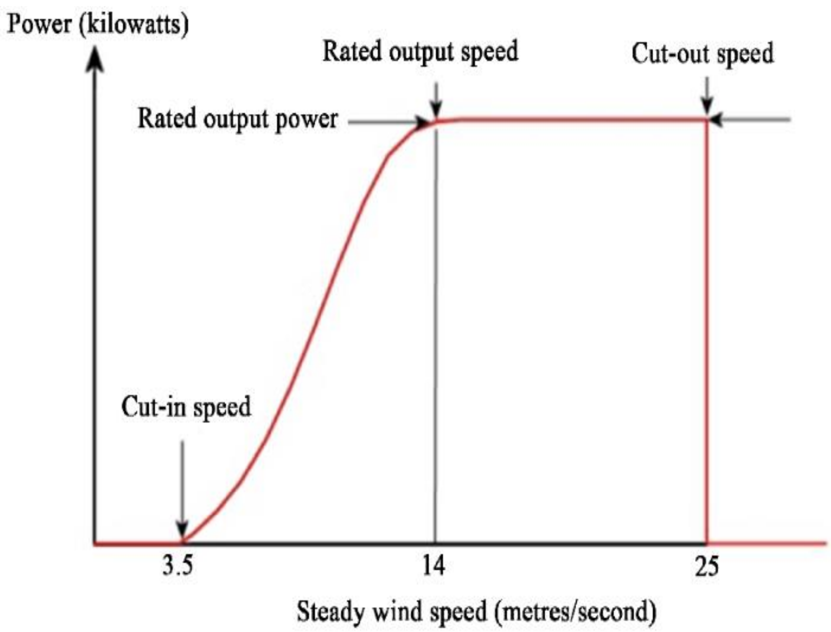

Figure 3.6: typical wind turbine power output versus wind speed *(Sachidonondo & Moneesh, 2023)*

The average wind speed (m/s) of the Huruta town at 10m height is recorded from the NASA is given in the table 3.5.

Table 3.5: Monthly average wind speed (m/s) at ten-meter height

year	Jan	Feb	Mar	Apr	May	Jun	Jul	Aug	Sep	Oct	Nov	Dec
2020	3.3	4.03	3.55	3.3	2.93	2.25	3.32	2.8	2.25	3.42	3.68	3.37
2021	3.64	3.48	4.45	3.52	2.91	2.75	4	2.3	2.08	3.31	3.83	3.78
2022	3.57	3.86	4.18	3.77	3.76	2.66	3.35	3.26	2.31	3.38	3.75	3.58
Monthly average	3.5	3.8	4	3.5	3.2	2.6	3.6	2.8	2.2	3.37	3.74	3.6

The wind-type DG is not feasible at the 10m height because, according to the monthly average wind speed data at 10m height given in Table 3.5, the wind speed at 10m is below the cut in speed and near to cut-in speed. Ten meters above the surface, the wind speed is minimum needed to generate wind power. The wind speed at average wind speed is not better generate enough power.

Table 3.6: Monthly average wind speed (m/s) at fifty-meter height

year	Jan	Feb	Mar	Apr	May	Jun	Jul	Aug	Sep	Oct	Nov	Dec
2020	4.68	5.73	5.01	4.68	4.2	3.16	4.61	3.9	3.27	5.02	5.34	5.36
2021	5.2	4.91	6.31	4.99	4.2	4	5.5	3.24	3.05	4.86	5.6	5.53
2022	5.16	5.45	5.89	5.36	5.35	3.8	4.88	4.59	3.41	5.02	5.52	5.22
Monthly average	5	5.3	5.7	5	4.5	3.36	5	3.9	3.2	4.9	5.4	5.37

The results presented in Table 3.6 show that even at a fifty-meter tower height, Huruta town's monthly average wind speed is not good. Wind-type DG is not feasible based on the data analyzed above, however solar-type DG is feasible. when wind speed exceeds the cut-in speed. This represents the range of wind speeds above (3-5 m/s) and below the rated speed (12-15 m/s). Wind energy generation is quite low, so to maximize power generation, maximum power tracking is required *(Sachidonondo & Moneesh, 2023)*.

3.7.3. Resource Assessment of DSTATCOM

The most effective and feasible device with faster response amongst the custom power devices is the Distribution Static synchronous compensator (DSTATCOM). The main advantage of DSTATCOM is the sophisticated power electronics control that effectively regulates the current injection into the distribution bus. Therefore, DSTATCOM can cancel the effect of poor load power factor, reduce the harmonics in load currents, and regulate the bus voltage during power failures such as sag and swell (N. H. Baharudin,, T. M. N. T. Mansur, R. Ali, S. I. S. Hassan , & P. Saad , 2021).

Both DSTATCOM (Distribution Static Synchronous Compensator) and STATCOM (Static Synchronous Compensator) are power electronic devices used to improve voltage profiles in distribution feeders (Tejas, Bhavesh , & Naimish, 2020).

DSTATCOM (Distribution Static Synchronous Compensator): A power electronics device used to improve voltage profiles in distribution feeders by injecting or absorbing reactive power.

STATCOM (Static Synchronous Compensator): A more powerful and versatile version of DSTATCOM, capable of providing both reactive power compensation and voltage regulation. While it is typically used in transmission systems, it can also be utilized in distribution systems for improved voltage profiles (Tejas, Bhavesh , & Naimish, 2020).

Table 3.7: Comparison of STATCOM and DSTATCOM (Tejas, Bhavesh , & Naimish, 2020)

Description	DSTATCOM	STATCOM
Installation	Installed closer to load	Installed at substation level
Rating in the same size	Lower rating in KVAr	Large rating in KVAr
Cost in the same size	Cost effective	More expensive
Control strategy	More complex strategy	Simple control strategy

Advantages of DSTATCOM

DSTATCOM have several advantages, including (Umar, 2017):

Faster response time: DSTATCOMs can respond to voltage fluctuations more quickly than STATCOM.

Improved power quality: DSTATCOMs can also mitigate other power quality issues, such as harmonics and flicker.

Reduced power losses: DSTATCOM can reduce power losses in the distribution system. Therefore, DSTATCOMs are often preferred for voltage profile improvement in distribution feeders, especially when fast response time and improved power quality are critical, whereas STATCOM mostly use in transmission power system to regulate voltage and enhancement of voltage profile to improve power quality.

Finally, the selection of DSTATCOM for proposed Dera (F-5) distribution feeder for voltage profile improvement depends on the specific requirements of the distribution feeder. DSTATCOM is a more cost-effective and feasible option.

3.8. Power Flow Analysis of Radial Distribution System

The general load flow techniques such as Gauss-Seidal, Newton-Raphson and Fast Decoupled load flow techniques cannot be applied to the distribution networks because of low reactance to resistance ratios(X/R). Distribution power flow methods are implemented to calculate line flows and voltage magnitude using forward and reverse sweeps along a radial line. Backward /forward sweep based distribution load flow is used, because of its accuracy and robust convergence characteristics (Salkuti, 2019).

Based on the accuracy and robustness use Backward/Forward sweep to load flow analysis. Backward /Forward sweep is a power load flow technique for radial network. BFS requires two computing cycle. At each node, the voltage beginning from the reference node to the end node is calculated using the forward sweep. The current or power flow solution starts from at the branch of the end nodes and move toward the branch connected to the reference node in the backward sweep (Khan, et al., 2022).

Analysis of load flow is needed to measure the bus voltage and branch currents in a distribution system. Backward/Forward sweep is used for load flow Analysis. Since The variables for the load flow analysis of distribution systems are different from that of transmission systems. This is because distribution network is radial in nature having high R/X ratio, whereas, the transmission system is loop in nature having high X/R ratio (Muquthiar, Gadana, & Visali, 2022).

3.8.1 Backward-Forward Sweep Load Flow Analysis of Radial Distribution System

Significant work is done before the optimal placement and size of DG and D-STATCOM in the distribution system network become known. The load flow of the current system uses the load flow method of backward and forward sweep. It is helping to evaluate electrical distribution networks' functioning effectiveness. After analyzing the existing power flow solution. DG and D-STATCOM are introduced into the backward/forward sweep technique by applying a static model of DG and D-STATCOM to load flow.

Kirchoff's current law (KCL) and Kirchoff's voltage law (KVL) are the foundation of the BFS algorithm. The three fundamental steps of the BFS algorithm are nodal current calculation (equivalent current injection), forward sweep or building of the branch current to the bus-voltage (BCBV) matrix, and backward sweep or formation of the bus injection to the branch-current matrix (BIBC). Simple matrix multiplication of BCBV and BIBC provides the solution. However, for a power system with n buses and m branches, the dimension of the BCBV is "(n − 1) xm," while the size of BIBC is "mx (n − 1)". In medium-voltage networks, the number of branches and buses is more significant and every MV/LV substation, switching substation, or network derivation represents a bus (Abdeljabbar & Saad, 2020).

Backward/forward sweep load flow method is used as the distribution load flow in this thesis, the over algorithm procedure is discussed below

Backward-Forward Sweep Load Flow Algorithm

BCBV and BIBC, and equivalent current injections are the basic step for developing the algorithm (Gurpreet & Asst.prof.Harmeet, 2017).

Step-1: Nodal current calculation (Bus current injection)

For the bus, the complex load S_i is expressed by

$$S_L(i) = P_L(i) + jQ_L(i) \tag{3.12}$$

From the complex power specified for each node as the equation above we can drive the equivalent current injection. The equivalent current injection at the kth iteration at the ith node in the load flow solution is represented below:

$$\begin{cases} I_L(i) = \left(\dfrac{P_L(i) + jQ_L(i)}{V(i)} \right)^* \\ I_L(i)^k = \left(\dfrac{P_L(i) + jQ_L(i)}{V(i)^k} \right)^* \end{cases} \tag{3.13}$$

Where: i=1,2…. N, k=1.2…Max-iteration.

$I_L(i)$ is s the load currents at the bus 'i'

V(i) is the bus voltages at the bus 'i'

P_L & Q_L are load demand and N is number of buses

Step-2: Formation of BIBC Matrix/Backward Sweep (Sunday, Hassan, Fajuke, & Kamilu, 2019)

Kirchhoff's current law (KCL), which is applied to the distribution network from the end node to the root node, is used to calculate the branch's current. By considering the equivalent injected current of each bus, we may build branch currents based on the sampled distribution system shown in Figure (3.7). The following will be the expression for each branch current:

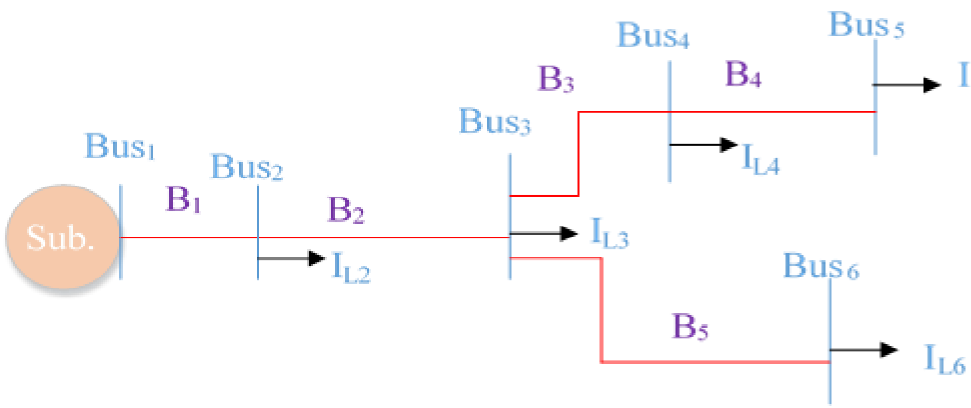

Figure 3.7: Sample radial distribution system

$$\begin{aligned}
B_5 &= I_{L6} \\
B_4 &= I_{L5} \\
B_3 &= I_{L4} + I_{L5} \\
B_2 &= I_{L3} + I_{L4} + I_{L5} + I_{L6} \\
B_1 &= I_{L2} + I_{L3} + I_{L4} + I_{L5} + I_{L6}
\end{aligned} \tag{3.14}$$

Furthermore, the bus injection to branch-current (BIBC) matrix can be obtained from above equation (3.14) as follows:

$$\begin{bmatrix} B_1 \\ B_2 \\ B_3 \\ B_4 \\ B_5 \end{bmatrix} = \begin{bmatrix} 1 & 1 & 1 & 1 & 1 \\ 0 & 1 & 1 & 1 & 1 \\ 0 & 0 & 1 & 1 & 0 \\ 0 & 0 & 0 & 1 & 0 \\ 0 & 0 & 0 & 0 & 1 \end{bmatrix} \begin{bmatrix} I_2 \\ I_3 \\ I_4 \\ I_5 \\ I_6 \end{bmatrix} \tag{3.15}$$

$$[B] = \begin{bmatrix} B_1 \\ B_2 \\ B_3 \\ B_4 \\ B_5 \end{bmatrix}, BIBC = \begin{bmatrix} 1 & 1 & 1 & 1 & 1 \\ 0 & 1 & 1 & 1 & 1 \\ 0 & 0 & 1 & 1 & 0 \\ 0 & 0 & 0 & 1 & 0 \\ 0 & 0 & 0 & 0 & 1 \end{bmatrix}, [I_L] = \begin{bmatrix} I_2 \\ I_3 \\ I_4 \\ I_5 \\ I_6 \end{bmatrix} \tag{3.16}$$

The general form of equation (3.16) can be expressed as follows:

$$[B] = [BIBC][I_L] \tag{3.17}$$

Step-3: Formation of BCBV Matrix/Forward Sweep (Zakir, Neem, & Neeraj, 2018)

In this step, the branch current, which was determined in stage one, and the impedance of each line are taken into consideration as Kirchhoff Voltage Laws (KVL) are used to compute each bus voltage from the source node to the end node. Finally, the following formula is taken to produce the Branch-Current to Bus Voltage (BCBV) matrix:

Brach-Current to Bus-Voltage (BCBV) matrix:

- The relation between branch current and bus voltages is then obtained
- For the former feeder, it can be seen that.

$$\begin{aligned} V_2 &= V_1 - B_1 Z_{12} \\ V_3 &= V_2 - B_2 Z_{23} = V_1 - B_1 Z_{12} - B_2 Z_{23} \\ V_4 &= V_3 - B_3 Z_{34} = V_1 - B_1 Z_{12} - B_2 Z_{23} - B_3 Z_{34} \\ V_5 &= V_4 - B_4 Z_{45} = V_1 - B_1 Z_{12} - B_2 Z_{23} - B_3 Z_{34} - B_4 Z_{45} \\ V_6 &= V_3 - B_5 Z_{56} = V_1 - B_1 Z_{12} - B_2 Z_{23} - B_5 Z_{36} \end{aligned} \tag{3.18}$$

Where, V_i is the bus voltage of Bus 'i'.

Z_{ij} is the line impedance between Bus 'i' and Bus 'j'.

From the above equation (3.18), the voltage at each bus can be obtained as the function of bus one (substation voltage). Thus, the bus voltage can be updated as

$$\begin{bmatrix} V_2 \\ V_3 \\ V_4 \\ V_5 \\ V_6 \end{bmatrix} = \begin{bmatrix} V_1 \\ V_1 \\ V_1 \\ V_1 \\ V_1 \end{bmatrix} - \begin{bmatrix} Z_{12} & 0 & 0 & 0 & 0 \\ Z_{12} & Z_{23} & 0 & 0 & 0 \\ Z_{12} & Z_{23} & Z_{34} & 0 & 0 \\ Z_{12} & Z_{23} & Z_{34} & Z_{45} & 0 \\ Z_{12} & Z_{12} & 0 & 0 & Z_{36} \end{bmatrix} \begin{bmatrix} B_1 \\ B_2 \\ B_3 \\ B_4 \\ B_5 \end{bmatrix} \tag{3.19}$$

From the given sample network BCBV is formulated as follow based on above equation (3.19).

$$[BCBV]=\begin{bmatrix}1&0&0&0&0\\1&1&0&0&0\\1&1&1&0&0\\1&1&1&1&0\\1&1&0&0&1\end{bmatrix}\begin{bmatrix}Z_{12}&0&0&0&0\\0&Z_{23}&0&0&0\\0&0&Z_{34}&0&0\\0&0&0&Z_{45}&0\\0&0&0&0&Z_{36}\end{bmatrix} \tag{3.20}$$

$$[BIBC]^T=\begin{bmatrix}1&1&1&1&1\\0&1&1&1&1\\0&0&1&1&0\\0&0&0&1&0\\0&0&0&0&1\end{bmatrix}^T,\ [Z_n]=\begin{bmatrix}Z_{12}&0&0&0&0\\0&Z_{23}&0&0&0\\0&0&Z_{34}&0&0\\0&0&0&Z_{45}&0\\0&0&0&0&Z_{36}\end{bmatrix}$$

$$[BCBV]=[BIBC]^T[Z_n] \tag{3.21}$$

$$\begin{bmatrix}V_1\\V_1\\V_1\\V_1\\V_1\end{bmatrix}-\begin{bmatrix}V_2\\V_3\\V_4\\V_5\\V_6\end{bmatrix}=\begin{bmatrix}1&0&0&0&0\\1&1&0&0&0\\1&1&1&0&0\\1&1&1&1&0\\1&1&0&0&1\end{bmatrix}\begin{bmatrix}Z_{12}&0&0&0&0\\0&Z_{23}&0&0&0\\0&0&Z_{34}&0&0\\0&0&0&Z_{45}&0\\0&0&0&0&Z_{36}\end{bmatrix}\begin{bmatrix}B_1\\B_2\\B_3\\B_4\\B_5\end{bmatrix} \tag{3.22}$$

The relationships between Bus current injections and Bus voltages could be expressed as above equation (3.22) and (3.17) can be written as:

$$\Delta V=[BCBV][BIBC][I_L] \tag{3.23}$$

The distribution load flow matrix (DLF) is formulated as follows based on the above equation (3.23):

$$[DLF]=[BCBV][BIBC] \tag{3.24}$$

By inserting equation (3.23) into equation (3.24), it gives:

$$\Delta V=[DLF][I_L] \tag{3.25}$$

The iterative solution for the distribution system load flow can be obtained as:

$$\left[\Delta V^{k+1}\right]=[DFL]\left[I_L^k\right] \tag{3.26}$$

$$\left[V^{k+1}\right]=[V_1]+\left[\Delta V^{k+1}\right] \tag{3.27}$$

Backward -Forward Sweep (BFS) Load Flow Algorithm (Sunday, Hassan, Fajuke, & Kamilu, 2019)

The backward- forward load flow algorithm described above may have the following steps for the load flow solution of distribution networks as shown below:

Step 1: Read System data like line data (resistance and reactance for each branch), and bus data (active and reactive load for each bus).

Step 2: Assume initialize the buses voltages as 1.0+j0 with zero angle value,

Step 3: Iteration k = k + 1, k=0,1,2… Maximum iteration, eps=0.0001 of error tolerance.

Step 4: Calculate each Bus current injection using equations (3.13).

$$I_i(k) = \left[{P_i(k) + Q_i(k)} \Big/ {V_i(k)} \right]^*$$

Step 5: Compute the [BCBV] and [BIBC] matrices that can be directly obtained from network topology on the above equation (3.16) and (3.20) and determine the branch current.

Step 6: Calculate the DLF matrix by using the equation (3.24).

Step 8: Compute [ΔV] =[BCBV][BIBC][I] and update voltages.

Step 9: Calculate the branch real and reactive power loss

$$PLoss_j(k) = B_j^2 R_j \text{ and } QLoss_j(k) = B_j^2 X_j \; \left\{ B_j \text{ is the } j^{th} \text{ branch current} \right\}$$

Step 10: Check if an error in voltage i.e., max ((│ΔV (k+1) │-│ΔV (k) │) if it is less than or equal eps, go to next step otherwise, go to step 3.

Step 10: Once the load flow has been converged and the bus voltage and branch currents have been determined, the power loss of each branch in the network must be determined

Step 11: Print the resulting load flow analysis and then stop.

3.8.2 Integration PQ Model of DG and of Static Model of DSTATCOM in BFS Load Flow Algorithm

The PQ model of PV-DG and the static model of D-STATCOM are integrated into the BFS load flow to calculate the power flow solution during the integration of DG and D-STATCOM (Sanam et al., 2017). (Samal et al., 2018). To compute the power flow solution, the BFS approach consists of two easy steps. that is forward and backward sweep. The load current is calculated using the former. Equations (3.13) and (3.14) can be used to determine the load current when BFS is not integrated with DG and D-STATCOM. Nonetheless, the load current can be altered during the integration of DG and D-STATCOM. For instance, the active and reactive power demand is changed and provided by the following when DG and D-STATCOM are installed at bus j:

$$P_L(j)' = P_L(j) - P_{DG}(j) \tag{3.28}$$

$$Q_L(j)' = Q_L(j) - Q_{DST}(j) \tag{3.29}$$

The modified load current, when DG and D-STATACOM are integrated at bus j, is calculated using modified active and reactive power demand obtained from equations (3.28) and (3.29) and expressed as follows:

$$I_L(j) = \left(\frac{P_L(j)' + Q_L(j)'}{V(j)} \right)^* \tag{3.30}$$

For kth iteration and j bus integration load current can be expressed as:

$$I_L(j)^k = \left(\frac{P_L(j)' + Q_L(j)'}{V(j)^k} \right)^* \tag{3.31}$$

Then the branch current is calculated as follows:

$$I(jk) = I(k) + \sum_{j \in m} I_L(j) \tag{3.32}$$

Where I (jk) represent phasor current in ‘jk’ branch, and ‘m’ represent all busses linked to ‘jk’ branch.

Then the forward sweep is applied for obtaining nodal voltage as follows:

$$V(k) = V(j) - I(jk) * Z(jk) \tag{3.33}$$

Where k is receiving end bus and j is sending end bus. Z(jk) is the impedance between the bus ‘j’ and ‘k’.

3.9. Optimal Placement and Sizing of DG and DSTATCOM

Optimal placement and sizing of the distribution network's DSTATCOM and DG to reduce power loss and improve the voltage profile. Integrating of DG and D-STATCOM for voltage profile and power loss mitigation. Separately and simultaneously integration of DSTATCOM and DG are more effective approaches to resolve the issues of DG and D-SATCOM location and sizing

(Prashant, Anwar, Sarwar, Ahmed, & Sherif, 2022). Whale optimization techniques are used to optimize distribution networks for factors like voltage profile, and power loss.

3.10. Whale Optimization Algorithm

Recently, Mirjalili and Lewis have presented a novel optimization approach to the metaheuristic algorithm known as the whale optimization algorithm in 2016. Whales are extremely clever moving animals. The unique method that humpback whales hunt became the model for the WOA. Usually, humpback whales choose to hunt tiny fish at the sea's surface. The bubble net feeding method is one of the special and unusual hunting techniques used by humpback whales. Using a circle or nine-shaped path, they swim around the prey and produce recognizable bubbles (P.Dinakara, V.C. Veera, & T.Gowri, 2019).

Finding appropriate locations in a radial network where a DG and DSTATCOM can be placed to minimize power loss and improve the voltage profile is necessary for optimal DG and DSTATCOM operation in a radial distribution system, provided that certain operating constraints are satisfied (Provas & Suvabrata, 2022).

The following sections describe the WOA mathematical model (P.Dinakara, V.C. Veera, & T.Gowri, 2019).

A. Encircling prey
B. Bubble net hunting method
C. Search prey

A): Encircling prey

This is similar to how humpback whales circle their prey after discovering it. The WOA technique identifies the immediate best candidate as the target victim or as the value that is closest to the ideal location, as the best position in the search area is not first detected. When the best search agent is identified, the other search agents adjust their positions to point in the direction of this search agent (Provas & Suvabrata, 2022).

WOA assumes that the target prey will be the current best candidate solution. In an attempt to find the greatest search agent, some try to upgrade their positions.

The behavior that is being modeled is as (P.Dinakara, V.C. Veera, & T.Gowri, 2019):

$$\vec{X}(t+1) = \vec{X}^{*}(t) - \vec{A}.\vec{D} \tag{3.34}$$

$$\vec{D} = \left| \vec{C} . \vec{X}^{*} - \vec{X}(t) \right| \tag{3.35}$$

$$\vec{A} = 2.\vec{a}.\vec{r} - \vec{a} \tag{3.36}$$

$$\vec{C} = 2.\vec{a} \tag{3.37}$$

Where $\vec{X}^{*}$, $\vec{X}$ denote the position of the best solution and position vector. The current iteration is denoted by t. $\vec{A}$, $\vec{C}$ are coefficient vectors. $\vec{a}$ is directly diminished from 2 to 0. $\vec{r}$ is a random vector [0, 1], $\vec{D}$ present the distance between whales and prey (best position).

B): Bubble net hunting Methods

Whales employ bubbles blasted from their blowholes to shock and capture fish closer to the surface while they bubble-net feed, diving well below schools of fish.

Bubble net hunting method have two approaches are there (P.Dinakara, V.C. Veera, & T.Gowri, 2019):

Shrinking Encircle prey

Here $\vec{A} \in [-a, a]$,where $\vec{A}$ is decreased from 2 to 0. Here $\vec{A}$ position is setting down at random values in between [−1,1]. The new position of $\vec{A}$ is obtained between the original position and the position of the current best agent. Figure (3.8) shows the possible positions from (X, Y) toward (X*, Y*) that can be achieved by $0 \leq A \leq 1$ in a 2D space represented by Equation (3.37)

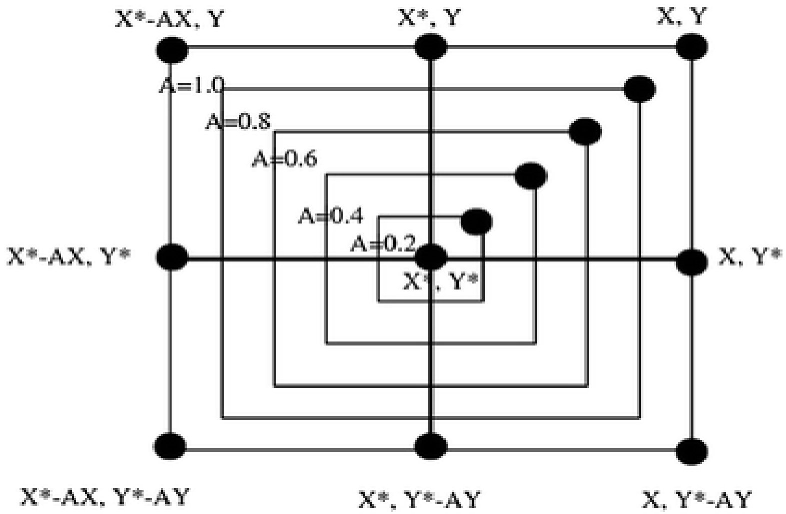

Figure 3.8: Bubble net search shrinking encircling mechanism *(P.Dinakara, V.C. Veera, & T.Gowri, 2019)*

Spring Position Updating

In this case, the distance is first evaluated at the intervals when the whale is located at (X, Y) and the prey is at (X*, Y*). Because humpback whales move in a helix, a formula (spiral) is created between the position of the prey and the whale to continue the helix-shaped movement. This can be shown like this *(P.Dinakara, V.C. Veera, & T.Gowri, 2019)*:

$$\vec{X}(t+1) = \vec{D}^{'} . e^{bl} . \cos(2\pi l) + \vec{X}^{*} \tag{3.38}$$

Whales hunt by swimming in two different circles around their prey at the same time. For the first two approaches, a probability of 50% is used to update the positions of whales.

$$\vec{X}(t+1) = \begin{cases} \vec{X}^{*}(t) - \vec{A}.\vec{D} & if \;\; p < 0.5 \\ \vec{D}^{'} . e^{bl} . \cos(2\pi l) + \vec{X}^{*} & if \;\; p \geq 0.5 \end{cases} \tag{3.39}$$

Where, $D^{'} = \left| \vec{X}^{*} - \vec{X}(t) \right|$, represent the distance between whales and the prey (best position). $l \in [-1,1]$, b is constant, p is random number [0,1]. The spiral updating position methods described on equation (3.39) present in figure (3.9).

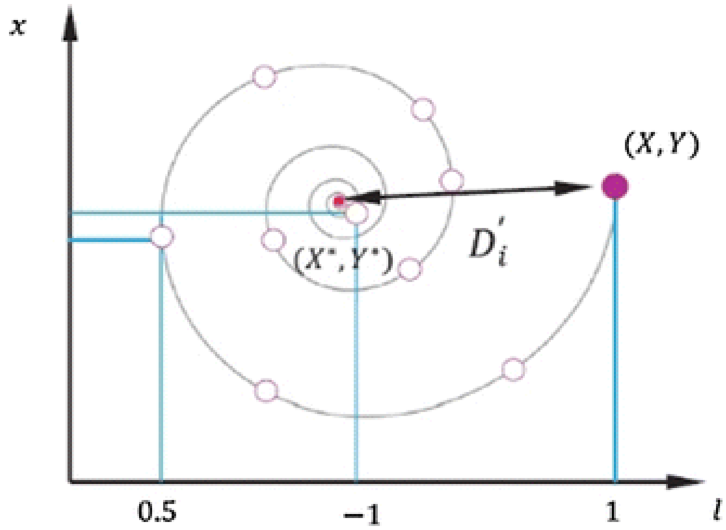

Figure 3.9: Bubble net search spiral updating position mechanism *(P.Dinakara, V.C. Veera, & T.Gowri, 2019)*

C): Search for Prey

To find the global optimum values updating has done with random select search agent rather than the best agent. This characterize as follows:

$$\vec{D} = \left| \vec{C}.\vec{X}_{rand} - \vec{X} \right| \tag{3.40}$$

$$\vec{X}(t+1) = \vec{X}_{rand}(t) - \vec{A}.\vec{D} \tag{3.41}$$

Where $\vec{X}_{rand}(t)$ is random Whales current iteration?

3.11. Problem Formulation of Multi-Objective function

Multi-objective function

The main goal of the suggested study is to determine the best placement and capacity of DG and D-STATCOM by minimizing fitness function. The fitness functions are multi-objective functions (MOF) consists three single functions combined by the weight sum method. In a radial distribution system, the best allocation of DG and D-STATCOM is used to reduce total active and reactive power losses and mitigate the voltage profile while meeting equality and inequality standards.

Power Loss and Voltage Profile

The distribution lines, balanced power nodes, and constant loads are represented by several branches that are components of the RDS. Equations (3.44) to (3.45), which refer to Figure 3.10, are used to get the power flow solution in the RDS with DG units and D-STATCOM integrated (Ashraf, Mohamed, & Salah, 2019).

$$P_{k+1} = P_k - P_{L,k+1} - R_{k,k+1}\left(\frac{P_k^2 + jQ_k^2}{|V_k|^2}\right) + P_{DG} \tag{3.42}$$

$$Q_{k+1} = Q_k - Q_{L,k+1} - X_{k,k+1}\left(\frac{P_k^2 + jQ_k^2}{|V_k|^2}\right) + Q_{DSTAT} \tag{3.43}$$

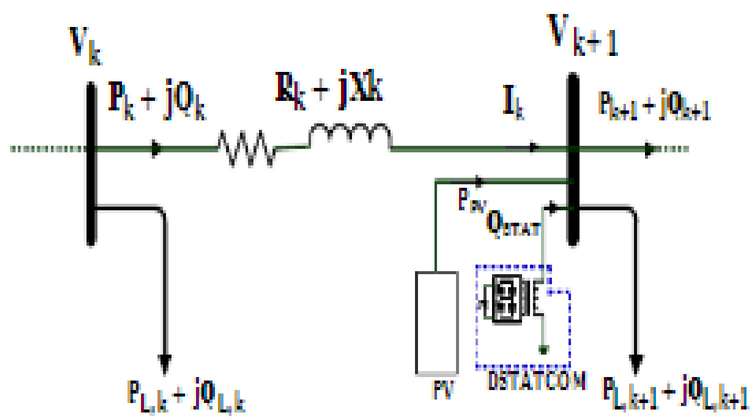

Figure 3.10: Schematic diagram of an RDS including PV &DSTATCOM

Where, between buses k and k1, are the reactance and resistance expressed in the parameters $X_{k,\ k-1}$ and $R_{k,\ k-1}$, respectively. The real and reactive power flows are denoted by P_k and Q_k, respecti vely. The following are the active and reactive power losses before the installation of DSTATCO M and DG.

$$P_{Loss(k,k+1)} = R_{k,k+1}\left(\frac{P_k^2 + jQ_k^2}{|V_k|^2}\right) \tag{3.44}$$

$$Q_{Loss(k,k+1)} = X_{k,k+1}\left(\frac{P_k^2 + jQ_k^2}{|V_k|^2}\right) \tag{3.45}$$

The total real power loss, and reactive power loss in the system P_{TL} and Q_{TL} is formulated respectively as:

$$\begin{cases} P_{TL} = \sum_{i=1}^{nb} P_{Loss}(i) \\ Q_{TL} = \sum_{i=1}^{nb} Q_{Loss}(i) \end{cases} \tag{3.46}$$

Power loss after the installation of D-STATCOM and DG in F five distribution feeder.

$$P_{DG/Dst,loss(k,k+1)} = R_{k,k+1} * \left(\frac{P^2{}_{DG/Dst,k} + Q^2_{DG/Dst,k}}{|V_k|^2} \right) \tag{3.47}$$

Figure (3.9) shows the one-line diagram of the distribution system with three nodes and a load at the end node. The resistance and reactance of the line, which links the load to the substation, are Total power loss in the system with DG and DSTATCOM is calculated by using Eq. (3.48)

$$P_{total\ loss\ with\ DG/Dst} = \sum_{k=1}^{n-1} P_{loss\ with\ DG/Dst_{(k,k+1)}} \tag{3.48}$$

indicated by the letters R and X, respectively. Figure (3.11) shows a basic explanation of voltage drop in radial distribution. Suppose that the complex load in bus two is represented by:

$$S_L = P_L + jQ_L \tag{3.49}$$

The current flow calculation in the feeder will be:

$$I = \left(\frac{S}{V_2} \right)^* \left(\frac{P_L + jQ_L}{V_2} \right)^* \tag{3.50}$$

The voltage drops due to distribution line only is shown in phasor diagram:

$$\begin{cases} v_1 - v_2 = I\left(R + jX\right) = \left(\frac{P_L - jQ_L}{V_2^*} \right)\left(R + jX\right) \\ v_1 - v_2 = \left(\frac{\left(P_L R + XQ_L\right) - j\left(XP_L - RQ_L\right)}{V_2} \right) \end{cases} \tag{3.51}$$

Where; R, X resistance and inductance; V_1, V_2 substation and load voltage; P_L, Q_L is real and reactive load.

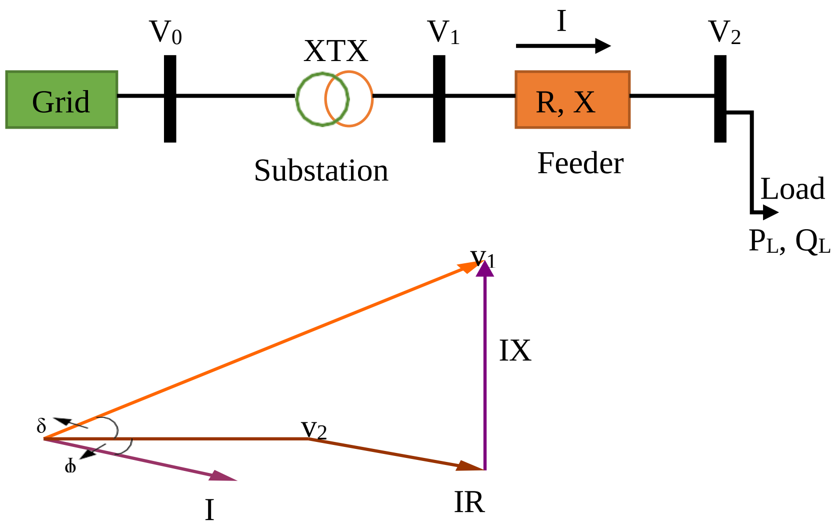

Figure 3.11: Sample radial distribution system and voltage phasor diagram

Loss minimization

First-objective function: feeder total active power losses can be formulated as follows:

$$f_1 = \sum_{i=1}^{nb} \left(R_i \times I_i^2 \right) \tag{3.52}$$

Second-objective function: feeder total reactive power losses can be formulated as follows:

$$f_2 = \sum_{i=1}^{nb} \left(X_i \times I_i^2 \right) \tag{3.53}$$

Where, f_1 and f_2 is the first & second objective functions associated with the system power loss minimization. I_i: is the current of line 'i', R_i: is the resistance of i^{th} line, X_i: is reactance of 'i^{th} line, nb: is the number of system branches.

$P_{DG/DST}$: Active power loss after integration of DG or DSTATCOM

$Q_{DG/DST}$: Reactive power loss after integration of DG or DSTATCOM

percentage of total power loss mitigation can be calculated by

$$\begin{cases} \%\ Active\ power\ loss\ mitigation = \left(\dfrac{P_L - P_{L@DG/DST}}{P_L} \right) \times 100 \\ \%\ \mathrm{Re}\,active\ power\ loss\ mitigation = \left(\dfrac{Q_L - Q_{L@DG/DST}}{Q_L} \right) \times 100 \end{cases} \tag{3.54}$$

Voltage Profile Mitigation

The third objective function is mitigating the voltage profile of the distribution network which is the Commutative voltage deviation index described as follow:

$$f_3 = \sum_{i=1}^{N} \left(1 - V_i\right)^2 \tag{3.55}$$

Where; f_3 is the third objective function associated voltage deviation index, V_i is the voltage of the i^{th} bus, and N is the number of the system bus.

The formulation of the general multi-objective function (MOF) and convert each single objective using the weight sum method and given by:

$$Minimize(MOF) = Min\left(w_1 \times f_1 + w_2 \times f_2 + w_3 \times f_3\right) \tag{3.56}$$

Where; $\sum_{i=1}^{3} w_i = 1$,MOF are multi-objective function, w_i is the selection suitable values of weight factor depends on important of minimization. w_1=0.5, w_2=0.4, and w_3=0.1 are the best combination.

Constraints

Equality and inequality constraints are two types of system constraints which are discussed below. The constraint-handling strategy for this study is the death penalty. In this method, all infeasible solutions are rejected and only feasible regions are explored of the radial distribution system (Alyu, 2022).

1.Equality constraints

The active and reactive powers flow in radial distribution system are included in the equality constrain, which may be written as follows:

$$P_s + \sum_{i=1}^{np} P_{DG} = \sum_{h=1}^{n} P_D(h) + \sum_{j=1}^{nl} P_{Loss}(j) \tag{3.57}$$

$$Q_s + \sum_{i=1}^{nc} Q_{DSTAT}(i) = \sum_{h=1}^{n} Q_D(h) + \sum_{j=1}^{nl} Q_{Loss}(j) \tag{3.58}$$

Where; P_s is active power and Q_s is reactive power are supplied power from substation.
P_D is active power and Q_D reactive power are the load of RDS. np is number of DG, nc is number of DSTATCOM and nl is number of lines in RDS (Assen & DR.Tefera, 2023).

2.Inquality constraints

A) Bus voltage limits

$$V_{\min} \le V_i \le V_{\max} \tag{3.59}$$

where, V_{max} and V_{min} are the upper and the lower voltage limits. As technical standard of IEEE 1547 bus voltage limit is ±5% of the nominal voltage that means V_{max} = 1.05pu and V_{min} = 0.95pu.

B) Total injected active power limit

DG is used to generate active power with an allowed range. In this case, the maximum limit of the total capacity of DG units is 60% of the total kW loading of this network, and its minimum limit is zero. The active power of the PV should be equal to or less than the active power load (Assen & DR.Tefera, 2023).

$$\sum_{i=1}^{np} P_{DG}(i) \leq \sum_{i=1}^{n} P_D(i) \tag{3.60}$$

where, P_D is the active power of the load and P_{DG} is injected active power by the DG units.

C)Total injected reactive power limit

D-STATCOM generates reactive power with an allowed range. In this case, the maximum limit of the total capacity of D-STATCOM units is 60% of the total kVAr loading of this network, and its minimum limit is zero. The reactive power of the DSTATCOM should equal to or less than the reactive load (Assen & DR.Tefera, 2023).

$$\sum_{i=1}^{np} Q_{DSTAT}(i) \leq \sum_{i=1}^{n} Q_D(i) \tag{3.61}$$

Where; Q_D is reactive power of the load and Q_{DSTAT} is an injected reactive power by DSTATCO M to RDS.

D) Line current limit

$$I_k \leq I_{\max,k} \tag{3.62}$$

Where; k=1, 2, 3………. NB and NB are number of bus.

Proposed Work steps of whale optimization algorithm

WOA a basic technique used optimal placing and sizing of DG and DSTATCM in F-5 distribution feeder for multi-objective, take following steps:

Step1: Initialization, the line impedance data and load data of the feeder as input.

Step 2: Calculate total power loss, and bus voltages using Forward-Backward sweep method

Step 3: Initialize the number of search agents to be optimized. If the search agents go beyond the boundaries then bring back to within the boundary by inserting the limits.

Step 4: Initialize the counter

Step 5: Calculate the fitness function for each search agent using Eq. (3.41) and obtain the initial best agent

Step 6: For each search agent update a, A, C, l and p using Eqs. (3.35), (3.36). Where l and p are random numbers.

Step 7: If ($p < 0.5$) go to Step 8 otherwise go to Step 10.

Step 8: If $|A| < 1$, then update the position of current search agent by using Eq. (3.40)

Step 9: If $|A| \geq 1$, then calculate new search agent and update its position by using Eq. (3.33).

Step 10: Update the position of current search agent by using Eq. (3.38).

Step 11: Go to Step 12, if the counter reaches the maximum value. Else go to Step 5.

Step 12: print the result.

3.12. Implementation of the WOA Algorithm to Identify the Optimal Size and Placement of DSTATCOM and DG

WOA, population (X i) is the position representation of each individual with N-dimensional search agent which is described as follows:

$$X_i = \left(X_{i1}\ X_{i2}\ X_{i3}............X_{iN}\right) \tag{3.63}$$

$$X_i = \left[Cap_{ij}, Loc_{ij}\right] \tag{3.64}$$

$$\begin{cases} X_{DG}(i) = \left[S_1, S_2....S_{NDG}, L_1, L_2.......L_{NDG}\right] \\ X_{DST}(i) = \left[S_1, S_2.......S_{NDST}, L_1, L_2..L_{NDST}\right] \end{cases} \tag{3.65}$$

$$X_{DG\&DST}(i) = \left[X_{DG}(i), X_{DST}(i)\right] \tag{3.66}$$

Where, L_1, L_2, L_{NDG}, L_1, L_2, L_{NDST} are location of DG and DSTATCOM, and NDG, NDST are number DG and DSTATCOM. S1, S2, SDG, S1, S2, SNDST are size of DG and DSTATCOM.

Table 3.8: Parameters of WOA algorithm and boundary of decision variables of the objective function

<table>
<tr><td rowspan="5">Parameters of WOA Algorithm</td><td colspan="2">Number of Population</td><td colspan="2">50</td></tr>
<tr><td colspan="2">Maximum Iteration</td><td colspan="2" rowspan="4">100</td></tr>
<tr><td>p (random variable)</td><td>[0 1]</td></tr>
<tr><td>A</td><td>[2 0]</td></tr>
<tr><td>L</td><td>[-1 1]</td></tr>
<tr><td colspan="2">Decision variables of objective function</td><td>Bus number (location)</td><td>Size of DG (MW)</td><td>Size of DSTAT(MVAr)</td></tr>
<tr><td rowspan="2">Boundary</td><td>Lower bound</td><td>2</td><td>0</td><td>0</td></tr>
<tr><td>Upper bound</td><td>118</td><td>4.23</td><td>2.538</td></tr>
</table>

Steps for the optimization algorithm:

The provided optimization algorithm for choosing the best position and sizing for the DG and D-STATCOM in the Awash Melkasa radial distribution feeder is put into population using the processes listed below.

Step 1: Read the distribution system data and line data, base MVA, base KVA, and bus voltage limits

Step 2: Compute the voltage profile at each bus and the real and reactive power of lines of the base case using the BFS load flow algorithm

Step 3: Determine a DG and D-STATCOM devices will be placed.

Step 4: Set the lower and upper bounds for system restrictions, as well as the control parameters for the Whale optimization algorithm (Population size, a, l, p, and the maximum iteration.)

Step 5: Generate numbers of population rows and two times the number of DG or (and) D-STATCOM column (Np´2* NDG or(and)N DST) population randomly. Set the iteration counter k=1.

Step 6: compute the current agent and best agent position of humpback whales.

Step 7: update the current agent position of the population using equations (3.35), (3.39) and (3.41).

Step 8: check boundary and position limits; Otherwise go to the next step.

Step 9: compute load flow system parameters with DG or(and) DST and evaluate each population using a multi-objective function.

Step 10: best agent as optimal solution which consists of optimal location and size of DG or (and) DST.

Step 11: Maximum iteration reached, go to next step. Otherwise, go back to Step 5 by setting the iteration index k=k+1.

Step 12: compute and update the new search agent and best agent position whales.

Step 13: Load flow analysis after integration of optimal location and size of DG or (and) D-STATCOM. Finally, evaluate system performance. The overall steps are shown in Figure 3.15 in flow chart form.

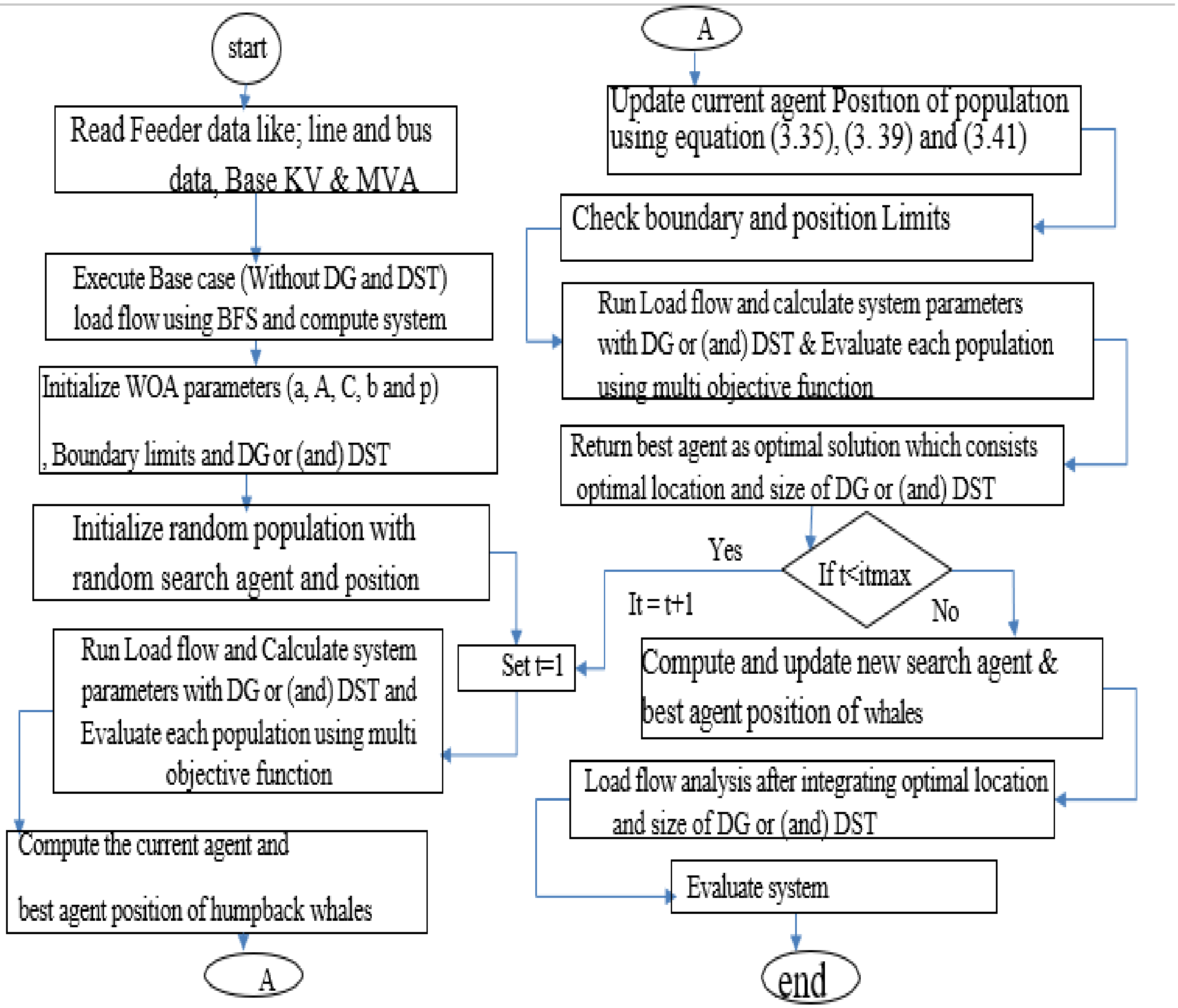

Figure 3.12: Flowchart proposed whale optimization algorithm

CHAPTER FOUR

4.SIMULATION RESULT ANALYSIS AND DISCUSSION

This chapter presents the outcomes of the simulations to analyses result using MATLAB (R2021a version) software. The simulation results are observed using MATLAB (R2021a) software.

The backward/forward sweep load flow technique has been used for power loss and voltage profile mitigation analysis of power flow using software tools. The distribution systems are evaluated using load flow analysis, which examines power losses, voltage profiles, and loss costs both with and without the integration of DG and D-STATCOM.

The optimum position and sizes for DG and D-STATCOM at the time of integration are selected using the whale optimization algorithm as a decision-making tool. In general, the base case and the perfect placement and size of DSTATCOM and DG after installation are the properties that determine the voltage profile and power loss of the distribution feeder.

Four distinct scenarios are compared and analyzed separately to obtain the best power loss and voltage profile mitigation scenario. The lists of scenarios are:

Scenario I: Base case or current system

Scenario II: DG Integration Only

Scenario III: Only D-STATCOM Integration

Scenario IV: Simultaneous DG and DSTATCOM Integration

4.1 Scenario I: Base case or current system

Base Case Load Flow Result

The base case-load flow simulation determines the current state of the distribution feeder. A load flow analysis of the distribution feeder was performed using the backward/forward sweep algorithm. The backward-forward sweep (BFS) method uses the line and bus data as input data obtained from Table 3.3. A Base voltage =15 KV and base MVA = 100 and these values convert the inputs to per-unit values before the algorithm runs. The overall reactive and active load demand of the F-5 feeder are 3.972 MVAr and 6.62 MW, respectively. The simulation result shows the system's overall reactive power loss is 987.991 KVAr, whereas, its total real power loss is 1298.84 KW. Such, a significant power loss is not cost-effective. Therefore, DG and D-STATCOM integration are solutions and tested in the next scenarios.

The voltage profile and power loss of the base case in each branch are shown in Figure 4.1. and Figure 4.2 respectively. At bus number 76, the minimum voltage is 0.8689 p. u., which is less than 0.95pu. The voltage magnitude is below the allowable range are forty-five and 12/100 (45.12%).

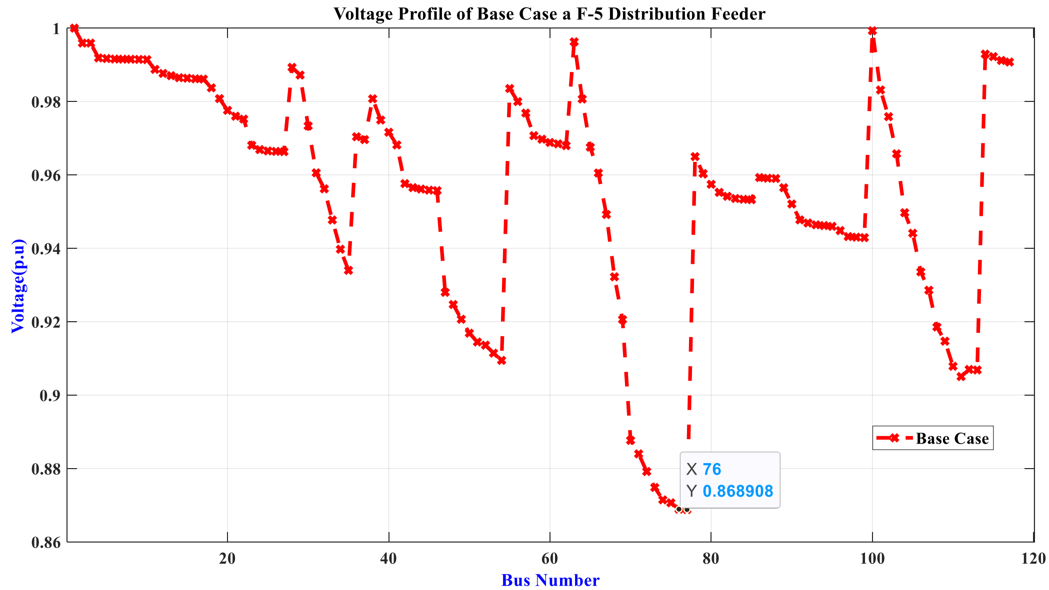

Figure 4.1: Base case voltage profile of Awash Melkasa F-5 feeder

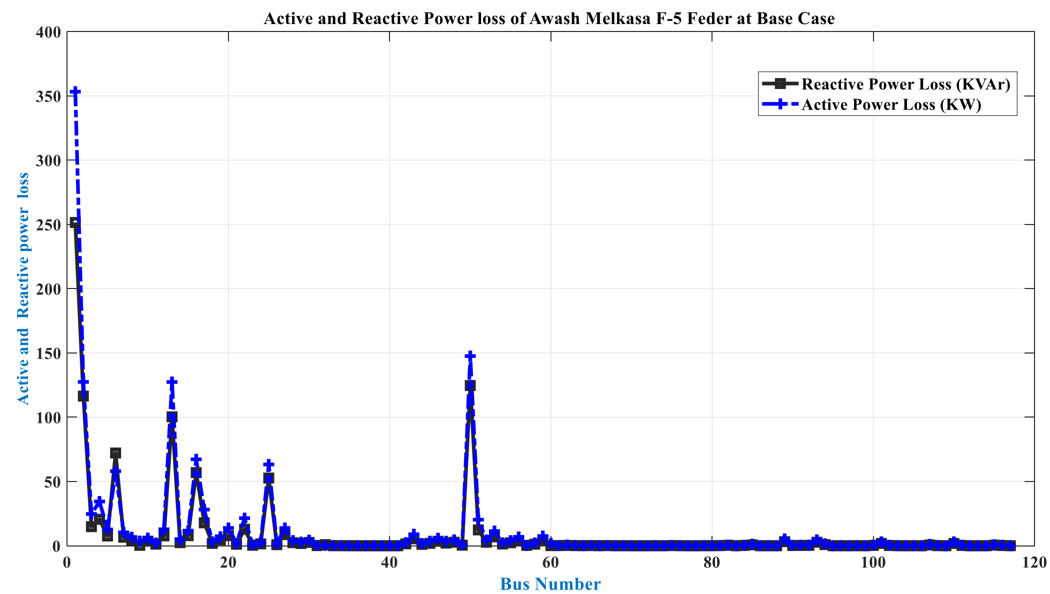

Figure 4.2: Base case active and reactive power loss of feeder F-five

4.2 Scenario II: DG Integration Only

The optimal placement and size of DG have been done based on the flow chart presented in Figure 3.11. A total of 50 population are randomly generated with two times the number of DG design variables. The decision variables are the capacity and placement of DG integrated into the system. The simulation results for the bus voltage profile and total active and reactive power loss for DG are shown in Figure 4.3 and Figure 4.4 respectively.

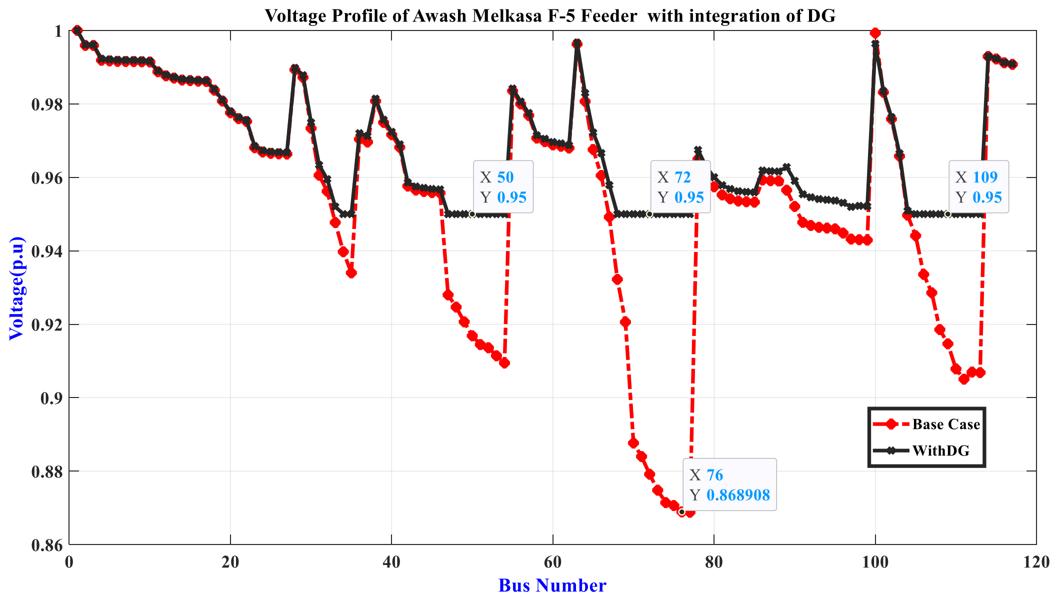

Figure 4.3: Voltage profile improvement using integration of DG

The simulation's output demonstrates that the incorporation of DG improves the voltage profile of the Awash Melkasa distribution feeder, shown in Figure 4.3. The voltage profile will increase to 0.95 (p. u) with the integration of DG. However, for DG integration, every bus voltage is more than or equal to 0.95(p.u.), the minimal threshold value.

The optimal installation of DG mitigates both active and reactive power losses while simultaneou sly improving the voltage profile of the Feeder as shown in Figure 4.4 below. The active power loss is decreased to 730. 5532KW.whereas, the reactive power loss reduces to 545.3182KVAr.

In general, the distribution feeder power loss and voltage profile mitigating with the help of DG integration is summarized and presented in Table 4.4. from this table, the effect of DG on power loss reduction and voltage profile improvement by considering the maximum penetration of DG was constant and the power factor is 0.9.

Table 4.1: Result summary of Scenario-II

Parameters	Base Case	DG1
Active power loss (KW)	1298.84	**730.5532**
Reactive power loss (KVAr)	987.991	**545.3182**
Execution time (sec.)	0.96038	**12.7244**
Minimum voltage (p.u) @bus No.	0.8689 @76	0.95@33
Maximum voltage deviation (%)	13.109	**4.4799**
Active power loss reduction (%)	NLL	**44.5578**
Reactive power loss reduction (%)	NLL	**44.6838**
DG Location (Bus No.)	NLL	@96
DG size in MW	NLL	1.129

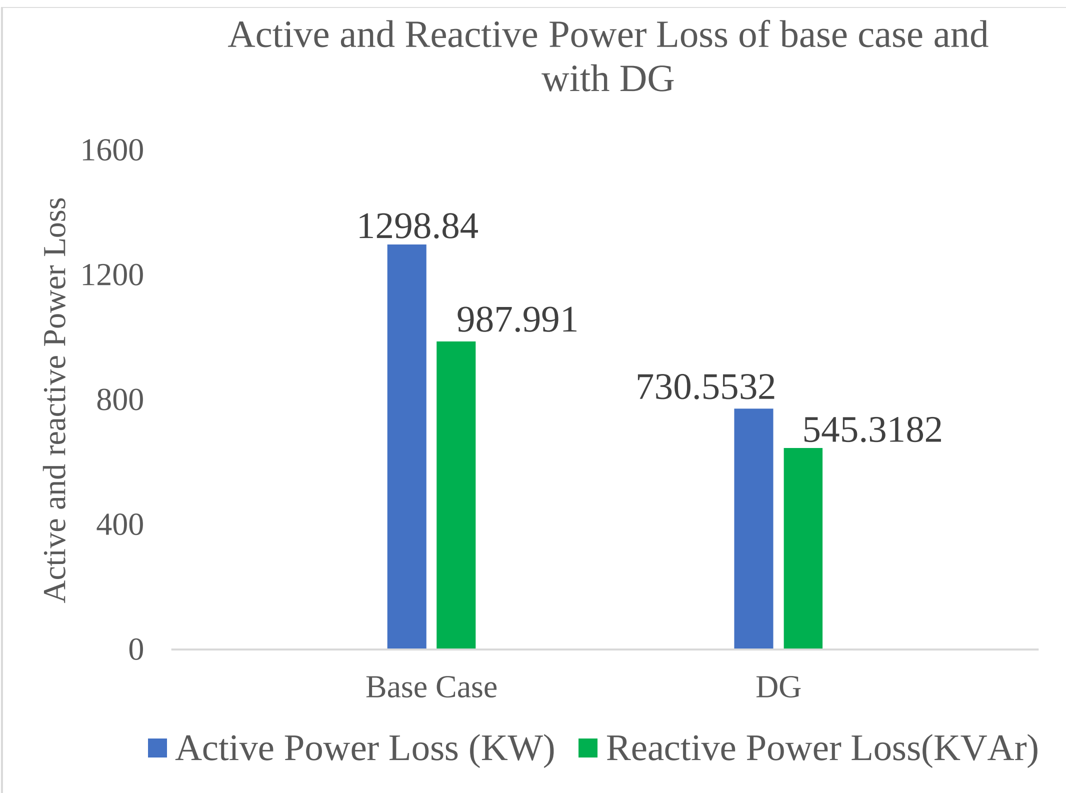

Figure 4.4: Total active and reactive power loss before and after DG installation

4.3 Scenario III: Only D-STATCOM Integration

The previous chapter discussion, D-STATCOM is used for power loss minimization and voltage profile improvement. The objective function and constraint are formulated and discussed in chapter three when D-STATCOM integration.

Based on the formulated objective function and constraints, WOA is used to find the optimal location and size of the required D-STATCOM. The result of the voltage profile and total active and reactive power loss are shown in Figure 4.5 and Figure 4.6.

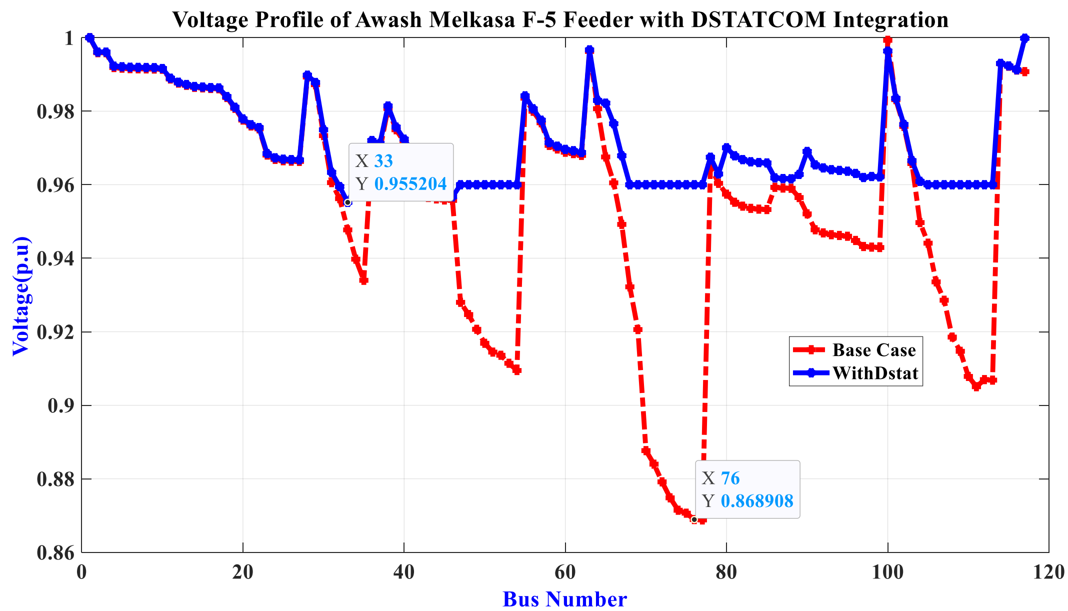

Figure 4.5: Voltage profile improvement using D-STATCOM

The voltage profile is improved when a single D-STATCOM integration occurs, as shown in Figure 4.5 above. The minimum voltage is 0.8689(p. u) before the installation of D-STATCOM. However, the addition of D-STATCOM voltage magnitude has increased to 0.955204(p. u). under the same condition, Figure 4.6 illustrates the power loss is mitigated when a single D-STATCOM integration at bus 65. For a single D-STATCOM installation, the active and reactive power loss is reduced by 26.456 percent and 26.497 percent respectively.

Table 4.2: Result summary of Scenario-III

Parameters	Base Case	Dstat1
Active power loss (KW)	1298.84	955.2189
Reactive power loss (KVAr)	987.991	726.2030
Execution time (sec.)	0.96038	13.7244
Minimum voltage (p.u) @bus No.	0.8689 @76	0.95802@33
Maximum voltage deviation (%)	13.109	4.198
Active power loss reduction (%)	NLL	26.456
Reactive power loss reduction (%)	NLL	26.497
DSTATCOM Location (Bus No.)	NLL	@65
DSTATCOM size in KVAr	NLL	1240

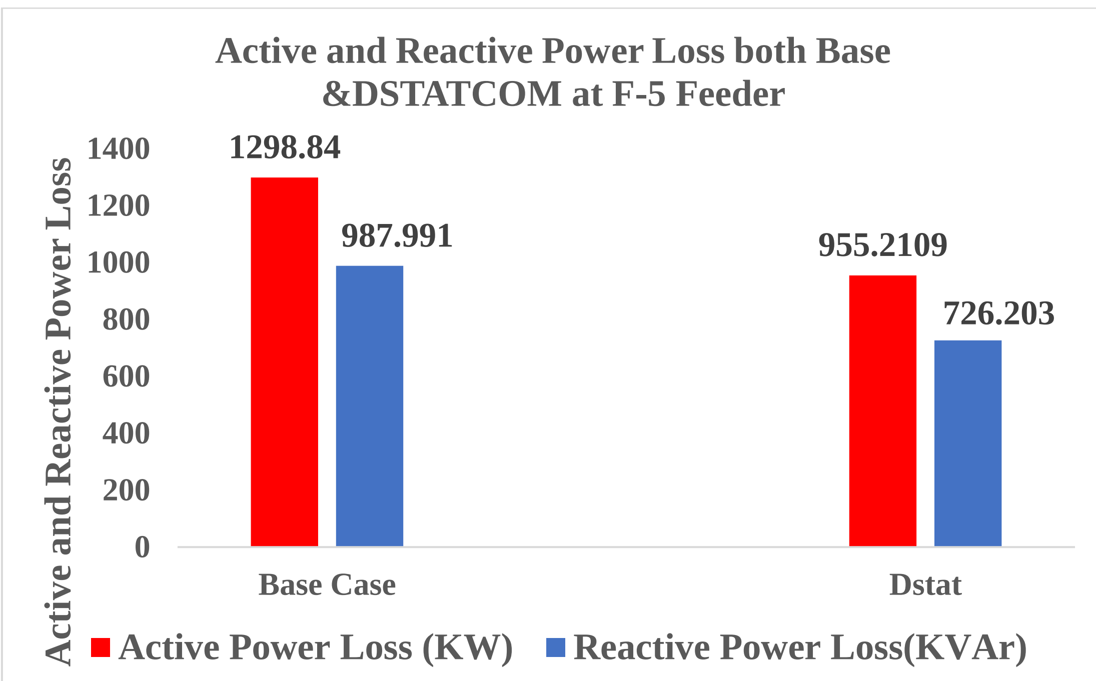

Figure 4.6: Total active and reactive power loss before and after DSTATCOM installation

4.4 Scenario IV: Simultaneous DG and DSTATCOM Integration

The previous discussion on scenarios II and III, DG and D-STATCOM integration improved the voltage profile and reduced power loss in the Awash Melkasa distribution system (F-five feeder) independently. The feeder F-five will not be improved well when DG and DSTATCOM integration is used independently. Through applying the WOA, the installations DG and D-STATCOM concurrently significantly improve the distribution system. The scenario where, simultaneous DG and D-STATCOM allocation is taken into consideration, Figure 4.7 shows the increase of the voltage profile and Figure 4.8 shows the reduction of the feeder total power loss.

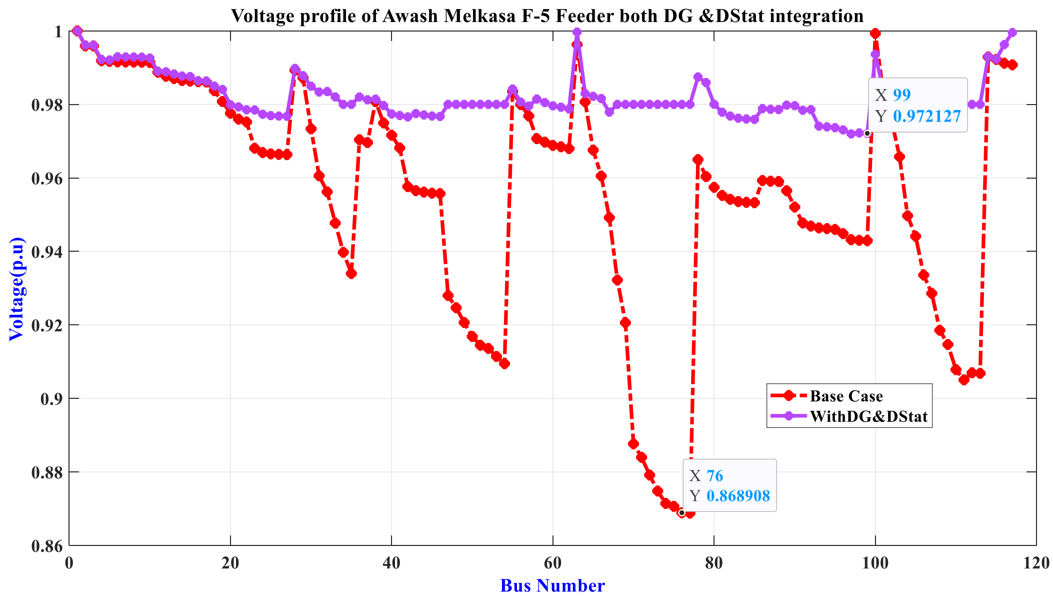

Figure 4.7: Voltage profile improvement using integration DG and D-STATCOM

Figure 4.7 illustrates that when integrating DG and D-STATCOM simultaneously, all bus voltage profiles are beyond the minimum nominal voltage. The base case's minimum voltage profile was 0.8689 p.u. However, after the installation of the DG and D-STATCOM, the voltage magnitude of the distribution feeder was significantly enhanced to 0.972127 p.u.

The overall active and reactive power losses of the feeder during simultaneous DG and D-STATCOM installation are also shown in Figure 4.8. When DG and D-STATCOM are installed, the reductions in active and reactive power loss are 79.117 % and 79.218%, respectively. This demonstrates that, from a technical standpoint, installing DG and DSTATCOM together was the best choice for reducing power loss and improving the voltage profile. The total size of single DG and DSTATCOM in scenarios II and III has no huge difference, as a result, the total investment cost for the two cases may not have a big gap. Therefore, installing simultaneously DG and D-STATCOM is preferable. The parameters due to the installation of both DG and D-STATCOM simultaneously are summarized and presented in Table 4.7 below.

Table 4.3: Results Summary of Scenario-IV

Parameters	**Base Case**	**Dstat-1&DG-1**
Active power loss (KW)	1298.84	271.2367
Reactive power loss (KVAr)	987.991	205.324
Minimum voltage (p.u) @bus No.	0.8689 @76	0.972127@99
Maximum voltage deviation (%)	13.109	2.773
Active power loss reduction (%)	-	79.117
Reactive power loss reduction (%)	-	79.218
DG location (Bus No,)	-	55
DG size in KW	-	1049
DSTATCOM Location (Bus No.)	-	105
DSTATCOM size in KVAr	-	1214

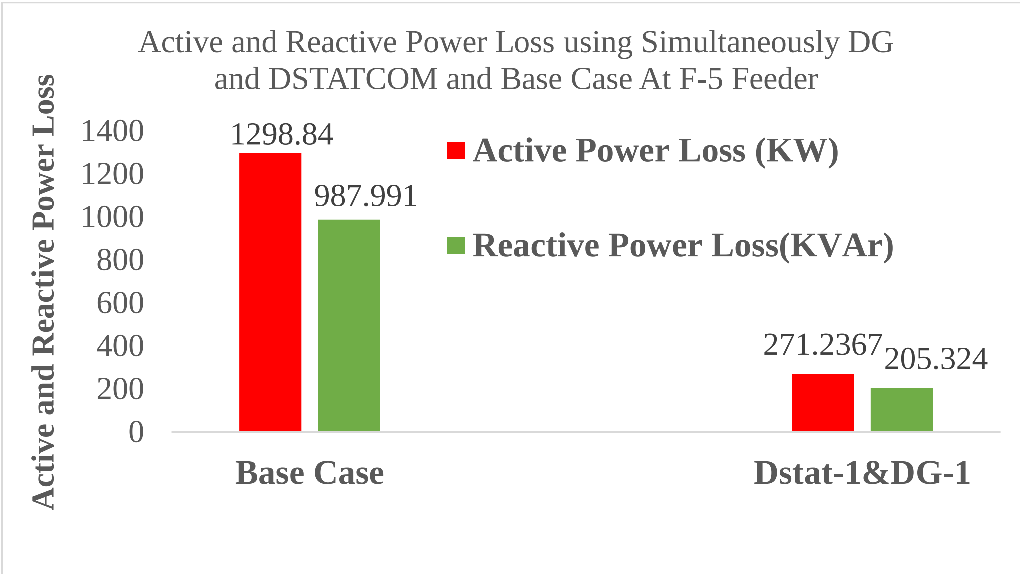

Figure 4.8: Power Loss after Simultaneously DG and D-STATCOM

4.5 General Discussion of the Results

Generally, the results from all scenarios are summarized and presented in Table 4.4. The percentage power loss reduction and enhanced voltage profile for each case are illustrated in Figures 4.9 and 4.10 respectively. The scenario two, distributed generation (DG) is installed to decrease power loss and enhance the voltage profile which analyzes the study of the F-5 feeder base case. The third scenario which is D-STATCOM integration is the best scenario based on the voltage profile improvement and power loss reduction. Finally, the greatest option for improving the Awash Melkasa F-5 feeders is scenario four, which integrates D-STATCOM and DG simultaneously into the feeder.

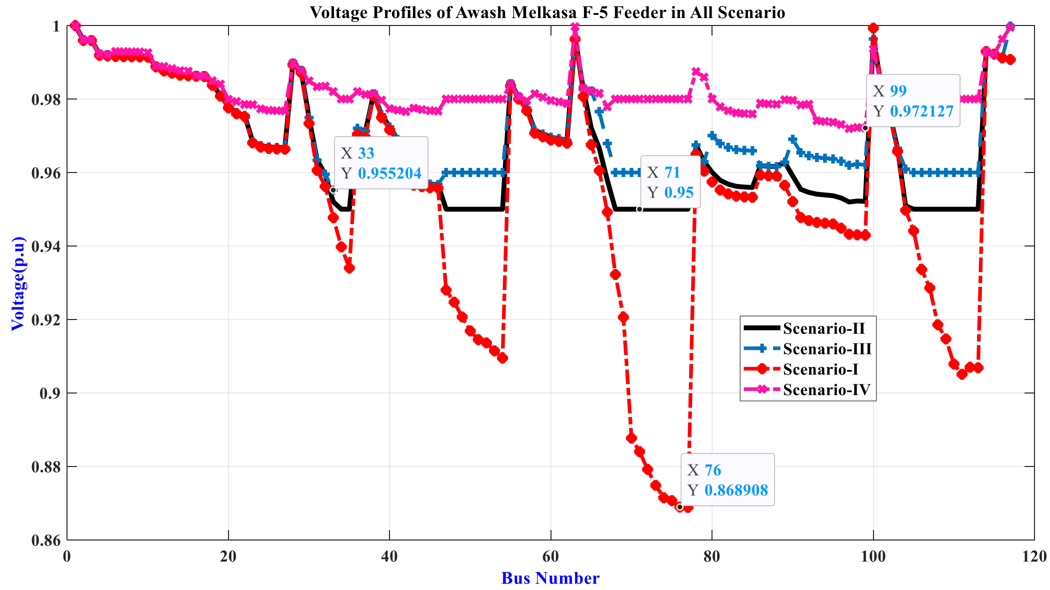

Figure 4.9: Voltage profile enhancement comparisons for all scenarios

Table 4.4: Result Summary of all Scenarios

Parameter Measurement	**Scenario I**	**Scenario II**	**Scenario III**	**Scenario IV**
Active power loss (KW)	1298.84	730.5532	955.2189	271.2367
Reactive power loss (KVAr)	987.991	545.3182	726.2030	205.324
Minimum voltage (p.u) @bus No.	0.8689@76	0.950@33	0.955204@33	0.9721@99
Maximum voltage deviation (%)	13.109	4.4799	4.198	2.773
Active power loss reduction (%)	-	44.5578	26.456	79.117
Reactive power loss reduction (%)	-	44.6838	26.497	79.218
DG location	-	@96	-	@55
DG size in MW	-	1129	-	1049
D-STATCOM Location	-	-	65	@105
D-STATCOM size in KVAr	-	-	1240	1214

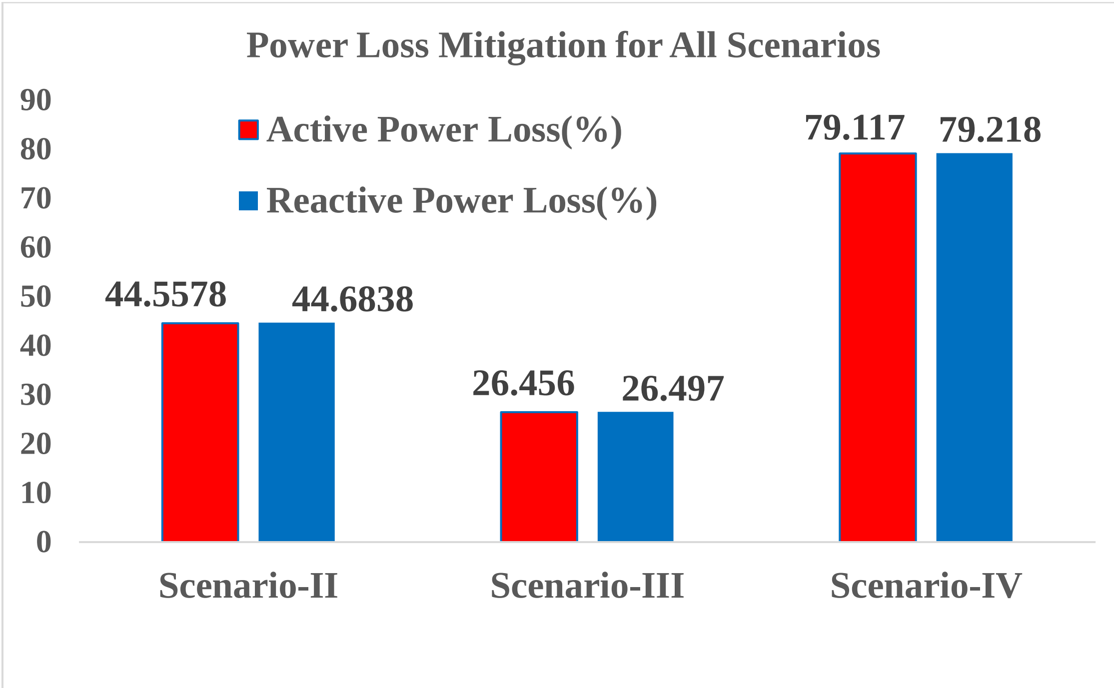

Figure 4.10: Total Power Loss Mitigation of all Scenarios

Table (4.8) shows above the voltage profile margins and the reduction in active and reactive power loss for each scenario. The findings indicate that, when implemented separately, each scenario contributes significantly to reducing the overall loss of active and reactive power and enhancing the voltage profile of the system. Nonetheless, it has been shown that the last scenario is simultaneous D-STATCOM, and DG allocation is the most effective for improving voltage profile and minimizing loss.

4.6. Cost Analysis and payback period

The economic feasibility of integrating devices into the Awash Melkasa (F-5) feeder is determined by saving the cost, which includes the cost of DG and D-STATCOM, and cost of energy loss, DG's energy supply, and total cost saving with a payback period.

Table 4.5: Ethiopia Electricity Prices

Ethiopia	Electric Price
Residential price	0.006
Business Prices	0.021
Measure	USD/KWh

Ethiopia Electricity price for business is ETB 1.223 KWh or 0.021 USD/KWh. The electricity price for residential is 0.349/KWh or 0.006 USD/KWh. this includes all components of electricity bill such, as cost of energy consumption, distribution and taxes shown Table (4.9) (Prices.com, 2023).

Cost of Energy Loss

The cost of energy loss in the feeder can be calculated by (Atma & Ashwani, 2022):

$$CEL = TAPF \times (EC \times H)\,ETB \tag{4.1}$$

Where, CEL is Total active power of the feeder, EC is energy cost rate (Birr/KWh), and a time measurement in hour (H).

EC=1.223Birr/KWh, H=8760h.

Cost Energy supplied by DG

The annually cost of supplied energy by DG can be calculated as:

$$CESDG = DG_{GP}(KW) \times (EC \times H) \tag{4.2}$$

Where, CESDG is Cost of energy supplied by DG and DG_{Gp} is generated power by DG.

$$CESDG = 1049\,KW \times 1.223 ETB / KWhr \times 8760 hr$$

$$CESDG = 11,238,440.52 \text{ ETB}$$

The total cost of energy loss of Awash Melkasa (F-5) feeder before DG and D-STATCOM installation (Scenario-1) can be calculated as follows.

Annual energy loss of Awash Melkasa (F-5) feeder as follows.

$$AEL = PL \times H \tag{4.3}$$

Where, AEL is annual energy loss and PL is total active power loss of feeder five.

From equation (4.3) annual energy loss calculated as follows.

$$AEL = PL \times 8760hrs$$
$$AEL = 1298.84KW * 8760hrs$$
$$AEL = 11,377838.4KWhr$$

Based on the new EEU tariff, the average of the first block and general tariff is 1.223 Birr//KWh as shown in Table (4.9) above.

Energy cost loss is Annual Energy loss multiplied by energy cost rate

Use equation (4.1) to evaluate annually cost of energy lost

$$ACEL = 11,377838.4\ KWhr \times 1.223ETB / KWhr$$
$$ACEL = 13,915,096.3632\ ETB$$

From simulation result simultaneously DG and D-STATCOM condition is preferred with 1049 KW DG and 1214 KVAr size of D-STATCOM.

After this integration DG and DSTATCOM, the power loss can be calculated as follows:

$$AEL = 355.4124KW * 8760hrs$$
$$AEL = 3,113,412.624KWhr$$
$$CEL = 3,113,412.624\ KWhr \times 1.223ETB / KWhr$$
$$CEL = 3,807,703.639ETB$$

The power loss after integration of DG and DSTATCOM simultaneously is 355.4124KW which means the cost of energy loss is reduce to 3,807,703.639 ETB per year. This shows that 10,107,392.72 (around ten million) Birr per year can be saved when DG and D-STATCOM integration in optimal size and location on the F-5 feeder.

The total cost of the proposed solution depends on the investment cost of DG and D- STATCOM. In previous chapter based on the assessment of DG choose solar PV-DG to integrate into F-5 feeder with DSTATCOM simultaneously. The total cost of solar PV-DG installation fluctuates from time to time. However, it changes at a decreasing rate. Thanks to the development of solar PV modules through technology, improvements in manufacturing, economies of scale, lower costs for the Balance of the System (BoS), and the rapid growth of solar PV-DG installations. The manufacturer and technology determine the cost of installation. However, the investment cost of PV-DG is estimated by using the U.S. Solar Photovoltaic System and Energy Storage Cost Benchmarks (Q1 2023) (Vingnesh , et al., 20223).

The investment cost of PV-DG in suggested distribution feeder is calculated as follows.

$$ICPVDG = PVDG_{GP} \times \mathrm{Cos}\,t\ in\ dollar\ \ per\ watt \tag{4.4}$$

Where, ICPVDG is investment cost of PV-DG, $PVDG_{GP}$ is power generating by PVDG and optimal capacity of DG in Scenario IV is 1049 KW.

$$ICPVDG = PDG \times USD\,/\,watt$$
$$ICPVDG = 1.049MW \times 1.49\$\,/\,w$$
$$ICPVDG = 1{,}563{,}010\ Dollar$$

Based on benchmark data of the USA for 2023, the average installed cost for a PV fixed-tilt utility-scale system is 1.49$/W.

So, the investment cost of solar based distribution generation is 1,563,010.00 $ or 90,913,727.05 8 ETB. Based on the Commercial Bank of Ethiopia (CBE) exchange rate on 24- May- 2024, (1$=58.1658 ETB). The cost of supplied energy by DG is 11,238,440.52 ETB per year.

Equation (4.4) can also be used to determine the cost of reactive power that the D-STATCOM provides. The D-STATCOM cost per KVAr is 50 dollars (Atma & Ashwani, 2022).

$$\mathrm{Cost}_{DSTATCOM} = Investment\_\mathrm{Cos}\,t_{DSTATCOM} \times \left(\frac{(1+B)^{nDST} \times B}{(1+B)^{nDST} - 1} \right) \tag{4.4}$$

Where, nDST=30 years is DSTATCOM length of life in year, B=0.1 is asset of return, $Investment_{cost}$=50$/KVAr and optimal capacity of DSTATCOM is 1214 KVAr in scenario IV. Investmentcost=60,700 Dollar. So, the investment cost of DSTATCOM is 60,700 $ or 3,530,664 .06 ETB. Based on the Commercial Bank of Ethiopia (CBE) exchange rate on 24- May- 2024, (1$=58.1658 ETB).

$$T\,\mathrm{Cos}\,t_{DSTATCOM} = 3{,}530{,}664.06\ ETB \left(\frac{(1+0.1)^{30} \times 0.1}{(1+0.1)^{30} - 1} \right)$$
$$T\,\mathrm{Cos}\,t_{DSTATCOM} = 3{,}530{,}664.06\ ETB \times 0.106079$$
$$T\,\mathrm{Cos}\,t_{DSTATCOM} = 374{,}530.192\ ETB$$

The optimized D- STATCOM capacity is 1214 KVAr. So that the total cost of D-STATCOM is 374,530.192 ETB.Based on the calculation of the total capital cost for DG and DSTATCOM, the economic feasibility of the investment was evaluated by computing the payback period. The payback period, which is the time required to recover the cost of an investment, is calculated as the ratio of net investment to net annual return. The net investment encompasses the entire cost of D-STATCOM and DG investments, while the net annual return includes the cost of energy supplied by DG and the cost savings from reduced losses.

$$Payback\ period = \frac{Net\ investment}{Net\ Annual\ \mathrm{Re}turn}$$

$$PB_{period} = \frac{Investment\ \cos t\ \ for\ DG + Investment\ \cos t\ for\ DSTATCOM\ /}{Saved\ energy\ loss\ \cos t + \cos t\ of\ \sup plied\ energy\ by\ DG}$$

$$PB_{period} = \frac{90,913.727.058\ ETB + 374,530.192\ ETB}{10,107,392.72\ ETB + 11,238,440.52\ ETB}$$

$$PB_{period} = \frac{91,261,252.25\ ETB}{21,345,833.24\ ETB} = 4.275\ years.$$

Table 4.6: Result summary of cost analysis

Annual Cost of energy and Investment cost of devices	Total cost of the system in ETB
Cost of Energy loss of feeder	13,915,096.3632
Cost of Energy Supplied by DG	11,238,440.52
Saving Energy Cost after DG and DSTATCOM integration	10,107,392.72
Investment Cost of DG	90,913,727.058
Investment Cost of DSTAT.	374,530.192
Net Investment Cost	91,261,252.25
Net Return Cost	21,345,833.24

NB net payback period is 4.275 years

5.CONCLUSIONS AND RECOMMENDATIONS

5.1. Conclusions

The main problems in the distribution system are power loss, poor voltage profile, high power interruption, distorted voltage and current at the customer end, and unstable voltage in the node of the system; thus, a technical solution is required to resolve those issue. The optimal size and location of the DG and D-STATCOM have been used in this thesis work to solve the power problems that occurs in the distribution system.

Basic methods that have been used in this thesis are backward -forward load flow analysis, and Whale optimization algorithm (WOA). A backward -forward load flow analysis method was used to find each bus voltage and active and reactive power losses before and after the integration of DG and D-STATCOM. The WOA was used to decide the optimal size and location of the two devices. The proposed method has been implemented on feeder F-5 (feeder five) of the Awash Melkas distribution substation. It has 117 branches and 118 buses. The base case real and reactive power losses are 1298.84 KW and 987.991KVAr respectively and forty-five and 12/100 (45.12%) buses have below standard voltage levels. Optimization problem was formulated as multi-objective functions comprising total real power loss, total reactive power loss, and voltage deviation for optimal siting and sizing of DG and D-STATCOM using the WOA algorithm. The simulation results were tested by considering different scenarios.

The integration Only DG (scenario-II), integration only D-STATCOM (scenario-III), and simultaneous integration (scenario- IV) scenarios were considered. The first two scenario which integration independently to improve voltage and reduce power loss. but the third scenarios are the best as compared the second scenario. Finally, scenario four was the best case for improve voltage profile and power loss mitigation of Awash Melkasa (F-5) feeder. The optimal simultaneous placement and sizing of DG and DSTATCOM were determined to be at buses 55 and 105 of the F-five feeder, with the DG rated at 1,049 MW and the DSTATCOM rated at 1,214 MVAr, respectively. After implementing the WOA method to study the effect of a DG and DSTATCOM on voltage profile and power loss. The effect of installation of DG on scenario II has no logger effect than the effect of DSTATCOM on scenario III was significant impact in the system. From the simulation results, the percentage of active power loss reduction was 44.5578%, 26.456 % and

79.117 % whereas the percentage of reactive power loss reduction was 44.6838%, 26.497 % and 79.218 % for scenario-II, scenario-III, and scenario-IV best-case respectively. Also, the minimum voltage level in the base case is improved from 0. 8689p.u to 0. 95p.u, 0.955204p. u, and 0.97227 p.u. Therefore, Scenario IV is the most effective Scenario for power loss reduction and voltage profile improvement as seen from the results. However, Cost analysis is required when developing a solution to a problem. In this regard, a cost-benefit analysis of the generated solution has been performed. The cost analysis showed that Simultaneous DG and D- STATCOM integration needs an initial capital cost of 91,261,252.25 birrs with a four year and three-month payback period. In another word, 21,345,833.24 ETB can be saved each year after four years and three months when applying this solution.

5.2 Recommendations

This study is beneficial to both the utility and customers, directly and indirectly. Some of the direct benefits of Awash Melkasa (F-5) feeder include reducing both active and reactive power loss. This improvement increases profit margins and raises the voltage level at the customer side to the required standard, leading to a reliable and secure power supply and greater customer satisfaction. I highly recommend that Ethiopia Electric Utility apply this method in the Awash Melkasa distribution system to reap these benefits.

5.3. Suggestions for Further Work

No scientific study can address all aspects and significant issues simultaneously; some points will need to be explored in future research. Here are some potential future research areas:

1. Impact of Harmonics: Investigate the impact of harmonics, as RES-based DG uses power electronics, which are major sources of harmonics injected into the system.

2. Expanded Objective Function: Consider other power system parameters in the objective function, such as stability issues and short circuit levels.

3. Algorithm Comparison: Compare the results of the WOA with other optimization algorithms and utilize hybrid WOA with other optimization techniques for mitigating power loss and voltage profile.

REFERENCE

Abayneh, B. (2022). *STUDY ON THE POWER LOSS REDUCTION AND VOLTAGE PROFILE IMPROVEMENT OF KOTEBE DISTRIBUTION SYSTEM BY OPTIMAL PLACEMENT OF D-STATCOM USING A HYBRID OF GENETIC ALGORITHM AND PARTICLE SWARM OPTIMIZATION METHOD.* Addis Ababa Institute of Technology, Electrical and Computer engineering.

Abdeljabbar, C., & Saad, O. (2020, Janury 17). An Improved Backward/Forward Sweep Power Flow Method Based on a New Network Information Organization for Radial Distribution Systems. (F. Salvatore, Ed.) *HIndawi*.

Adetokun, B. B., & Muriithi, C. M. (2021, Murch). Application and control of flexible alternating current transmission system devices for voltage stability enhancement of renewable-integrated power grid. *Heliyon, 7*(3).

Alireza, N., Yiming, Z., Negar, N., & Mohammad, H. (2021). Multi-Objective Optimal Placement and Sizing of Distribution Static Compensator in Radial Distribution Networks with Variable Residential,Commertial and industrial Demands Considering Reliability.

Alyu, A. B. (2022). *Performance Enhancement of Distribution System Using Optimal Allocation of Solar Based Distributed Generation and D-STATCOM* . Adama Science and Technology University.

Argaw, A. (2021). *DISTRIBUTION NETWORK OPTIMIZATION BY OPTIMAL SIZING AND PLACEMENT OF D-STATCOM USING TEACHING AND LEARING BASED OPTIMIZATION ALGORITHIM (CASE STUDY: YIRGALEM SUBSTATION).*

Asghar, W. (2024, April 5). Per Unit System in PE Power Exam. *Study for FE*, 3-4. Retrieved from https://books.google.com.et/books/about/Fundamentals_of_Engineering_FE_Electrica.

Ashraf, R., Mohamed, E., & Salah, K. (2019, February). Performance Assessment of a Realistic Egyptian Distribution Network Including PV Penetration With DSTATCOM. *IEEE*, 4-6. doi:10.1109/ITCE.2019.8648473

Asmaa, N., Abdullah, S., & Heba, K. (2022, Aprill). Local and remote control of automatic voltage regulators in distribution networks with different variations and uncertainties: Practical cases study. *ELSEIER*, *205*.

Assen , B. A., & DR.Tefera, T. Y. (2023, Agust). Optimal Placement and Size of Multiple PV-DG Units for Power Loss Reduction and Voltage Profile Improvment in Dilla Distribution Network. (H. W. Bereket, M. Kibret, Z. G. Muluken, G. M. Eshetu, & A. A. Addisu, Eds.) *Springer*, 179.

Atma, R. G., & Ashwani, K. (2022, April 20). Optimal Placement of DSTATCCOM Using Sensitivity Approches in Mesh Distributin System with Time Variant Loads Models Under Load Growth. *REsearchGate*, 4. Retrieved from www.SCiencedirect.com

Ayman, M. (2022, October). Learn how to Interpret and Design Single-Line Diagrams(SLD) for Complex Projects. *EEP*, 1-2.

Ayooluwa, P. A., Funso, K. A., Kehinde, A. M., Sunday, A. S., Oludamilare, B. A., & Olusola, K. A. (2022, February 15). Integration of Solar Photovoltaic Distribution Generators in Distribution Networks Based on Site's Condition. (J. H. Werne, Ed.) *Solar*, 52-63.

B. M., M. T., & B. T. (2020). Optimal DG Unit Placement and Sizing in Radial Distribution Network for Power Loss Minimization and Voltage Stability Enhancement.

Bazilah, I., Noor, I. A., Muhammed, L. O., Kanenara, N. V., Mohd, A. M., & Muhammed, N. M. (2020). A Comprehensive Review on Optimal Location and Sizing of Reactive Power Compensation Using Hybrid-Based Approaches for Power Loss Reduction, Voltage Stability Improvement, Voltage Profile Enhancement and Loadability Enhancement.

Bhavna , R. (2023). Distribution Flexible AC Transmissin Sytem (D-FACTs).

Bikash, K. S., Aashish, K. B., Jalpa H., J., & Mohan, L. K. (2022, Decemberr). Solar-DG and DSTATCOM Concurrent Planning in Reconfigured Distribution Sytem Using APSO andGWO-PSO Based on Novel Objective Function. *energies*.

Daware, K. (2018, November). Electric power distribution system. *ResearchGate*, 5-6.

Dikio, I., & Ezenwa, U. (2018). Impact of Distribution Generation from Solar Energy on Power Sytem Distribution in Nigeria. *Electrical and electronics*.

Ganguly, A., Manna, N., Mondal, S., & Roy, P. (2020). Power Flow Congestion Management Using Distributed FACTS Devices. *VOL 7*(ISSUE 07).

Gurpreet, K., & Asst.prof.Harmeet, S. G. (2017, July). Power Flow Analysis of Radial Distribution System using Backward/Forward Sweep Method. *IJRASET, 5*(VII), 204-207.

Hermanus, L. W., Ramesh, C., & Raj, N. (2020, September). PV Based Distribution Generation Power Protection. *Renewable Energy Focus, 34*, 58.

Kallon, M. A., Nyakoe, G. N., & Muriithi, C. M. (2021). Development of D-STATCOM Optimal Sizing and Location Techniques Based on IA-GA for Power Loss Reduction and Voltage Profile Enhancement in an RDN.

Khan, M. H., Abasin, U., Abraiz, K., Haris, s. Z., Mohammad , A., Ahmad , A. A., & Nusim , U. (2022). Optimal Sizing and Allocation of Distributed Generation in the Radial Power Distribution System Using Honey Badger Algorithm.

KJV, A. P. (2010). *Technical Data Sheet.* DNV.

Mohammed, B. L., Ahmet, T., & Yeliz, Y. (2015, June). Mitigation of Power Quality Problems Using Distribution Synchronous Compoensator. *WILEY, 8*(7), 1312-1328.

Muhammad, I. A., Syed, A. A., & Omar, A. (2022). A novel hybrid optimization-based algorithm for the single and multi-objective achievement with optimal DG alocation in distribution network.

Muquthiar, A. S., Gadana, L. M., & Visali, N. (2022). Enhancement of Voltage Profile in the Distribution System by Reconfiguring with DG and Placement using Equilibrium Optimizer.

N. H. Baharudin,, T. M. N. T. Mansur, R. Ali, S. I. S. Hassan , & P. Saad . (2021). Technical and Economic Evaluation of a Solar Photovoltaic (PV) based Distribution Static Synchronous Compensator (DSTATCOM). 1-2.

P.Dinakara, P. R., V.C. Veera, R., & T.Gowri, M. (2019, Augest 12). Whale Optimization Algorithm for Optimal sizing of Renewable Resource for Loss Reduction in Distribution System. *Springer open*, 3-5.

Pareja, L. A., Lezama, J. M., & Carmona, O. G. (2023). Optimal Integration of Distribution Network Reconfiguration and Condactor Selection in Power Distribution System via MILP.

Prashant, Anwar, S. S., Sarwar, M., Ahmed, A., & Sherif, S. G. (2022). "optimal location and sizing of distribution genarator in power system network with power quality enhancement using fuzzy logic controlled D-STATCOM".

Prices.com, G. P. (2023). *Ethiopia Electricity Prices.* Retrieved from Global Petrol Price.com

Provas, K. R., & Suvabrata, M. (2022, May 27). Whale Optimization Algorithm -Based DG Alloatment for loss Minimization of Distribution network. *IGI Global*, 52.

R. S., & Jordehi, A. R. (2017, September). Optimal placement and sizing of distribution static compensator (D-STATCOM) in electric distribution networks. *ELSEIER*, *77*, 688-694.

S.Balakumar, Akililu, G., Samuel, K., & K.Bamash, K. (2021). Improvement of Voltage Profile and Loss Reduction in Distribution Network Using Moth Flame Algorithm: Wolaita Sodo,Ethiopia.

Saad, O., & Abdeljabbar , C. (2020). An Improved Backward/Forward Sweep Power Flow Method Based on a Nework Information Organization for Radial Distribution Systems. *Journal of Electrical and Computer Engineerimg*.

Sachidonondo, S., & Moneesh, K. (2023, May 1). Reference Module in Earth System and Enviromental Sciences. *ScienceDirect*.

Salkuti, S. R. (2019). Optimal Location and Sizing of DG and D-STATCOM in Distribution Network.

Singh, E. J. (2018, August). Real Time Study on Technical and non-technical Losses in Distribution System and reduction techniques. *5*(3).

Sunday, A. S., Hassan, A. A., Fajuke, I. D., & Kamilu, A. S. (2019). Load Flow Analysis of Nigerian Radial Distribution Network Using Backward/Forward Sweep Techniques. *VLSI*, *2*(3), 5.

Talukdar, B. K. (2019). Electrical Distribution Power system.

Tanish, D., Srijan, C., & Tajender, M. (2022, May). Load Flow Analysis Using Forward and Backward Sweep, and Minimizing Power Losses Using Genetic Algorithm. *IJAEM*, *4*(5), 763-5252.

Tejas, Z., Bhavesh , B., & Naimish, Z. (2020, December). Comparison of Control Strategies for DSTATCOM in Three-Phase, Four-Wire Distribution System for Power Quality Improvement Under Various Source Voltage and Load Conditions. *ijepes*.

Tesfay, K. G. (2018). *SIZING AND PLACEMENT OF DISTRIBUTED GENERATION INDISTRIBUTION SYSTEMS FOR VOLTAGE IMPROVEMENT AND POWERLOSS REDUCTION.* BAHIR DAR INSTITUTE OF TECHNOLOGY, FACULTY OF ELECTRICAL AND COMPUTERENGINEERING.

Umar, M. (2017). *Application of Improved Bacterial Foraging Algorithm to the Optimal Siting and Sizing of D-STATCOM in Radial Distribution Networks.* ResearchGate.

Vingnesh , R., Jarett, Z., Michael, W., Eric, O., David, F., Jal, D., . . . Paul, D. (20223). *U.S. Solar PhotoVoltic System and Energy Storage Cost Benchmarks,with Minimum Sustainable Prices Analysis Q1 2023.* Department of Solar Energy Office. NREL.

www.Maps.com. (2023).

Zaenab, M., Riskiani, Idar, C. G., & Agus, S. (2022, Novemeber 16). Study of Distribution Static Componsator(D-STATCOM) Installation in Melkassar Electric Energy Distribution Sstem. *APL Quantum*.

Zakir, H., Neem, S., & Neeraj, G. (2018, November 5). Steady State Analysis of Distribution Sytem With Wind Generation Uncertainty. *12*, 306. Retrieved from scholar.waset.org

APPENDIXES

Appendixes-A: Annually Interruption Data for Awash Melkasa substation outgoing Feeders

Table Appendix-A1: Three-year (2013,2014 and 2015E.C) interruption

Feeder name	Interruption	2013E.C	2014E.C	2015E.C	PL(MW) 2014E.C
F-01	TNFI	20	28	28	1.67
	TNDI	82.633	167.8	178.99	
F-02	TNFI	97	61	55	0.89
	TNDI	189.124	135.5	78.84	
F-03	TNFI	183	165	23	1.44
	TNDI	221.993	157.32	47.5	
F-04	TNFI	428	549	275	4.22
	TNDI	411.313	558.56	383.98	
F-05	TNFI	488	1108	336	6.32
	TNDI	527.112	1788.4	532.26	
Amude	TNFI	316	418	236	1.46
	TNDI	373.075	830	369.57	
Industry 1	TNFI	77	711	53	5.55
	TNDI	124.728	709.1	51.80	
Industry 2	TNFI	*	265	61	4.37
	TNDI	*	614.8	62.07	

Note: TNFI=Total Number of Frequency Interruption

TNDI=Total Number of Duration Interruption (Hr.) *=No recorded data

PL=Peak Load

Table Appendix-A2:2013 E.C interruption data of Awash Melkasa substation outgoing feeder

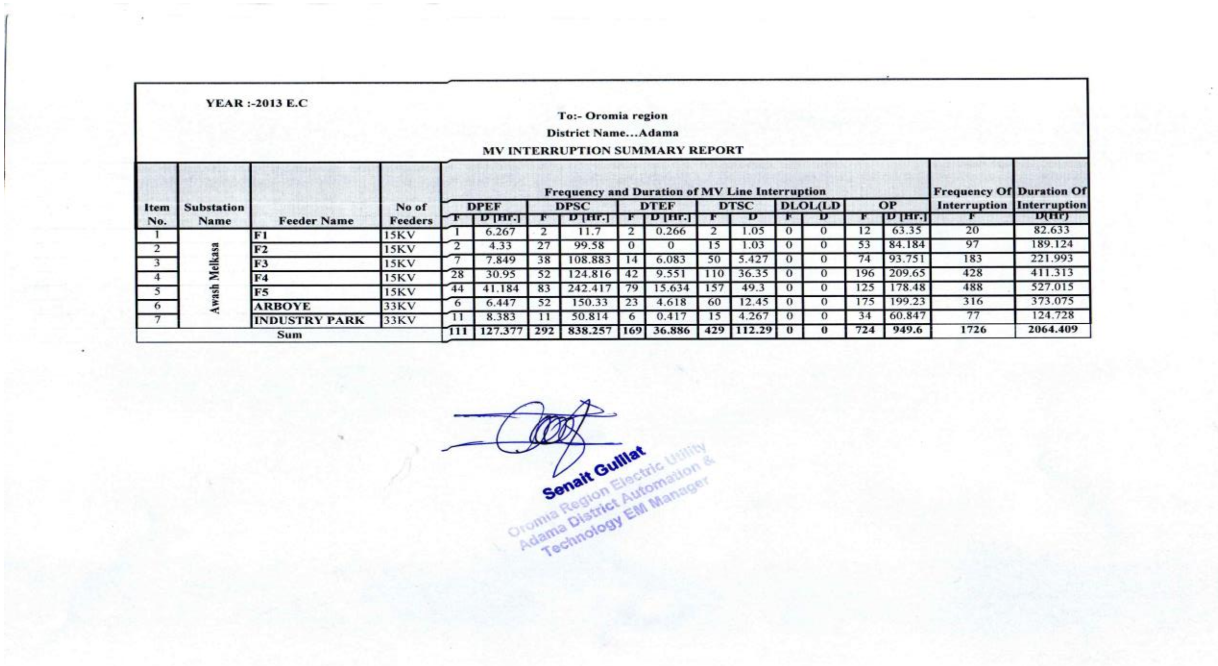

YEAR :-2013 E.C To:- Oromia region District Name…Adama MV INTERRUPTION SUMMARY REPORT																	
Item No.	Substation Name	Feeder Name	No of Feeders	Frequency and Duration of MV Line Interruption												Frequency Of Interruption	Duration Of Interruption
				DPEF		DPSC		DTEF		DTSC		DLOL(LD		OP			
				F	D [Hr.]	F	D [Hr.]	F	D [Hr.]	F	D	F	D	F	D [Hr.]	F	D(Hr)
1	Awash Melkasa	F1	15KV	1	6.267	2	11.7	2	0.266	2	1.05	0	0	12	63.35	20	82.633
2		F2	15KV	2	4.33	27	99.58	0	0	15	1.03	0	0	53	84.184	97	189.124
3		F3	15KV	7	7.849	38	108.883	14	6.083	50	5.427	0	0	74	93.751	183	221.993
4		F4	15KV	28	30.95	52	124.816	42	9.551	110	36.35	0	0	196	209.65	428	411.313
5		F5	15KV	44	41.184	83	242.417	79	15.634	157	49.3	0	0	125	178.48	488	527.015
6		ARBOYE	33KV	6	6.447	52	150.33	23	4.618	60	12.45	0	0	175	199.23	316	373.075
7		INDUSTRY PARK	33KV	11	8.383	11	50.814	6	0.417	15	4.267	0	0	34	60.847	77	124.728
Sum				111	127.377	292	838.257	169	36.886	429	112.3	0	0	724	949.6	1726	2064.409

Where DFET is duration of permanent earth fault, DTEF is duration of temporary fault, DPSC is duration of permanent short circuit fault, and LDC is duration of interruption by load dispatch center. OP is interruption of operation due to maintenance and emergency. The recorded data of 2013 E.C in above table appendix-B are in Awash Melkasa substation outgoing feeder are six feeders have recorded data on the report of 2013.Total interruption frequency of years and total number of durations of industry 2 is no data on the report.

2014 E.C interruption data of Awash Melkasa substation outgoing feeder

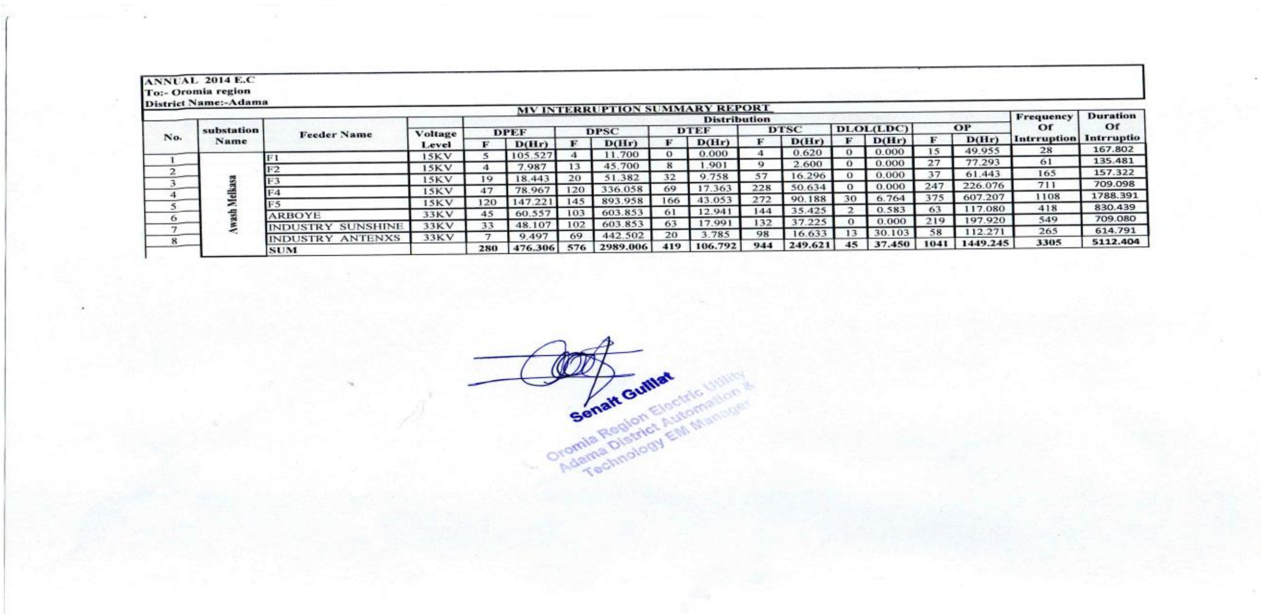

ANNUAL 2014 E.C
To:- Oromia region
District Name:-Adama

MV INTERRUPTION SUMMARY REPORT

No.	substation Name	Feeder Name	Voltage Level	Distribution												Frequency Of Intrruption	Duration Of Intrruptio
				DPEF		DPSC		DTEF		DTSC		DLOL(LDC)		OP			
				F	D(Hr)	F	D(Hr)	F	D(Hr)	F	D(Hr)	F	D(Hr)	F	D(Hr)		
1	Awash Melkasa	F1	15KV	5	105.527	4	11.700	0	0.000	4	0.620	0	0.000	15	49.955	28	167.802
2		F2	15KV	4	7.987	13	45.700	8	1.901	9	2.600	0	0.000	27	77.293	61	135.481
3		F3	15KV	19	18.443	20	51.382	32	9.758	57	16.296	0	0.000	37	61.443	165	157.322
4		F4	15KV	47	78.967	120	336.058	69	17.363	228	50.634	0	0.000	247	226.076	711	709.098
5		F5	15KV	120	147.221	145	893.958	166	43.053	272	90.188	30	6.764	375	607.207	1108	1788.391
6		ARBOYE	33KV	45	60.557	103	603.853	61	12.941	144	35.425	2	0.583	63	117.080	418	830.439
7		INDUSTRY SUNSHINE	33KV	33	48.107	102	603.853	63	17.991	132	37.225	0	0.000	219	197.920	549	709.080
8		INDUSTRY ANTENXS	33KV	7	9.497	69	442.502	20	3.785	98	16.633	13	30.103	58	112.271	265	614.791
		SUM		280	476.306	576	2989.006	419	106.792	944	249.621	45	37.450	1041	1449.245	3305	5112.404

ANNUAL 2014 E.C
To:- Oromia region
District Name:-Adama

MV INTERRUPTION SUMMARY REPORT

No.	substation Name	Feeder Name	Voltage Level	Distribution												Frequency Of Intrruption	Duration Of Intrruption
				DPEF		DPSC		DTEF		DTSC		DLOL(LDC)		OP			
				F	D(Hr)	F	D(Hr)	F	D(Hr)	F	D(Hr)	F	D(Hr)	F	D(Hr)		
1	Awash Melkasa	F1	15KV	5	105.527	4	11.700	0	0.000	4	0.620	0	0.000	15	49.955	28	167.802
2		F2	15KV	4	7.987	13	45.700	8	1.901	9	2.600	0	0.000	27	77.293	61	135.481
3		F3	15KV	19	18.443	20	51.382	32	9.758	57	16.296	0	0.000	37	61.443	165	157.322
4		F4	15KV	47	78.967	120	336.058	69	17.363	228	50.634	0	0.000	247	226.076	711	709.098
5		F5	15KV	120	147.221	145	893.958	166	43.053	272	90.188	30	6.764	375	607.207	1108	1788.391
6		ARBOYE	33KV	45	60.557	103	603.853	61	12.941	144	35.425	2	0.583	63	117.080	418	830.439
7		INDUSTRY SUNSHINE	33KV	33	48.107	102	603.853	63	17.991	132	37.225	0	0.000	219	197.920	549	709.080
8		INDUSTRY ANTENXS	33KV	7	9.497	69	442.502	20	3.785	98	16.633	13	30.103	58	112.271	265	614.791
		SUM		**280**	**476.306**	**576**	**2989.006**	**419**	**106.792**	**944**	**249.621**	**45**	**37.450**	**1041**	**1449.245**	**3305**	**5112.404**

Where; F is the frequency of earthing and short-circuit fault interruption, D is duration of short-circuit, earthing fault, operation and LD is load dispatch and Hr. is hours.

Table Appendix-A3:2015 E.C interruption data of Awash Melkasa substation outgoing feeder

Month :-Annual 2015 E.C
To:- Oromia region
District Name:-Adama

MV INTERRUPTION SUMMARY REPORT

No.	substation Name	Feeder Name	Voltage Level	Distribution DPEF F	DPEF D(Hr)	DPSC F	DPSC D(Hr)	DTEF F	DTEF D(Hr)	DTSC F	DTSC D(Hr)	DLOL(LDC) F	DLOL(LDC) D(Hr)	OP F	OP D(Hr)	Frequency Of Intrruption (No.)	Duration Of Intrruption (Hr.)
1	Awash Melkasa	F1	15KV	1	24.28	15	116.53	0	0.00	6	0.87	1	4.00	5	33.30	28	178.99
2		F2	15KV	2	11.33	13	37.90	2	0.18	14	3.32	0	0.00	24	26.10	55	78.84
3		F3	15KV	0	0.00	8	24.80	0	0.00	2	0.20	1	4.97	12	17.53	23	47.50
4		F4	15KV	6	14.93	85	251.17	9	0.93	114	22.82	5	13.68	56	80.43	275	383.98
5		F5	15KV	37	107.32	94	383.77	48	8.37	141	22.51	0	0.00	16	10.20	336	532.17
6		ARBOYE	33KV	7	32.04	61	159.77	4	0.70	55	8.60	13	58.86	96	109.59	236	369.56
7		INDUSTRY SUNSHINE	33KV	3	13.17	7	10.53	8	1.87	19	2.38	3	0.53	13	23.32	53	51.80
8		INDUSTRY ANTENXS	33KV	7	13.73	11	24.72	9	1.23	21	3.10	0	0.00	13	19.28	61	62.07
		SUM		**63**	**216.81**	**294**	**1009.20**	**80**	**13.28**	**372**	**63.81**	**23**	**82.05**	**213**	**319.75**	**1067**	**1704.90**

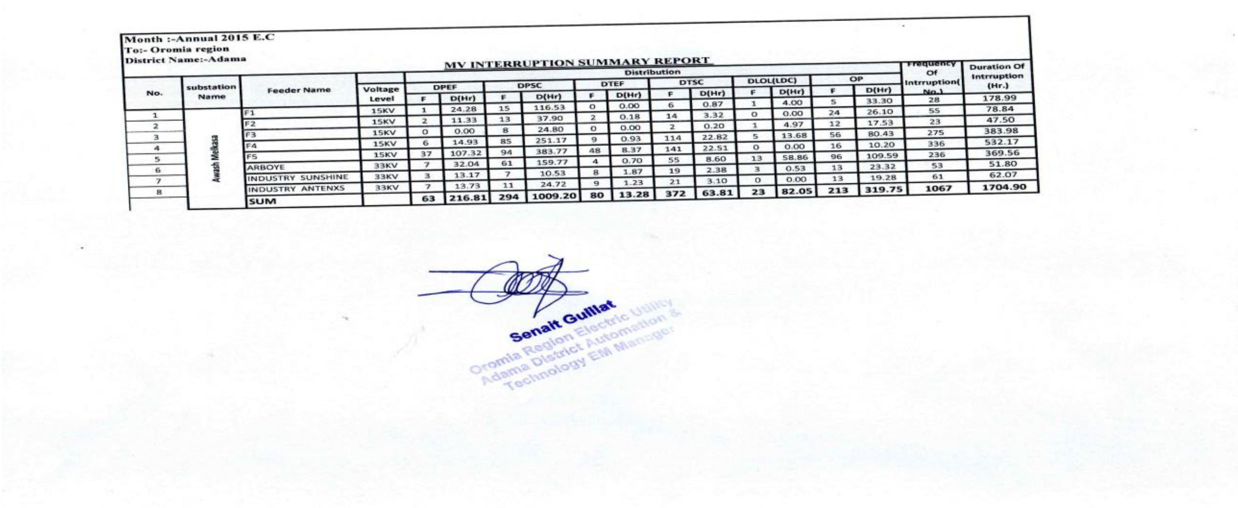

Total interruption of three consecutive years of feeder five from above are

- First year: TNFI is 488 and TNDI is 527.015
- Second year: TNFI is 1108 and TNDI is 1788.391
- Third year: TNFI is 336 and TNDI is 532.17 respectively.

From those three years maximum frequency of interruption and duration (Hrs.) can be recorded in second years (2013). According to the data frequency of interrupting and duration increased from 2013 to 2014 and back decrease those value from 2014 to 2015.

Table Appendix-A4: feeder of Awash Melkasa distribution substation with their network types

Adama District MV Feeders With Their Network Types and data that gathered in 2014.E.C															
No.	Substation	Feeder Name	voltage level	Feeder Capacity(CT)	Feeder Peak load(MVA)	Feeder Length (km)	Network Type		concrete/wooden pole Length(km)		Forced Permanet		Planned /Operation		
							Number of Concrete Pole	Number of Wooden pole	concrete pole(km)	wooden pole(km)	SAIFI (FP)	SAIDI (hrs) (FP)	SAIFI (P/OP)	SAIDI (hrs) (p/op)	
1	Awash Melkasa	F1	15KV	600/5	1.67	6.836	0	162	0	6.836	10.28	68.565	13.5	56.653	
2		F2	15KV	600/5	0.89	11.568	0	251	0	11.568	39	81.564	40	80.739	
3		F3	15KV	600/5	1.44	4.886	0	110	0	4.886	118.5	112.06	55.5	77.597	
4		F4	15KV	600/5	4.22	97.637	5	1945	0.447	97.165	348	342.34	221.5	217.86	
5		F5	15KV	600/5	8.74	161.175	159	2899	13.145	148.03	388	622.53	204.5	334.03	
6		ARBOYE	33KV	150/1	1.46	91.437	893	157	83.462	7.974	359	530.99	94	147.78	
7		INDUSTRY SUNSHINE	33KV	150/1	5.55	38.645	693	0	37.962	0	235.5	268.74	197	197.08	
8		INDUSTRY ANTENXS	33KV	150/1	4.37						103.5	251.26	58	112.27	

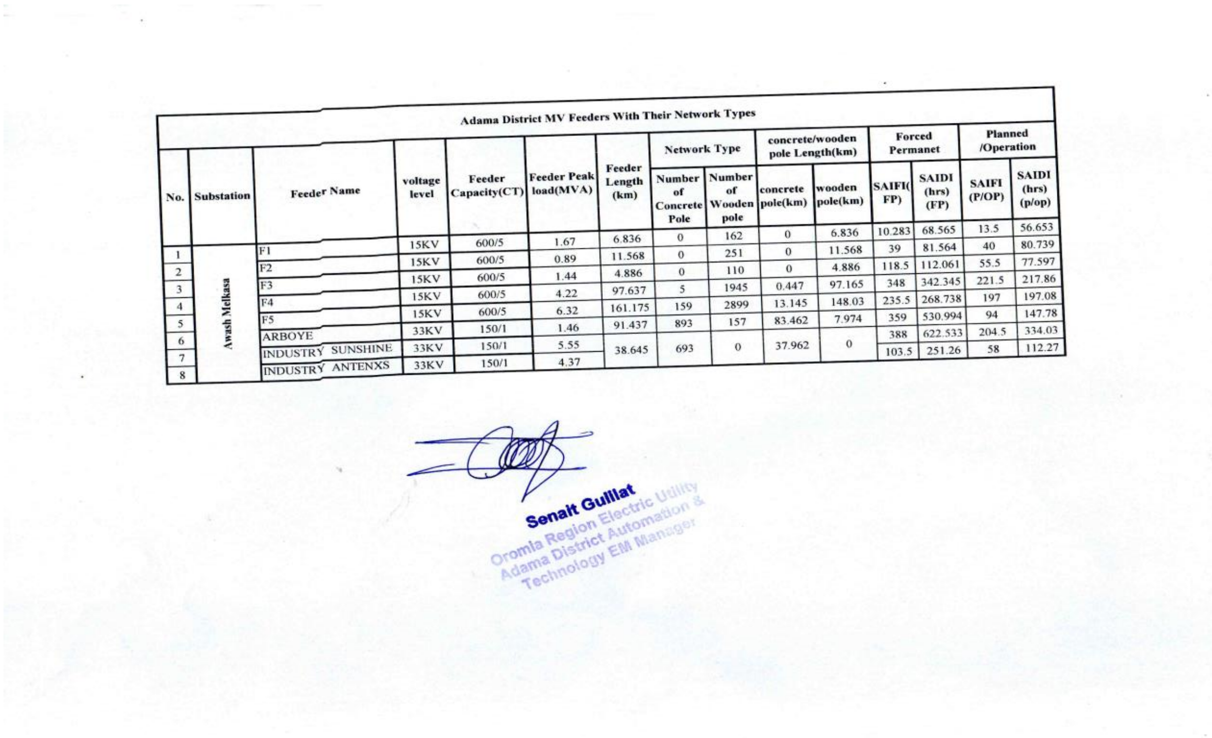

Adama District MV Feeders With Their Network Types														
No.	Substation	Feeder Name	voltage level	Feeder Capacity(CT)	Feeder Peak load(MVA)	Feeder Length (km)	Network Type		concrete/wooden pole Length(km)		Forced Permanet		Planned /Operation	
							Number of Concrete Pole	Number of Wooden pole	concrete pole(km)	wooden pole(km)	SAIFI(FP)	SAIDI (hrs) (FP)	SAIFI (P/OP)	SAIDI (hrs) (p/op)
1	Awash Melkasa	F1	15KV	600/5	1.67	6.836	0	162	0	6.836	10.283	68.565	13.5	56.653
2		F2	15KV	600/5	0.89	11.568	0	251	0	11.568	39	81.564	40	80.739
3		F3	15KV	600/5	1.44	4.886	0	110	0	4.886	118.5	112.061	55.5	77.597
4		F4	15KV	600/5	4.22	97.637	5	1945	0.447	97.165	348	342.345	221.5	217.86
5		F5	15KV	600/5	6.32	161.175	159	2899	13.145	148.03	235.5	268.738	197	197.08
6		ARBOYE	33KV	150/1	1.46	91.437	893	157	83.462	7.974	359	530.994	94	147.78
7		INDUSTRY SUNSHINE	33KV	150/1	5.55	38.645	693	0	37.962	0	388	622.533	204.5	334.03
8		INDUSTRY ANTENXS	33KV	150/1	4.37						103.5	251.26	58	112.27

Senait Gulilat
Oromia Region Electric Utility
Adama District Automation &
Technology EM Manager

The data on the above table the peak load of the Awash Melkasa substation outgoing feeder is feeder five. The highest number of wooden pole and travel long distance to supply the load.

Where; MV is medium voltage, CT is current transformer, and FP is forced permanent interrupd.

P/O is planned/operation interruption, SAIFI is system average interruption frequency index and SAIDI is system average interruption duration index.

Table Appendix-A5 distribution transformer capacity and voltage level of F-5 feeder

TAG_NUMBER	NODES_GPS_PATH_START_LAT	NODES_GPS_PATH_START_LNG	VOLTAG	CAPACITY
DT-057311	8.2885984	39.4851024	15	50
DT-057312	8.2737041	39.4880208	15	100
DT-057260	8.14944369	39.35049812	15	630
DT-010313	8.238772787	39.27032372	15	100
DT-010312	8.195784816	39.24642811	15	100
DT-010272	8.27060458	39.49005761	15	315
DT-010193	8.144601561	39.23748734	15	100
DT-010192	8.16478451	39.23192962	15	50
DT-010191	8.141907881	39.23537458	15	100
DT-010157	8.39830034	39.33640012	15	200
DT-009988	8.22569214	39.26271025	15	25
DT-009989	8.14337682	39.28146541	15	100
DT-009987	8.16798534	39.28917087	15	200
DT-009985	8.16454407	39.28050152	15	100
DT-009986	8.10720131	39.27547792	15	100
DT-045820	8.24614445	39.58101529	15	100
DT-045819	8.24311355	39.57867235	15	200
DT-045818	8.28461398	39.49058426	15	100
DT-045817	8.27164113	39.49693328	15	50
DT-045816	8.24184723	39.58661759	15	25
DT-045815	8.28535461	39.63482306	15	200
DT-045814	8.26855561	39.62291561	15	50
DT-045813	8.2652383	39.6067021	15	50
DT-045812	8.24306218	39.57827686	15	25
DT-045811	8.2628429	39.52955301	15	25
DT-045810	8.26325121	39.529589	15	25
DT-045809	8.25719581	39.52340047	15	50
DT-045808	8.27419525	39.49431558	15	100
DT-021371	8.28020471	39.4897591	15	50
DT-021274	8.27734097	39.49442482	15	315
DT-021266	8.27884146	39.491585	15	315
DT-021252	8.28109122	39.50399292	15	50
DT-021199	8.27958762	39.50212719	15	200
DT-021198	8.28066679	39.49982276	15	100
DT-021197	8.27624479	39.49813211	15	100
DT-021196	8.27491736	39.4948215	15	50
DT-021195	8.27597723	39.48965546	15	315
DT-021194	8.28417878	39.48551371	15	200
DT-012086	8.1310194	39.34816328	15	50
DT-020523	8.14505805	39.34526165	15	315
DT-012076	8.14788406	39.35802833	15	315
DT-012081	8.1569095	39.3627913	15	25

Senait Guillat
Oromia Region Electric Utility
Adama District Automation &
Technology EM Manager

DT-012091	8.11709849	39.28426447	15	100
DT-012090	8.12719697	39.29848692	15	50
DT-020522	8.09190289	39.33531049	15	25
DT-012080	8.16211401	39.36757564	15	100
DT-012089	8.14913816	39.33574733	15	50
DT-012088	8.09172351	39.33545277	15	200
DT-012085	8.12967566	39.34654727	15	50
DT-012087	8.10614738	39.33759231	15	50
DT-020521	8.15133749	39.35729003	15	200
DT-012077	8.14973458	39.35492869	15	315
DT-012075	8.14833744	39.35273179	15	25
DT-012084	8.14541933	39.34764768	15	100
DT-012083	8.1462844	39.35126041	15	315
DT-012079	8.14491254	39.35593868	15	25
DT-012082	8.15310442	39.36079607	15	50
DT-012078	8.15387842	39.35864227	15	315
DT-012074	8.15022863	39.34992474	15	315
DT-012073	8.14936881	39.35053332	15	315
DT-011940	8.1269505	39.40537879	15	315
DT-012015	8.26399656	39.32880522	15	25
DT-012018	8.24846331	39.34142711	15	50
DT-012017	8.24049111	39.32798741	15	50
DT-012016	8.24147974	39.33063643	15	50
DT-011936	8.1228119	39.2890316	15	50
DT-011939	8.12954681	39.38109742	15	100
DT-011935	8.13963303	39.24004837	15	100
DT-011938	8.14767951	39.34466324	15	100
DT-011937	8.13451647	39.30668997	15	100
DT-010734	8.291232898	39.48766493	15	100
DT-010733	8.291930524	39.47649563	15	100
DT-010732	8.294333238	39.44629529	15	100
DT-010731	8.274707221	39.41212026	15	50
DT-010729	8.297891817	39.41188507	15	50
DT-010730	8.333065636	39.38155632	15	25
DT-010760	8.324343637	39.47200544	15	100
DT-010756	8.297580974	39.4690105	15	100
DT-010755	8.293260229	39.44064589	15	100
DT-010753	8.277223762	39.40052734	15	200
DT-010752	8.277011532	39.40131658	15	200
DT-010717	8.276964761	39.40132563	15	200
DT-010716	8.287919113	39.38377669	15	50
DT-010715	8.292252808	39.37878409	15	315
DT-010757	8.304817658	39.44245311	15	200
DT-010754	8.280388936	39.40829066	15	25

Senait Gulilat
Oromia Region Electric Utility
Adama District Automation &
Technology EM Manager

DT-010751	8.278102353	39.40388856	15	200
DT-010687	8.325967756	39.31294424	15	100
DT-010682	8.333901144	39.32101157	15	200
DT-010728	8.328016168	39.32401883	15	200
DT-010727	8.317233562	39.32995087	15	100
DT-010725	8.319218396	39.32382312	15	100
DT-010724	8.331485018	39.32184641	15	50
DT-010723	8.318084283	39.31760534	15	50
DT-010722	8.320563147	39.3164509	15	25
DT-010721	8.322128677	39.31859868	15	100
DT-010690	8.330017347	39.31505959	15	50
DT-010689	8.330527176	39.30795911	15	315
DT-010688	8.327479558	39.30800823	15	315
DT-010686	8.327470841	39.31440538	15	315
DT-010685	8.326687175	39.31844512	15	315
DT-010683	8.329874352	39.31931047	15	315
DT-010368	8.342288705	39.32119455	15	200
DT-010714	8.320129844	39.3272265	15	200
DT-010713	8.323685532	39.32613149	15	100

Senait Gulilat
Oromia Region Electric Utility
Adama District Automation &
Technology EM Manager

Appendix- B: Standard conductor type and impedance per km

The electrical parameters for conductors for modeling the feeder of the Awash Melkasa distribution system taken from standard books and manufacturer catalogs are shown in the table below. All Aluminum conductor (AAC) datasheet (KJV, 2010)

Table Appendix-B: All Aluminum Conductor (AAC)

AAC (DIN 48201-5)								
Nominal aluminium area	Number and diameter	Cross-sectional	Overall diameter	Weight	Calculated Breaking Load		Calculated DC Resistance At 20°C	Breaking length
mm^2	mm	mm^2	mm	Kg/Km	kgf	kN	Ohms/Km	Km
16	7/1.70	15.89	5.10	43	290	2.84	1.80170	6.740
25	7/2.10	24.25	6.30	66	425	4.17	1.18060	6.440
35	7/2.50	34.36	7.50	94	589	5.78	0.83320	6.270
50	7/3.00	49.48	9.00	135	810	7.94	0.57860	6.000
50	19/1.80	48.35	9.00	133	862	8.45	0.59500	6.480
70	19/2.10	85.81	10.50	181	1154	11.32	0.43710	6.380
95	19/2.50	93.27	12.50	256	1599	15.68	0.30840	6.260
120	19/2.80	117.00	14.00	322	1915	18.78	0.24590	5.950
150	37/2.25	147.10	15.75	405	2580	25.30	0.19600	6.370
185	37/2.50	181.60	17.50	500	3114	30.54	0.15880	6.230
240	61/2.25	242.50	20.25	669	4029	39.51	0.11920	6.030
300	61/2.50	299.40	22.50	826	4864	47.70	0.09651	5.900
400	61/2.89	400.10	26.01	1104	6206	60.86	0.72220	5.630
500	61/3.23	499.80	29.07	1379	7614	74.67	0.05782	5.530
625	91/2.96	626.20	32.56	1733	9713	95.25	0.04625	5.600
800	91/3.35	802.10	36.85	2219	12072	118.39	0.03610	5.440
1000	91/3.74	999.70	41.14	2766	14863	145.76	0.02897	5.370

All aluminum conductors are made up of one or more wire strands of aluminum wire depends on usage .AAC have a very high degree of corrosion resistance.

Advantages of AAC conductors are

- AAC conductor have high conductivity
- AAC conductor is corrosion resistant

Table Appedix-B1: Conductor type of F-5 feeder with length and impedance

n0.	Transformer name	GPS	km distance(km)	traformer size	conductor type	Conductor size	imedance
1	DT-010157	8.3983,39.3364	2.1	200KVA	AAC	50	1.21485+j0.7287
2	DT-010368	8.342289,321194	4.962	200kva	AAC	50	2.870517+j1.721814
3	DT-010659	8.3377,39.320382	0.55	200kva	AAC	50	0.318175+j0.19085
4	DT-010682	8.333901,39.321012	0.48	200kva	AAC	50	0.27768+j0.16656
5	DT-010724	8.331485,39.321847	0.43	50	AAC	25	0.393355+j0.155594
6	DT-010683	8.329874,39.319311	0.38	315	AAC	50	0.21983+j0.13186
7	t-off	8.326657,39.320198	0.19	0	AAC	50	0.109915+j0.06593
8	t-off	8.325599,39.321448	0.24	0	AAC	50	0.13884+j0.08328
9	t-off	8.321966,39.321122	0.42	0	AAC	50	0.24297+j0.14574
10	DT-010711	8.32159,39.321071	0.044	200kva	AAC	50	0.025454+j0.015268
11	DT-010725	8.319219,39.323823	0.65	100kva	AAC	50	0.376025+j0.22555
12	DT-010712	8.316286,39.322308	0.25	100kva	AAC	50	0.144625+j0.08675
13	t-off	8.302366,39.323331	1.6	0	AAC	50	0.9256+j0.5552
14	DT-010660	8.242904,39.272711	8.8	50kva	AAC	50	5.0908+j3.0536
15	DT-010313	8.238773,39.270324	0.55	100kva	AAC	50	0.318175+j0.19085
16	DT-009988	8.225692,39.26271	1.7	25	AAC	50	0.98345+j0.5899
17	DT-010312	8.195785,39.246428	3.8	100kva	AAC	50	2.1983+j1.3186
18	DT-010300	8.160661,39.240326	4.1	50	AAC	50	2.37185+j1.4227
19	t-off	8.14791,39.236853	1.1	0	AAC	50	0.63653+0.3817
20	DT-045810	8.263251,39.529589	0.086	25	AAC	50	0.049751+j0.029842
21	DT-010192	8.164784,39.231929	2.4	50	AAC	50	1.3884+j0.8328
22	DT-010193	8.144601,39.237487	0.39	100kva	AAC	50	0.225615+j0.13533
23	DT-010191	8.141908,39.235374	0.48	100kva	AAC	50	0.27768+j0.16656
24	DT-012089	8.149138,39.335747	3.8	50	AAC	50	2.1983+j1.3186
25	DT-011935	8.139633,39.240048	0.605	100kva	AAC	50/35	0.363587+j0.210254
26	DT-011938	8.147679,39.344663	1.1	100	AAC	50	0.6942+j0.3817
27	DT-011936	8.122812,39.289032	0.39	50kva	AAC	50	0.225615+j0.13533
28	DT-012090	8.127197,39.298487	1.2	50kva	AAC	50	0.6942+j0.4164
29	DT-011937	8.134516,39.30669	1.2	100kva	AAC	50	0.6942+j0.4164
30	t-off	8.32543,39.325064	0.11	0	AAC	50	0.63635+j0.03817
31	t-off	8.281344	2.3		AAC	50	1.33055+j0.7981
32	DT-012075	8.148338,39.352732	0.15	25kva	AAC	50	0.86775+j0.05205
33	DT-011938	8.147679,39.344663	1.1	100	AAC	50	0.6942+j0.3817
34	DT-012083	8.146284,39.35126	0.28	315	AAC	50	0.16198+j0.09716
35	t-off	8.148002,39.351364	0.43	0	AAC	50	0.248755+j0.14921
36	DT-012077	8.149734,39.354929	0.29	315	AAC	50	0.167765+j0.10063
37	DT-045810	8.263251,39.529589	0.086	25	AAC	50	0.049751+j0.029842
38	DT-020521	8.151338,39.35729	0.27	200	AAC	50	0.156195+j0.09369
39	DT-012078	8.153878,39.358642	0.39	315	AAC	50	0.225615+j0.13533
40	DT-012082	8.153104,39.360796	0.26	50	AAC	50	0.15041+j0.09022
41	DT-012081	8.15691,39.362791	0.46	25	AAC	50	0.26611+j0.15962
42	DT-012080	8.162114,39.367576	0.81	100	AAC	50	0468585+j0.28107
43	DT-010685	8.326687,39.318445	0.2	315	AAC	50	0.1157+j0.0694
44	DT-010690	8.330017,39.31506	0.74	50	AAC	50	0.42809+j0.25678
45	DT-010686	8.327471,39.314405	0.15	315	AAC	50	0.086775+j0.05205
46	DT-010687	8.325968,39.312944	0.3	100	AAC	50	0.17355+j0.1041
47	t-off	8.275977,39.491162	0.31	0	AAC	35	0.179335+j0.10757
48	DT-010689	8.330527,39.307959	0.35	315	AAC	50	0.202475+j0.12145
49	DT-010728	8.328016,39.324019	0.57	200	AAC	50	0.329745+j0.19779
50	DT-010730	8.333066,39.381556	8.2	25	AAC	50	4.7437+j2.8454
51	t-off	8.146033,39.348514	0.21	0	AAC	50	0.121485+j0.07287
52	DT-010715	8.292253,39.378784	2.9	315	AAC	50	1.67765+j1.0063
53	DT-010716	8.287919,39.383777	0.86	50	AAC	50	0.49751+j0.29842
54	DT-010730	8.333066,39.381556	8.2	25	AAC	50	4.7437+j2.8454
55	DT-010754	8.280389,39.408291	0.46	25	AAC	50	0.26611+j0.15962
56	DT-010731	8.274707,39.41212	1	50	AAC	50	0.5785+j0.347
57	t-off	8.293172,39.439638	3.4	0	AAC	95	1.9669+j1.1798
58	DT-010755	8.29326,39.440646	0.12	100	AAC	95	0.06942+j0.04164
59	DT-010732	8.294333,39.446295	0.69	100	AAC	50	0.399165+j0.23943
60	t-off	8.294043,39.466514	2.4	0	AAC	50	1.3884+j0.8328
61	DT-010733	8.291931,39.476496	1.5	100	AAC	50	0.86775+j0.05205
62	DT-021198	8.280667,39.499823	0.72	100	AAC	50	0.41652+j0.24984
63	DT-021197	8.276245,39.498132	0.43	100	AAC	50	0.248755+j0.14921
64	DT-021194	8.284179,39.485514	0.34	200	AAC	50	0.19669+j0.11798
65	DT-021196	8.274917,39.494822	0.2	50	AAC	50	0.1157+j0.0694
66	DT-021195	8.275977,39.489656	0.65	315	AAC	50	0.376025+j0.22555

Senait Gulilat

Oromia Region Electric Utility
Adama District Automation &
Technology EM Manager

67	DT-010272	8.270604,39.490058	0.94	315	AAC	35	0.908886+j0.334734
68	DT-045808	8.274195,39.494316	0.59	100	AAC	50	0.341315+j0.20473
69	DT-045817	8.271641,39.496933	0.53	50	AAC	50	0.306605+j0.18391
70	DT-045809	8.257196,39.5234	3.7	50	AAC	50	2.14045+j1.2839
71	DT-057312	8.273704,39.488021	0.88	100	AAC	50	0.50908+j0.30536
72	DT-045812	8.243062,39.578277	6.6	25	AAC	50	3.8181+j2.2902
73	DT-045819	8.243113,39.578672	0.038	200	AAC	50	0.021983+j0.013186
74	DT-045820	8.246145,39.581015	0.42	100	AAC	50	0.24297+j0.14574
75	DT-045816	8.241847,39.586617	1.2	25	AAC	50	0.6942+j0.4164
76	DT-045813	8.265238,39606702	3.3	50	AAC	50	1.90905+j1.1451
77	DT-045814	8.268556,39.622915	2.3	50	AAC	50	1.33055+j0.7981
78	DT-045815	8.285355,39.634823	2.1	200	AAC	50	1.21485+j0.7287
79	DT-010721	8.322129,39.318599	0.28	100	AAC	50	0.16198+j0.09716
80	DT-010722	8.320563,39.316451	0.51	25	AAC	25	0.295035+j0.12697
81	DT-010723	8.318084,39.317605	0.43	50	AAC	50	0.60231+j0.190536
82	DT-012015	8.263997,39.328805	4.5	25	AAC	95	1.38825+j1.4598
83	DT-012017	8.240491,39.327987	3	50	AAC	95	0.9255+j0.9732
84	DT-012016	8.24148,39.330636	0.19	50	AAC	95	0.058615+j0.061636
85	DT-012018	8.248463,39.341427	1.4	50	AAC	95	0.4319+j0.45416
86	DT-009989	8.143377,39.281466	7.3	100	AAC	50	4.22305+j2.5331
87	DT-009985	8.164544,39.280502	0.64	100	AAC	50	0.37024+j0.22208
88	DT-009987	8.167985,39.289171	1.3	200	AAC	50	0.75205+j0.4511
89	DT-012091	8.117098,39.284264	0.66	100	AAC	50	0.376025+j0.22555
90	DT-009986	8.107201,39.275478	1.8	100	AAC	50	1.0413+j0.6246
91	DT-021274	8.277341,39.494425	0.4	315	AAC	50	0.2314+j0.1388
92	DT-012086	8.131019,39.348163	2.1	50	AAC	50	1.21485+j0.7287
93	DT-012085	8.129676,39.346547	0.24	50	AAC	50	0.13884+j0.08328
94	DT-012087	8.106147,39.337592	2.9	50	AAC	50	1.67765+j1.0063
95	DT-012088	8.091724,39.335453	2.7	200	AAC	50	1.56195+j0.9369
96	DT-020522	8.091903,39.335311	0.026	25	AAC	50	0.015041+j0.009022
97	DT-012073	8.149369,39.350533	0.18	315	AAC	50	0.10413+j0.06246
98	DT-057260	8.149444,39.350498	0.012	630	AAC	50	0.006942+j0.004164
99	DT-012074	8.150229,39.349925	0.11	315	AAC	50	0.063635+j0.03817
100	DT-012076	8.147884,39.358028	0.4	315	AAC	50	0.2314+0.1388
101	DT-012079	8.144912,39.355939	0.4	25	AAC	50	0.2314+0.1388
102	DT-011939	8.129547,39.381098	5.93	100	AAC	50	3.430505+j2.05771
103	DT-011940	8.126951,39.405379	2.87	315	AAC	50	1.660295+j0.99589
104	DT-010713	8.323686,39.326131	0.31	100	AAC	50	0.179335+j0.10757
105	DT-010714	8.32013,39.327226	0.45	200	AAC	50	0.260325+j0.15615
106	DT-010727	8.317234,39.329951	0.48	100	AAC	50	0.27768+j0.16656
107	DT-010751	8.278103,39.403889	0.53	200	AAC	50	0.306605+j0.18391
108	DT-010753	8.277224,39.400527	0.34	200	AAC	50	0.19669+j0.11798
109	DT-010752	8.277012,39.401317	0.06	200	AAC	50	0.03471+j0.02082
110	DT-010717	8.276965,39.401326	0.006	200	AAC	50	0.003471+j0.002082
111	DT-010729	8.297892,39.411885	4.4	50	AAC	50	2.5454+j1.5268
112	DT-077375	8.304799,39.442405	1.3	200	AAC	50	0.75205+j0.4511
113	DT-010757	8.304818,39.442453	0.01	200	AAC	50	0.005785+j0.00347
114	DT-010756	8.297581,39.469011	0.52	100	AAC	50	0.30082+j0.18044
115	DT-010760	8.324344,39.472005	3	100	AAC	50	1.7355+j1.041
116	DT-076911	8.281233,39.475442	1	200	AAC	50	0.5785+j0.3470
117	DT-076912	8.277624,39.473462	0.53	300	AAC	50	0.306605+j0.18391
118	DT-076913	8.269517,39.475248	1.5	200	AAC	50	0.86775+j0.5205

165.166

Senait Gullat
Oromia Region Electric Utility
Adama District Automation &
Technology EM Manager

Appendix -C: Sample MATLAB code for This Thesis

Appendix-C1: Subprogram for the formation of BIBC Matrix

```
Function finalres=BIBC_BCBV_PROCESS(nbus,radial_check,baseKV,baseMVA,data_pass_to
_loadflow)
[finalinedata]=LINE_DATA (nbus, radial_check);
from_node=finalinedata(:,2).';to_node=finalinedata(:,3).';
path_number=finalinedata(:,1).';
for km=1:nbus
   node_name_final{km}=num2str(km);
end
network_final_model=digraph (to_node, from_node,path_number,node_name_final);
while(1)
   for kmx=2: length(node_name_final)
      bfdata=bfsearch(network_final_model,node_name_final{kmx});
      memchk=ismember(bfdata, num2str(1));
      filp_nodes_edges=[];
      if(isempty(find(memchk)))
         preid=predecessors(network_final_model,node_name_final{kmx});
         for kmd1=1: length(preid)
            filp_nodes_edges=[filp_nodes_edges ;[str2num(preid{kmd1})
str2num(node_name_final{kmx})]];
         end
         edgedata=network_final_model.Edges;
         if(~isempty(filp_nodes_edges))
edgenum=findedge (network_final_model, filp_nodes_edges(:,1),filp_nodes_edges(:,2));
         ss=edgedata(edgenum,:);
         wval=ss.Weight;
         network_final_model=rmedge(network_final_model,edgenum);
```

```
        network_final_model=addedge(network_final_model, filp_nodes_edges(:,2),
filp_nodes_edges(:,1),wval);
            end
        end
    end
    count=0;
    for kit=1:length(node_name_final)
        bfdata=bfsearch(network_final_model,node_name_final{kit});
        memchk=ismember(bfdata, num2str(1));
        if(~isempty(find(memchk)))
            count=count+1;
        end
    end
    if(count==length(node_name_final))
        break;
    end

end
final_network_to_source=network_final_model;
network_edges=network_final_model.Edges;
node_number_data=network_edges.EndNodes;
edgenum=findedge(network_final_model, node_number_data(:,1),node_number_data(:,2));
edgedata=network_final_model.Edges;
ss=edgedata(edgenum,:);
wval=ss.Weight;
network_final_model=rmedge(network_final_model,edgenum);
network_final_model=addedge(network_final_model, node_number_data(:,2),
node_number_data(:,1),wval);
[linedata_value]=LINE_DATA(nbus,[],radial_check);
VBASE=(baseKV^2)/baseMVA;
```

```
PBASE=baseMVA*1000;
linedata_value(:,4:5)=linedata_value(:,4:5)/VBASE;
rxdata=complex(linedata_value(:,4),linedata_value(:,5));
finaldlf=DLF_MATRIX_GENERATE(node_name_final,final_network_to_source,...
   network_final_model,rxdata);
busdata_value=BUS_DATA(nbus,data_pass_to_loadflow);
load_percentage=data_pass_to_loadflow{33};
busdata_value(:,[2 3])=busdata_value(:,[2 3])*(load_percentage/100);
busdata_value(:,[2 3])=busdata_value(:,[2 3]);
busdata_value(:,2:3)=(busdata_value(:,2:3)/PBASE);
resistance_val=linedata_value(:,4);reactance_val=linedata_value(:,5);
actual_imped=complex(resistance_val,reactance_val);
finalres{1}=finaldlf;
finalres{2}=busdata_value;
finalres{3}=resistance_val;
finalres{4}=reactance_val;
finalres{5}=actual_imped;
finalres{6}=linedata_value;
finalres{7}=PBASE;
```

Appendix-C2: Base case Backward-forward Sweep load flow

```
functionfinalres_out=withoDG()
tic,clc,clear
source_num=[1];
% Read the line and bus data from excel file
  LINEDATA=xlsread('Feederdata.xlsx','linedata');
  BUSDATA=xlsread('Feederdata.xlsx','busdata');
baseKV=15;baseMVA=100;
PBASE=baseMVA*1000;                          %  Change to KVA
ZBASE=(baseKV^2)/baseMVA;                    % Base impedance
busdata_value=BUSDATA;linedata_value=LINEDATA;
linedata_value(:,4:5)=linedata_value(:,4:5)/ZBASE;     % per unit
conversion
R_val=linedata_value(:,4);                      % per unit resistance
```

```
X_val=linedata_value(:,5);                                    % per unit
reactance impe_perunit=complex(R_val,X_val);
busdata_value(:,2:3)=(busdata_value(:,2:3)/PBASE);                    %
Per unit conversion
imped_value=impe_perunit;
[bibc_matrix]=bibc_gen(linedata_value,busdata_value);calling bibc matrix
bibc_matrix(source_num,:=[]
;bibc_matrix(:,source_num)=
[];
final_bibc_matrix=bibc_matr
ix';
% diag of collum vector is happend
final_bcbv_matrix=final_bibc_matrix'*diag(impe_perunit);
final_dlf_matrix=final_bcbv_matrix*final_bibc_matrix;
load_comp_d=complex(busdata_value(:,2),busdata_value(:,3));                %
complex power load
load_comp_g=zeros(size(busdata_value,1),1);

% 33x1 matrix
load_final_matrix=(load_comp_d-load_comp_g);                         %
ingected power Pi=Pd-Pg
load_final_matrix(length(source_num))=[];                                  %
out of source node
initvolt_value=ones(size(busdata_value,1)-length(source_num),1);

% 32x1 initial bus voltage 1.0 p.u
voltagedrop_value=initial_volt_value;

% Convergency with max
iter max_iter=100;
% error_volt_tolr =0.2e-3; % maximum iteration
% while max_iter==100 && error_volt_tolr<=0.2e-
3 for i=1:max_iter
    %% backward sweep
    I_inject=conj(load_final_matrix./voltagedrop_value);
% injected current at each bus
    IB=final_bibc_matrix*I_inject;
%get the cumulative injected current flowing through each branch
    volt_old=voltagedrop_value;
    voltdrop_each=final_dlf_matrix*I_inject;
 %Voltage drop w.r.t. substation bus.
    voltagedrop_value=initial_volt_value-voltdrop_each;
```

```
        volt1_old=(volt_old);
        volt_new=(voltagedrop_value);
        % tolerance must definend
        error_tolr=max(abs(volt1_old-volt_new));                          %%
    must be defien max error
    end
    %  end final_volt_data=[ones(length(source_num),1);voltagedrop_value];       %
    voltage profile
    % ????
    locvoltm=find(final_volt_data>1);%if voltage is above 1 pu set as 1 pu
final_volt_data(locvoltm)=1;

from_node=linedata_value(:,2);to_node=linedata_value(:,3);

     for
    ind=1:length(from_node)
        %each branch voltage drop
        volt_diff_old(ind,:)=final_volt_data(from_node(ind))-
    final_volt_data(to_node(ind));

    end

    voltdiff_new_=abs(volt_diff_d);

    % magnitude of voltage drop for each branch

    %% Loss calculation

    ploss=sum(abs(IB).^2.*resistance_val)*10^5; qloss=sum(abs(IB).^2.*reactance_val)*10^5;

    total_lossp=sum(ploss(loc1));

    total_lossq=sum(qloss(loc2));

    final_voltage=abs(final_volt_data);

    % CVD=sum((1-

    final_voltage(:,1)).^2)

    %% consruct the cell arrays

    finalres_out{1}=total_lossp;

    finalres_out{2}=total_lossq;

    finalres_out{3}=final_voltage

    ; finalres_out{4}=ploss;

    finalres_out{5}= CVD;

    toc
```